THE ROLE OF CA^{2+}/CALMODULIN-DEPENDENT KINASE II IN NORMAL AND ABNORMAL EARLY POSTNATAL DEVELOPMENT

By

Richard M. Gustin

Dissertation

Submitted to the Faculty of the

Graduate School of Vanderbilt University

in partial fulfillment of the requirements

for the degree of

DOCTOR OF PHILOSOPHY

In

Pharmacology

August, 2010

Nashville, Tennessee

Approved:

Professor Roger J. Colbran

Professor Vsevolod Gurevich

Professor Pat Levitt

Professor David Zald

Professor Joey V. Barnett

To my wife Gena Stefanie Gustin,

my parents Richard Gustin and Deborah Petrell,

and my entire family for all their love and support.

I want to send a special thanks to the

thousands of furry little lives that made this possible.

ACKNOWLEDGMENTS

This research was made possible through funding received by the following:

- National Institutes of Health/National Institute of General Medical Science, Vanderbilt University Department of Pharmacology Training Grant: Richard M. Gustin, 2-T32-GM07628

- National Institute of Neurological Disorder and Stroke, National Research Service Award: Richard M. Gustin, F31NS061537

- Vanderbilt University Kennedy Center Hobbs Development Grant: Roger J. Colbran

- National Institutes of Health/National Institute of Mental Health: Roger J. Colbran, R01MH063232-10

TABLE OF CONTENTS

Page

LIST OF FIGURES

CHAPTER I

INTRODUCTION

Learning and Memory

Understanding molecular mechanisms underlying normal learning and memory processes are fundamental to neuroscience research. Common research methods use rodent models with genetic and/or environmental perturbations to cause dysfunction that can be demonstrated in neurobehavioral paradigms. Using these manipulations one can identify proteins of interest that may have altered expression, subcellular localization, and/or activation states. The effects of protein misregulation in the diseased state can shed light on how these proteins function in normal learning and memory. Additionally, identification of signaling cascades that are altered in the diseased state can themselves lead to identification of therapeutic targets for the treatment of disease.

Hippocampus

Found in the medial temporal lobe, the hippocampus is a region of the brain that plays a crucial role in forming declarative or explicit memories (Figure 1A). The hippocampus emerged as an integral component of memory when it was discovered that individuals who had undergone temporal lobe lobotomies, as well as those that had certain forms of amnesia, had significant deficiencies in the ability to form new memories, without other noticeable cognitive deficits (Squire and Zola-Morgan, 1991; Milner et al., 1998). Numerous studies using animal models have demonstrated that

disruption of hippocampal neuronal circuitry, whether through lesion (Mishkin, 1978; Chen et al., 1996; Deacon et al., 2002; Dillon et al., 2008), genetic manipulation (Silva et al., 1992b; Silva et al., 1992a; Chen et al., 1994; Mayford et al., 1995; Giese et al., 1998; Elgersma et al., 2002; Wang et al., 2003), or pharmacological intervention (Morris et al., 1986; McHugh et al., 2008; Wang et al., 2008), leads to altered learning and memory.

In addition to the functional importance of the hippocampus, the anatomy of the hippocampus lends itself to experimental manipulation (Figure 1B). The hippocampal circuitry seen in Figure 1B describes the axonal inputs projecting from the neocortex to the dentate gyrus making up the perforant pathway. The mossy fiber pathway extends from the dentate gyrus to the Cornu Ammonis (CA) 3 region of the hippocampus. The CA3 receives additional innervation through the commissural fibers extending from the contralateral hippocampus. CA3 neurons project onto the CA1 region of the hippocampus through what is known as the Schaffer collateral pathway. The circuit is complete as the CA1 sends axonal projections back to the neocortex. The anatomical structure of the hippocampus and its circuitry, intact in isolated slices, has allowed the hippocampus to become a very well studied model of cellular learning and memory. In particular, altered physiological properties at the Schaffer-collateral synapse (Figure 1B) have been linked to a number of learning and memory deficits (Jiang et al., 1998; Moretti et al., 2006; Son et al., 2006; Polydoro et al., 2009).

Understanding mechanisms of altered physiology in disease models of hippocampal-dependent learning and memory allows for the design of hypotheses that can lead to the identification of therapeutic targets, which may be manipulated to reverse or prevent the memory dysfunction (van Woerden et al., 2007). Though complex, this is

Figure 1

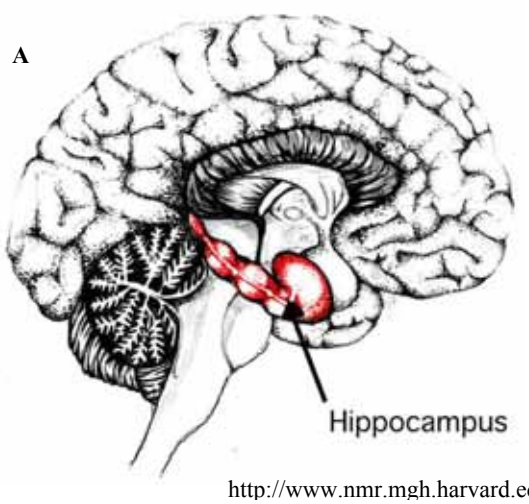

http://www.nmr.mgh.harvard.edu/~bradd/hippocampus.jpg

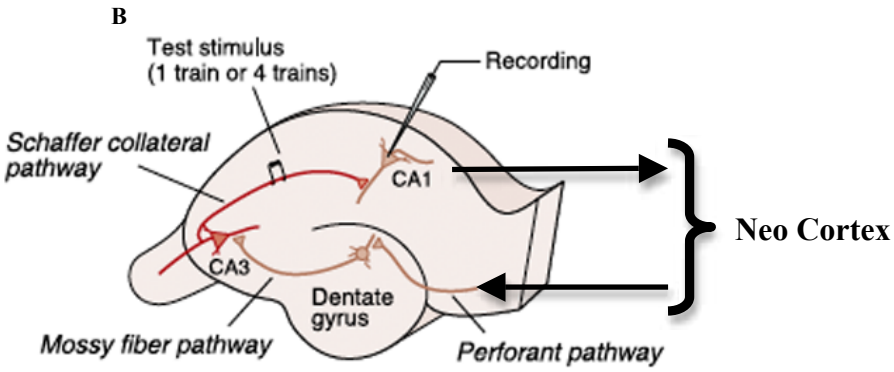

Adapted from Kandel 2001

Figure 1. Hippocampus location and architecture. **A.** The human hippocampus (shown in red) is a brain region found deep in the temporal lobe that is important in normal learning and memory processes. **B.** A schematic of the cellular architecture of the rodent hippocampus depicts the innervation of the dentate gyrus of the hippocampus by neurons projecting from the entorhinal cortex, known as the perforant pathway. Granular cells of the dentate gyrus project via the Mossy fiber pathway synapsing onto pyramidal cells of the CA3 region of the hippocampus. Additionally, CA3 is innervated by commissural fibers extending from the contralateral hippocampus. CA3 projections synapse on pyramidal cells of CA1, making up the Schaffer collateral pathway. The circuit is completed as CA1 projects back to the neocortex. The well characterized Schaffer collateral pathway can be manipulated electrophyiologically, seen in B, as electrical stimulation of the Schaffer collateral can lead to electrical changes recorded in the CA1 pyramidal neurons.

possible in the hippocampus due to the vast knowledge of how hippocampal physiology relates to learning and memory behaviors.

Neuron

Hippocampal function depends on communication between excitatory glutamatergic neurons, of which the pyramidal cells are the major neuronal cell type making up the hippocampus. The morphology of typical hippocampal pyramidal neurons can be seen in a golgi-stain of the CA1 region of the hippocampus (Figure 2A). Under higher magnification dendrites can be visualized, studded with dendritic spines, the site of synaptic transmission (Figure 2A, right). The dendritic spines form connections with presynaptic axon terminals creating a structure called the synapse (Figure 2B). Activity-dependent regulation of the strength of synapses (synaptic plasticity) can modulate the number, size, morphology, and subcellular protein composition of dendritic spines (Chang and Greenough, 1984; Moser et al., 1994; Isaac et al., 1995; Liao et al., 1995; Marrs et al., 2001; Bourne and Harris, 2008). Moreover, it is thought that synaptic plasticity is the cellular basis for learning and memory.

Dendritic spines are specialized structures that extend from the dendritic shaft and allow for communication between the presynaptic and postsynaptic neuron (Figure 2B). Vesicles in presynaptic axon terminals store neurotransmitter, and are able to release their contents into the synapse upon depolarization of the presynaptic neuron. The neurotransmitter is able to traverse the synaptic cleft and activate receptors on the dendritic spine of the postsynaptic neuron, altering downstream signaling initially in the postsynaptic density (PSD), and then throughout the neuron. The PSD contains all the

Figure 2

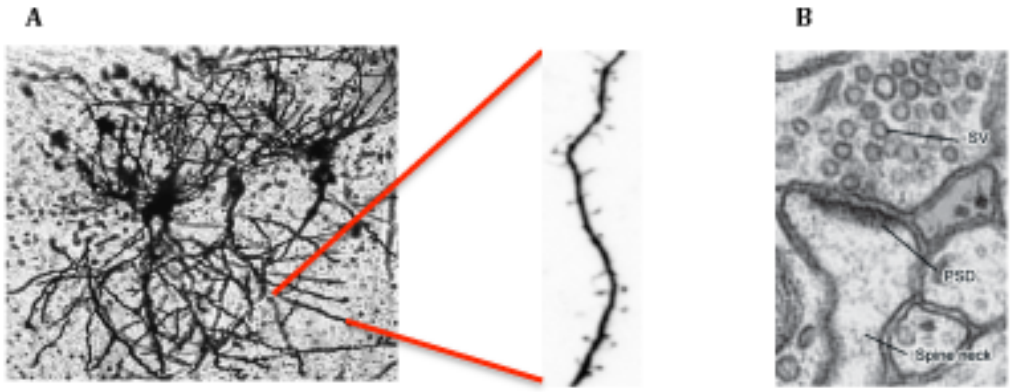

Adapted from Marrs et al., 2001 and Shang and Hoogenraad, 2007

Figure 2. Neuronal and dendritic spine structure. **A.** The left panel shows a golgi-stain of pyramidal cells of the CA1 region of the hippocampus, in slice preparations. The tightly packed pyramidal cells contain dense dendritic arborizations. Under higher magnification (A. right panel) an eGFP transfected dendrite reveals the dendritic spines that dot the length of the dendrite. **B.** An electromicograph image shows both presynaptic and postsynaptic elements that form the synapse. The characteristic synaptic vesicle (SV) laden presynaptic terminal (top) forms connections with the postsynaptic neuron via dendritic spines. The electron rich area of the dendritic spine is known as the PSD. The spin neck, which extends from the dendrite is also visible. (Images taken from Marrs et al, 2001 and Shang and Hoogenraad, 2007).

machinery needed for the transduction of presynaptic signals into intracellular molecular responses. This consists of scaffolding proteins (e.g., PSD-95), receptors and channels (e.g., NMDAR, AMPAR), kinases (e.g., CaMKII), as well as a number of other adhesion, cytoskeletal, translational, and regulatory proteins. Through protein/protein interactions this collection of 400-1000 proteins (Sheng and Hoogenraad, 2007) are able to spatially and temporally organize signaling complexes at the PSD for efficient and specific dissemination of presynaptic messages (Figure 3). It is hypothesized that altered expression, localization, or activation of PSD proteins that affect these protein/protein interactions can lead to learning and memory dysfunction.

Glutamate family of receptors

Glutamate is a major excitatory neurotransmitter in the hippocampus as well as the entire central nervous system (CNS). Glutamate released by presynaptic axon terminals can traverse the synaptic cleft and activate a number of receptors on the postsynaptic membrane, including metabotropic glutamate receptors (mGluRs) and ionotropic glutamate receptors (iGluRs). mGluRs are G-protein coupled receptors (GPCRs), which are able to alter intracellular signaling cascades upon glutamate binding. iGluRs function as ion channels, opening in response to glutamate activation. For the purposes of this dissertation I will focus on the ionotropic family of glutamate receptors.

N-methyl-D-aspartate receptors (NMDAR)

A member of the ionotropic glutamate family of receptors, NMDARs are voltage-gated and ligand-gated cation channels that play important roles in synaptic plasticity and

Figure 3

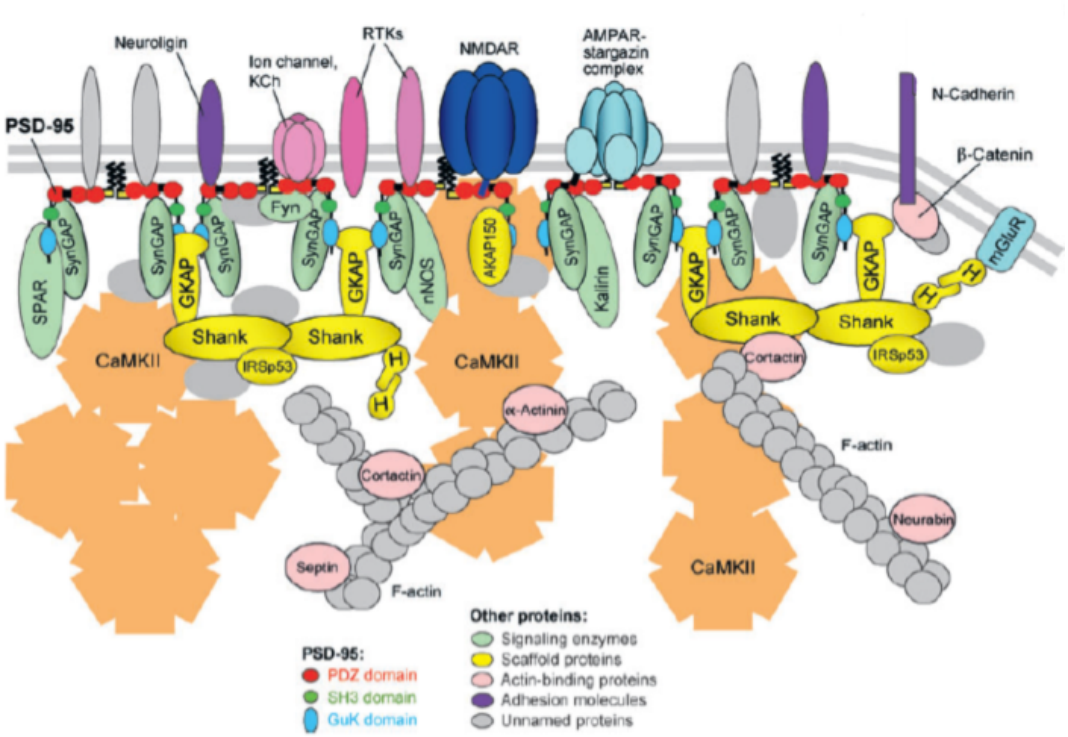

Adapted from Sheng and Hoogenraad 2007

Figure 3. Representation of a postsynaptic density (PSD). This cartoon represents an electron dense area of the dendritic spine seen in figure 1B. An estimated 400-1000 proteins are present in a PSD. These proteins are necessary for rapid dissemination of both electrical and chemical signals relayed from presynaptic neurons. Signal transduction from the PSD initiates changes in spine morphology, gene expression, and altered protein activation/localization that is important in changes in synaptic strength, which in turn affects learning and memory.

learning and memory (Morris et al., 1986; Bliss and Collingridge, 1993). Additionally, these receptors are involved in brain development and are crucial in synaptogenesis (Stephenson et al., 2008).

The heterotetrameric transmembrane NMDARs are comprised of a combination of NR1, NR2 (A-D), and NR3 (A and B) subunits (Hollmann et al., 1989; Moriyoshi et al., 1991; Monyer et al., 1992). Along with NR1, NR2B and NR2A are the predominate subunits found in the adult hippocampus, with NR3 being expressed in the immature brain. Each subunit of the NMDA receptor contains (1) an extracellular agonist binding N-terminal domain, (2) three transmembrane domains with an intracellular reentrant loop between transmembrane domains 1 and 2, forming the channel pore, and (3) an intracellular C-terminal domain important for posttranslational modification of the receptor, trafficking, and protein/protein interactions. Functional NMDARs are formed by the association of two obligatory NR1 subunits (Forrest et al., 1994; Behe et al., 1995), which contain an extracellular binding pocket for the co-agonist, glycine (Monyer et al., 1992; Anson et al., 1998; Banke and Traynelis, 2003), and two additional NR2 subunits (Sheng et al., 1994), which contain the extracellular glutamate binding domain (Planells-Cases et al., 1993; Anson et al., 1998).

NMDA receptors are localized to the PSD in part by the direct interaction of NR2A and NR2B with PSD-95 (Roche et al., 2001), a member of the membrane-associated guanylate kinase (MAGUK) family of scaffolding proteins that is enriched in the PSD. Stable localization of NMDA receptors at postsynaptic and extrasynaptic membranes is vital for receptor regulation and neuronal function (Barria and Malinow, 2002; Mohrmann et al., 2002).

Activation of NMDARs is a unique process requiring the coordination of several simultaneous events. In the inactive state, the pore of the channel is blocked by an Mg^{2+} ion, thus depolarization of the postsynaptic membrane is required for removal of the Mg^{2+} block. Along with depolarization of the postsynaptic cell, coincident binding of glutamate, as well as the co-agonist glycine, is needed to activate the receptor. Once active, Ca^{2+} is conducted through the pore altering local intracellular Ca^{2+} concentrations in the dendritic spine leading to activation of signaling cascades that modulate synaptic plasticity. Desensitization of the NMDAR is enhanced by activation of CaMKII (Sessoms-Sikes et al., 2005). This desensitization is thought to occur through phosphorylation at residue Ser1303 of the NR2B subunit by CaMKII (Colbran lab unpublished data). Furthermore, it is hypothesized that this phosphorylation results in alterations of Ca^{2+} concentrations that can modulate synaptic plasticity and learning and memory.

α-amino-3-hydroxy-5-methyl-4-isoxazolepropionic acid receptors (AMPAR)

The primary receptors responsible for fast excitatory neurotransmission in the brain are the AMPARs, another member of the ionotropic glutamate receptor family. These ligand-gated ion channels, activated by glutamate, are a major conductor of Na^{+} and in some cases Ca^{2+} ions leading to depolarization of postsynaptic neurons. Activity-dependent trafficking of AMPARs in and out of the postsynaptic membrane is thought to underlie a number of forms of synaptic plasticity, including LTP and LTD (Barry and Ziff, 2002; Malinow and Malenka, 2002; Bredt and Nicoll, 2003). Altered trafficking of

AMPARs due to changes in phosphorylation of the receptor can lead to deficits in learning and memory (Lee et al., 2003; Crombag et al., 2008).

Functional AMPARs exist as heterotetramers made up of a combination of four subunits, which are encoded from four separate genes (GluR1-GluR4) (Hollmann and Heinemann, 1994; Rosenmund et al., 1998). All four subunits can be found in the brain, with GluR4 found predominantly in the immature brain. In the mature hippocampus GluR1, GluR2, and GluR3 are the major subunits expressed. These subunits combine to primarily form heteromers of either GluR1/GluR2 homodimers or GluR2/GluR3 homodimers (Wenthold et al., 1996). Structurally, AMPARs contain (1) a large extracellular N-terminal domain that contains the site for glutamate binding, (2) three transmembrane domains with a cation pore formed between transmembrane domain 1 and 2, and (3) a C-terminal domain. Posttranslational modification and protein/protein interactions in the C-terminal domain can direct trafficking and subcellular localization of the receptors, as well as affect function of the receptors (Kessels and Malinow, 2009).

Insertion or removal of AMPARs from the postsynaptic membrane dictates the strength of the synapse (Barry and Ziff, 2002; Malinow and Malenka, 2002; Bredt and Nicoll, 2003). This can be influenced by the subunit composition of individual receptors and the presence of long-tail (GluR1/4) or short-tail (GluR2/3) cytoplasmic C-termini. It has been documented that heterotetrameric GluR2/3 containing AMPARs, that have short cytoplasmic tails, constitutively traffic in and out of the synapse, whereas synaptic activity is needed to drive AMPARs containing GluR1/2 subunits, in which a long-tail cytoplasmic domain is present (GluR1) (Shi et al., 2001). Although AMPAR trafficking is not completely understood it is thought that phosphorylation of intracellular sites on

the receptor can affect the subcellular localization of the receptor. For example, synaptic insertion of AMPARs can be enhanced by phosphorylation of Ser845 by PKA (Roche et al., 1996; Song and Huganir, 2002; Esteban et al., 2003). CaMKII activation is known to enhance synaptic insertion and can modulate AMPAR conductance through phosphorylation of Ser831 (Barria et al., 1997; Mammen et al., 1997), along with PKC phosphorylation at Ser818 and Ser831 (Roche et al., 1996; Boehm et al., 2006). Alternatively, dephosphorylation of Ser845/Ser831 (Kameyama et al., 1998; Lee et al., 2000) along with phosphorylation of Ser880 by PKC can remove AMPARs from the synapse (Chung et al., 2000; Matsuda et al., 2000). Changes in phosphorylation of the receptor, which affect AMPAR binding to PDZ domain proteins, are thought to lead to altered receptor localization (Chung et al., 2000).

When activated, AMPARs are able to rapidly conduct Na^+ ions, leading to a depolarization of the postsynaptic neuron. These receptors are responsible for the fast component of the excitatory postsynaptic potential (EPSP) and are a crucial component of synaptic plasticity and learning and memory (Kessels and Malinow, 2009).

Ca^{2+}/calmodulin-dependent kinase II (CaMKII)

Ca^{2+}/calmodulin-dependent kinase II (CaMKII) is a multifunctional kinase that plays an integral role in the normal learning and memory process. CaMKII acts as a Ca^{2+} sensor, integrating local transient changes in Ca^{2+} concentration to a variety of functional responses. It is thought that CaMKII localization, protein interactions, and activity state dictate how the calcium signal will be decoded and what cellular responses will occur (Soderling, 2000; Lisman et al., 2002; Colbran and Brown, 2004).

A highly abundant protein, CaMKII accounts for ~1-2% of the total protein in the hippocampus, furthermore CaMKII levels in the PSD have been estimated to account for 2-10% of the total protein present (Hanson and Schulman, 1992b; Colbran, 2004). There are four isoforms of CaMKII (α, β, δ, and γ) encoded on four separate genes, all of which can undergo alternative splicing accounting for 30 mRNA products. CaMKIIα and CaMKIIβ are the major isoforms found in the brain, and more specifically the hippocampus. CaMKII exists as a homo- or hetero- multimeric protein containing twelve individual subunits. The individual subunits assemble through the C-terminal association domain to form a dodecomeric structure (two stacked, hexameric rings) (Kolodziej et al., 2000; Morris and Torok, 2001).

A single CaMKII subunit consists of an N-terminal catalytic domain (residues 1-272), an internal regulatory domain (residues 273-314), and a C-terminal association domain (residues 315-478) (Figure 4A). The association domain, through intersubunit interactions, acts as a scaffold to form the functional holoenzyme structure. The regulatory domain is the site of calmodulin binding and contains phosphorylation sites at Thr286 and Thr305/306, which can further modulate kinase activity and subcellular localization (Figure 4B) (Lisman et al., 2002; Colbran, 2004; Griffith, 2004).

CaMKII responds to transient changes in local Ca^{2+} concentrations, with varying sensitivity to the duration and frequency of these changes (De Koninck and Schulman, 1998). Calcium-dependent activation of CaMKII occurs when increasing intracellular Ca^{2+} binds to calmodulin, the Ca^{2+}/calmodulin complex is able to bind to the regulatory domain of CaMKII removing the autoinhibition and activating the kinase. CaMKII is now able to bind to, and phosphorylate, its target substrates. The active kinase is also

Figure 4

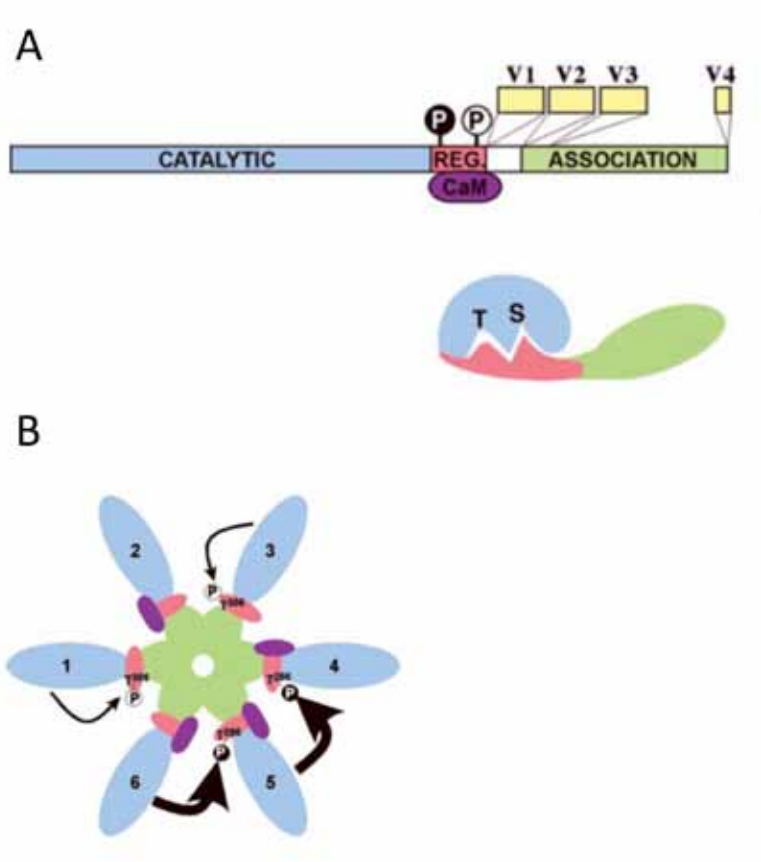

Figure 4. CaMKII structure and regulation. **A.** A schematic representation of a single subunit of CaMKII, which is comprised of an N-terminal catalytic domain (Blue), a regulatory domain (Red) that contains autophosphorylation sites, and a calmodulin binding site that are crucial in the regulation of the kinase, variable regions (Yellow) that are sites of alternative splicing, and a C-terminal association domain allowing for subunit oligomerization. In the inactive state the catalytic domain binds to auto-inhibitory sites in the regulatory domain preventing ATP (T-site) and substrate (S-site) binding. **B.** CaMKII exists as a dodecomeric structure formed by two-stacked hexameric rings (for simplicity only one ring is shown in B.). Ca^{2+}/calmodulin binding to the regulatory domain releases the catalytic domain from auto-inhibition activating the kinase. When two adjacent subunits are bound to Ca^{2+}/calmodulin the kinase can undergo inter-subunit trans-autophosphorylation at Thr286 rendering the kinase autonomously active as Ca^{2+}/calmodulin dissociate (subunits 4 and 5 in the diagram). The absence of calmodulin can lead to inter-subunit Thr305/306 phosphorylation, which prevents calmodulin binding, and thus Thr286 phosphorylation. (Figure adapted from Colbran, 2004)

primed to undergo intersubunit trans-autophosphorylation at Thr286 (Bradshaw et al., 2002), increasing the affinity for Ca^{2+}/calmodulin 1000-fold, "trapping" the kinase in the active conformation (Meyer et al., 1992). Thr286 phosphorylation also confers autonomous activity to the kinase, so as intracellular Ca^{2+} returns to basal levels and the Ca^{2+}/calmodulin complex dissociates, CaMKII is able to remain active due to the Thr286 phosphorylation, which prevents autoinhibition through steric hindrance (Lai et al., 1986; Lou et al., 1986; Miller and Kennedy, 1986; Schworer et al., 1986). Moreover, this phosphorylation is thought to be a form of "molecular memory" at the level of dendritic spines, integrating transient changes in Ca^{2+} levels to long-term signals that induce changes in synaptic strength (Figure 4B) (Colbran 2004).

Calcium-independent activity of CaMKII is revealed as Ca^{2+}/calmodulin dissociates from the kinase. Intra-subunit phosphorylation of Thr305/306 in the regulatory domain prevents further Ca^{2+}/calmodulin binding (Colbran and Soderling, 1990; Hanson and Schulman, 1992a; Mukherji et al., 1994). However, the previous phosphorylation at Thr286 keeps the kinase in an active conformation able to interact with and phosphorylate substrates. When CaMKII is dephosphorylated at Thr286 the kinase is locked in an inactive form until the kinase can be reset by dephosphorylation of Thr305/306. However, it is not completely understood how differential phosphorylation of subunits within the CaMKII holoenzyme, at Thr286, Thr305/306, as well as other sites, affects the activity level or the subcellular localization of the kinase (Figure 4B).

Specific functions of CaMKII are intimately coupled to its subcellular localization within the neuron (Figure 5). For example, in order for calcium-dependent activation of CaMKII to occur, the kinase must be localized to regions within the cell that are sites of

Figure 5

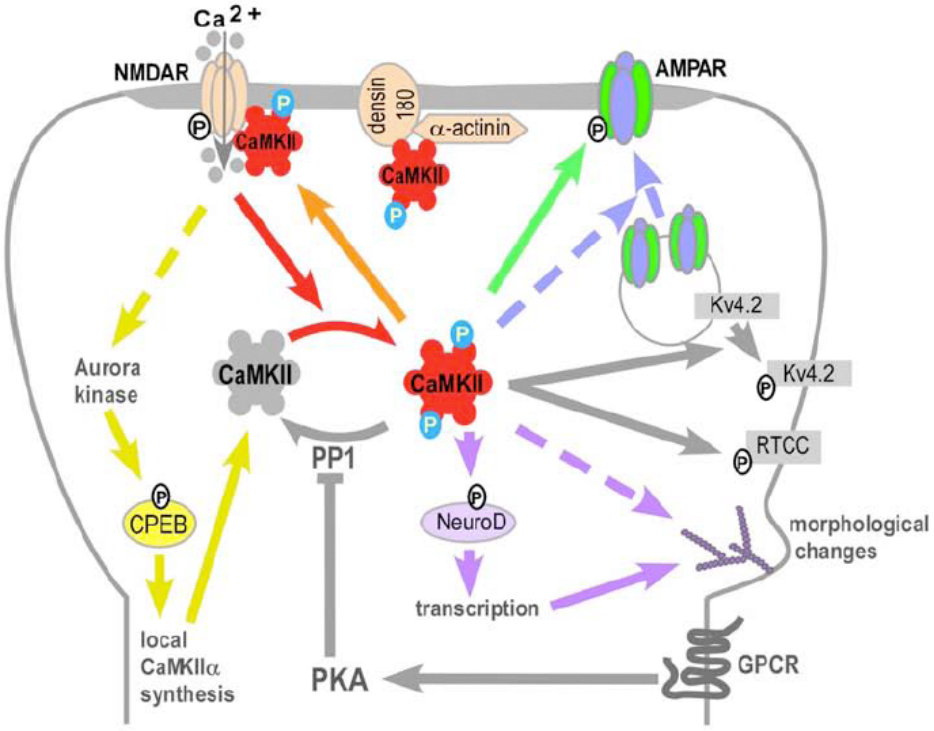

Figure 5. Phosphorylation-dependent subcellular localization and function of CaMKII. Ca^{2+}/calmodulin activation of CaMKII leads to translocation and differential phosphorylation of CaMKII (see text). Thr286 phosphorylation increases the affinity of CaMKII to the PSD where it can interact with and, through phosphorylation, modulate a number of substrates including the NMDAR and AMPAR. Activation of the multifunctional CaMKII leads to changes in local CaMKII synthesis, gene transcription, morphological changes, as well as receptor trafficking and changes in receptor function. (Figure adapted from Colbran and Brown, 2004)

Ca^{2+} entry. Additionally, activity of the enzyme is useless if CaMKII is not appropriately localized to sites where its substrates are localized. Phosphorylation state dependent subcellular localization of CaMKII is able to position the kinase, both temporally and spatially, within the cell to efficiently modulate cellular functions (Colbran 2004). In addition to modulating the activity of the kinase, differential phosphorylation of CaMKII can dictate subcellular localization of the kinase. CaMKII phosphorylation at residue Thr286 (see above) stabilizes the kinase at the PSD. It has been demonstrated that there is a greater than 2-fold increase in the amount of CaMKII (Strack et al., 1997a) and the size of the PSD (Dosemeci et al., 2001) after CaMKII Thr286 phosphorylation following LTP induction. This is thought to be due to an increased affinity of CaMKII for PSD enriched proteins, such as the NR2B subunit of the NMDAR (Strack and Colbran, 1998). CaMKII is able to interact (directly or indirectly) with a number of PSD-associated proteins (α-actinin, densin-180, SAP-97, PSD-95, synGAPβ, and F-Actin) that may participate in targeting CaMKII to the PSD (Shen et al., 1998; Strack et al., 2000b; Li et al., 2001; Robison et al., 2005b; Nikandrova et al., 2010). Presumably, translocation of activated CaMKII into the PSD positions the kinase in close proximity to its substrates to facilitate and alter molecular learning and memory functions (Robison et al., 2005a; Tsui and Malenka, 2006).

Holoenzyme subunit composition can also affect subcellular localization. Although the CaMKII α and β subunits are 90% homologous, CaMKIIβ has the ability to bind to F-Actin through an F-Actin binding domain located in the association domain (Shen et al., 1998; Fink et al., 2003). The interaction between CaMKIIβ and F-Actin can be modulated by Ca^{2+}/calmodulin, causing dissociation of the complex when CaMKII is

activated (Ohta et al., 1986). At present it is unknown how the subunit composition (i.e. α:β ratio), within individual twelve subunit holoenzymes, affects CaMKII targeting to F-Actin or how this affects subcellular localization of the kinase.

I have described how activation can drive the translocation of CaMKII into the PSD (Strack et al., 1997a; Migues et al., 2006). Once Ca^{2+} levels drop and Ca^{2+}/calmodulin dissociates from CaMKII, the autonomously active kinase (Thr286 phosphorylated) remains in the PSD able to regulate its substrates. A rapid intrasubunit phosphorylation of Thr305/306 follows Ca^{2+}/calmodulin dissociation, which prevents any additional Ca^{2+}/calmodulin from binding the kinase. The PSD-associated CaMKII can be dephosphorylated by protein phosphatase 1 (PP1) (Strack et al., 1997b), which removes the Thr286 phospho-group rendering the kinase inactive. The Thr305/306 phosphorylation drives translocation of CaMKII out of the PSD into more cytosolic locations, removing the kinase from the vicinity of its PSD-associated targets. This can be demonstrated in genetically modified mice where the residues Thr305/306 of the CaMKIIα subunit are mutated to alanines. These mice have an increased CaMKII associated with the PSD (Elgersma et al., 2002). Additionally, mice that harbor a mutation in CaMKIIα that replaces the threonine at residue 305 to an aspartate leads to a decrease in the amount of CaMKII associated with the PSD (Elgersma et al., 2002). Together this suggests that Thr305/306 is, in part, responsible for the decreased affinity and dissociation of CaMKII from the PSD. After phosphorylated at Thr305/306 the kinase must be "reset" (i.e. dephosphorylated at Thr305/306) before it can be activated again by changes in Ca2+ levels. Protein phosphatase 2A (PP2A) dephosphorylates cytosolic CaMKII (Strack et al., 1997b) resetting the kinase, making it available for

subsequent activation by Ca^{2+}/calmodulin. This tight regulation of CaMKII, dictating its activation state, subcellular localization, and interacting partners, is crucial for normal synaptic plasticity and learning and memory to occur. Any perturbations that affect CaMKII expression or regulation can drastically alter normal cellular function and lead to deficits in learning and memory (see below).

Synaptic plasticity

Synaptic plasticity refers to the strengthening or weakening of synapses during learning and memory or synaptogenesis. Changes in protein composition and function results in remodeling of dendritic spines that leads to the insertion or removal of AMPARs from the synapse. This can be detected electrophysiologically as long-term pontentiation (LTP) or depression (LTD), respectively (Barry and Ziff, 2002; Malinow and Malenka, 2002; Bredt and Nicoll, 2003; Kessels and Malinow, 2009).

LTP is a cellular correlate to learning and memory consisting of two major phases, an early-phase (E-LTP) and a late-phase (L-LTP). Experimentally, LTP can be generated by high-frequency stimulation (HFS) of CA3 afferents leading to a potentiation of excitatory postsynaptic potentials (EPSPs) in CA1 neurons (Fig. 1B) (Bliss and Lomo, 1973). E-LTP is the immediate response to a HFS, which is protein synthesis-independent and is sustainable for 30 minutes to one hour. L-LTP is dependent on protein synthesis and can last for days to weeks and even months (Kandel, 2001).

CaMKII is known to play a fundamental role in molecular mechanisms of synaptic plasticity and LTP (Figure 6) (Fink and Meyer, 2002; Lisman et al., 2002; Matynia et al., 2002; Colbran and Brown, 2004). LTP begins with the release of

glutamate from the presynaptic terminal into the synapse. The coincident depolarization of the postsynaptic membrane, often due to AMPAR activation, and binding of glutamate to postsynaptic NMDARs displaces Mg^{2+} from the ion channel pore and activates the receptor. Now active, the NMDARs conduct Ca^{2+} ions, changing the local concentration of Ca^{2+} at the PSD, thus activating CaMKII (see above). Activation of CaMKII allows the kinase to translocate to the PSD where it can bind to and phosphorylate target proteins, such as the GluR1 subunit of the AMPAR at Ser831. CaMKII activation leads to increased expression of AMPARs at the postsynaptic membrane and phosphorylation of the GuR1 subunit at Ser831enhances conductance of the receptor, leading to long-term changes in the strength of the synapse. This is visualized electrophyisologically as a potentiation of the excitatory postsynaptic potential (EPSP). There are numerous mouse models linking misregulation of CaMKII to hippocampal LTP and learning and memory deficits, highlighting the importance of CaMKII in normal learning processes (Silva et al., 1992b; Silva et al., 1992a; Bach et al., 1995; Mayford et al., 1995; Mayford et al., 1996; Giese et al., 1998; Elgersma et al., 2002; Miller et al., 2002; Hinds et al., 2003; Wang et al., 2003).

CaMKII and Learning and Memory

The role of CaMKII in the normal learning and memory process has been widely studied using both *in vitro, ex vivo* and *in vivo* paradigms. Altering CaMKII expression, phosphorylation state (activity), or subcellular localization can profoundly affect the molecular mechanisms that drive learning and memory. To fully understand how changes on a molecular level can lead to alterations in behavioral output, it first must be

Figure 6

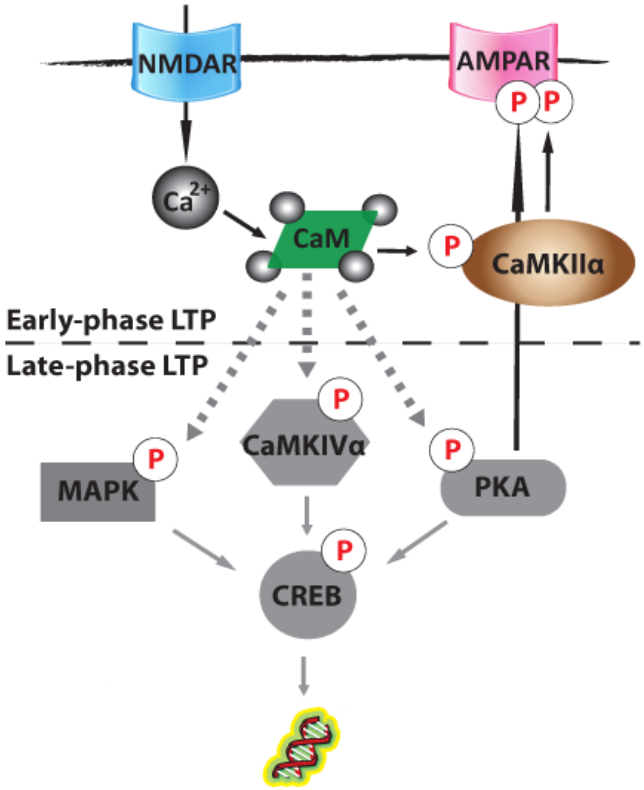

Figure 6. Long-term potentiation (LTP). NMDAR activation leads to an increase in intracellular Ca^{2+}. The Ca^{2+} is able to bind to CaM and through binding can activate a number of kinases associated with E-LTP and L-LTP. In E-LTP activation of CaMKIIα and PKA leads to phosporylation of AMPAR at Ser831 and Ser845, respectively. The activation of these kinases leads to an increased trafficking of AMPARs to the synapse, as well as an increase in AMPAR conductance leading to a potentiation of AMPAR responses that can last for 1-3 hours. L-LTP, unlike E-LTP, is dependent on protein synthesis. Ca^{2+}/CaM activation of a number of signaling pathways, such as Mitogen-activated protein kinase (MAPK), CaMKIV, and Protein kinase A (PKA), leads to cAMP response element binding protein (CREB) phosphorylation and gene transcription. The activation of gene transcription in the context of L-LTP can lead to potentiation of AMPAR responses that can last for months.

known how manipulating the function and/or regulation of the kinase leads to learning and memory deficits.

Using electrophysiological techniques it has been shown that induction of LTP in the hippocampus leads to an enhanced AMPAR response to glutamate due to an increased number of AMPARs in the postsynaptic membrane (Shi et al., 1999; Shi et al., 2001). The same alteration of AMPAR response to glutamate can be detected if exogenous CaMKIIα is added to hippocampal slices (Lledo et al., 1995; Poncer et al., 2002; Thiagarajan et al., 2002) and has been shown to be CaMKII dependent (Hayashi et al., 2000). Additionally, there is an increase of CaMKII levels, and CaMKII activity, in the PSD following LTP (Strack et al., 1997a). Similarly, if CaMKII activity is inhibited using CaMKII antagonists, LTP is blocked (Chen et al., 2001). It is important to note that inhibition of CaMKII prior to, but not after, HFS blocks LTP (Sanhueza et al., 2007). These experiments directly show that CaMKII is a crucial player in the cellular mechanisms that are responsible for the induction of LTP.

The creation of genetically modified mice, that alter learning and memory in behavioral paradigms, have greatly enhanced the understanding of the role CaMKII is playing in learning and memory (Table 1). In attempts to understand the contribution of CaMKIIα autonomous activity on learning and memory, the laboratory of Alcino Silva created CaMKIIα-Thr286Ala knock-in (KI) mice by homologous recombination using a point mutation strategy to change the encoding of the amino acid threonine at position 286 to an alanine. Mice harboring this CaMKIIα (Thr286 to Ala) KI mutation cannot autophosphorylate at position 286, thus preventing autonomous activity of the kinase (Giese et al., 1998). The CaMKIIα in these mice can still be activated by

Ca^{2+}/calmodulin; however, without autonomous activity, when Ca^{2+} returns to basal levels in the neuron CaMKII no longer has the capacity to "remember" previous changes in intracellular Ca^{2+}, losing the ability to act as a "molecular memory" protein. The loss of autonomous CaMKII activity in these mice leads to profound electrophysiological and learning and memory deficit (Giese et al., 1998).

Immunoblot and immunocytochemical analysis of total CaMKIIα from the hippocampus of adult KI mice was unchanged from that of WT. Ca^{2+}/calmodulin-dependent CaMKII activity was unaltered, however the Ca^{2+}/calmodulin-independent activity was reduced, not absent, in the KI mice. CaMKIIβ activity may be compensating for the decreased CaMKIIα activity (Giese et al., 1998; Elgersma et al., 2004); Although CaMKIIβ expression has not been evaluated (see chapter 5).

Electrophysiological mechanisms were tested in the KI mice to identify potential deficiencies associated with learning and memory. Field recordings in hippocampal slices revealed no changes in basal synaptic transmission properties in KI compared to WT mice. LTP experiments were used as a cellular correlate to learning and memory. Hippocampal slices from KI mice showed a deficiency in fEPSP potentiation compared to WT slices using a number of LTP induction protocols (2-theta burst, 10 Hz, 100Hz stimulation) (Giese et al., 1998).

The LTP deficit in the KI slices suggested a potential hippocampal-dependent learning and memory deficit. Hippocampal-dependent special learning was assayed using the Morris water maze (MWM) behavioral task. During training, KI mice demonstrated a significantly higher escape latency to find a hidden platform. Additionally, during the probe trial WT mice spent significantly more time in the target

quadrant compared to the other three quadrants, whereas KI mice did not show preference for the target quadrant over any other quadrant. Accordingly, the WT mice had significantly more platform crosses than the KI mice. The MWM revealed a dramatic learning and memory deficit in the KI mice compared to the WT mice, consistent with an important physiological role for the electrophysiological deficits shown in these animals (Giese et al., 1998).

A number of other genetically modified mice altering the expression, activity, and/or subcellular localization of CaMKII have demonstrated the crucial role for normal CaMKII regulation and function for proper hippocampal learning and memory to occur. The changes in hippocampal PSD expression, electrophysiological properties, and behavioral phenotypes in these other CaMKII mutant mice are outlined in Table 1.

Summary

CaMKII functions as a serine/threonine kinase as well as a scaffolding protein that is able to coordinate the interaction of multiple proteins into larger signaling complexes, which CaMKII can regulate through its kinase activity. CaMKII is activated by increases in local intracellular Ca^{2+} levels and can act as a "molecular memory" switch, integrating subsequent Ca^{2+} signals to affect cellular changes leading to synaptic plasticity.

This research project aims to understand how CaMKII expression, phosphorylation, and subcellular localization are altered due to genetic and environmental perturbations during early postnatal development. Using mouse models of a neurodevelopmental disorder, an environmental stressor, and a CaMKIIα mutation, I

will show that alterations in normal CaMKII regulation that occur prior to adolescence can drastically affect biochemical, electrophysiological, and behavioral measures related to learning and memory. I will attempt to identify molecular mechanisms that lead to dysfunction to gain a better understanding of how signaling pathways involved in molecular memory develop. This may shed light on potential therapeutic targets that themselves can be manipulated, during these early postnatal time points, to rescue or prevent learning and memory deficits from occurring later in life.

Table 1

CaMKII Mutant Mice	Localization within PSD		Electrophysiological Properties			Behavior	References
	α	β	LTP	LTD	Basal Properties		
CaMKIIα-KO	-	↑	Reduced	?	-Normal synaptic transmission -Reduced PPF	-MWM deficit -Fear Condition deficit -Increased activity (open-field; Y-maze)	Silva et al., 1992a Silva et al., 1992b Elgersma et al., 2002
CaMKIIα-T286A	↓	↓	Reduced	?	-Normal synaptic transmission	-MWM deficit	Giese et al., 1998 Gustin et al., unpublished
CaMKIIα-T286D (Tg)	?	?	Normal	Increased	-Normal synaptic transmission -Normal PPF	-Barnes maze deficiency	Mayford et al., 1995 Bach et al., 1995
CaMKIIα-T305D	↓	-	Reduced	Increased (potentiates at 10 Hz)	-Normal synaptic transmission	-MWM deficit -Context fear deficit	Elgersma et al., 2002
CaMKIIα-TT305/306VA	-	↑	Enhanced (decreased threshold)	-No change at low frequency -Enhanced (10 Hz)	-Normal synaptic transmission	-Reversal learning MWM deficit -Discrimination deficit (fear conditioning)	Elgersma et al., 2002
CaMKIIα-Δ-3' UTR	↓	-	Normal Early-LTP Reduced Late-LTP	?	-Normal synaptic transmission -Normal PPF	-MWM deficit -Fear conditioning deficit (context/cue 24 hr) -Novel object deficit (24 hr)	Miller et al., 2002
CaMKIIα-F89G (Tg)	?	?	Increased (potentiates at 10 Hz)	Increased	-Normal synaptic transmission -Normal PPF	-Novel object deficit -Fear conditioning deficit (context/cue)	Wang et al., 2003
CaMKIIα-Δ-CA3	?	?	?	?	-Normal synaptic transmission -Normal PPF -Increased frequency facilitation	?	Hinds et al., 2003

Table Legend: - (no change), ↑ (increase), ↓ (decrease), **?** (unknown), **MWM** (Morris water maze), **PPF** (paired-plus facilitation)

CHAPTER II

METHODS

Mice/Breeding

1) Angelman Syndrome mouse model: All mice were maintained on C57/SV-129 mixed background. WT males (*Ube3a* M+/P+) were bred with AS females (*Ube3a* M-/P+) to generate WT and AS littermates. PCR analysis (described previously by Jiang et al., 1998) was performed on ear punches to genotype the offspring and confirmed by western blot analysis of E6-AP. Male and female mice were used in this analysis.

2) Early-life stress model: All mice were generated by C57BL/6J breeding pairs. Prior to beginning the stress experiments, females had to successfully rear two litters of pups to weaning age (P21). Dams pregnant with their third litters (E17-E19), were moved into standard cages and were housed individually. After the pups reached P2, the litter was culled to five pups (selecting for males). The Dam and her five remaining pups were placed in a mouse cage with a wire mesh floor (McMaster-Carr cat. #9656T112, fabricated in the Vanderbilt machine shop). The wire mesh floor was elevated ~ 2-2.5 cm off the bottom of the cage. The bottom of the cage contained 10% of the normal corncob bedding as a standard cage (~ 60 ml). Additionally, a 2.5 cm x 5 cm nesting square was placed in the cage with the dam and her pups. The control mice were moved and the litters culled as described for the ES mice; however, they were always kept in a standard mouse cage. Additionally, the control dams were given a 5 cm x 5 cm nesting square

when moved at P2. All experiments described were done at adolescent (P24-P28) and adult (~P90) time points.

3) CaMKIIα-Thr286Ala KI mice were maintained on a C57BL/6J background. Breeding pairs consisted of heterozygous males and females that generated WT, HET, and KI mice in a 1:2:1 ratio. PCR analysis (described previously by Giese et al., 1998) was performed on ear punches to genotype the offspring. Animal genotypes were confirmed using western blot analysis of CaMKIIα-Thr286 phosphorylation.

Western Blot Analysis

Protein gel samples were heated at 60°C for 10 minutes and fractionated by SDS-polyacrylamide gel electrophoresis (PAGE). Proteins were transferred in 10mM N-cyclohexyl-3-amino propanesulfonic acid (CAPS) with 10% methanol buffer onto nitrocellulose membranes. Membranes were stained with 0.2% Ponceau-S and digitally scanned in order to compare total protein levels in each lane by densitometric scanning of the 45-116 kDa molecular weight range using ImageJ (NIH). Membranes were then blocked in 5% milk in Tris-Buffered Solution with Tween-20 (TTBS) at 4°C overnight. Membranes were then incubated with primary antibody in 5% milk in TTBS overnight at 4°C. Membranes were washed 4 x 10 minutes in TTBS, incubated with secondary antibody in 5% milk in TTBS for 1 hour and 30 minutes, washed 4 x 10 minutes in TTBS, and developed using Western Lighting Enhanced Luminol Reagent-Plus (Plus-ECL). X-ray films exposed in a linear range were quantified using ImageJ for densitometric analysis as described previously (Brown et al., 2005). Western blot signals were then normalized for variations in total protein loading in the corresponding lane, as

quantified from Ponceau-S stained membranes, thereby avoiding potential problems associated with quantifying a single protein for use as a loading control. All phosphoproteins were normalized to the total amount of the respective protein detected unless otherwise stated.

Immunohistochemisty

Mice were deeply anesthetized and transcardially perfused with 10 ml ice-cold 1M phosphate buffered saline (PBS; pH 7.3) followed by 20 ml ice-cold 4% paraformaldehyde (PFA) in PBS. The brain was carefully removed and post-fixed overnight in 4% PFA at 4°C. The brain was placed in a 50 ml conical tube containing 15% sucrose in PBS for 8-10 hours at 4°C (until the brain sinks), and then moved to a 50 ml conical tube containing 30% sucrose in PBS overnight at 4°C. The brain was then mounted on a cryostat, frozen with cryospray, and 40 μM coronal slices were collected. The slices were placed into 24-well plates containing cryopretectant (300 ml ethylene glycol, 300 ml glycerol, 0.2 M phosphate buffer, and 300 ml H_2O) and stored at 4°C. Slices were washed 3 x 10 minutes in 0.01 M PBS. Slices were then placed in 0.6% hydrogen peroxide in 0.01 M PBS for 30 minutes, then the solution was changed and incubated for an additional 10 minutes. The slices were then washed 3 x 10 minutes in 0.01 M PBS and blocked for 1 hour in 5% normal goat serum (NGS) in 0.2% Triton X-100 in PBS. The slices were then incubated for 2 days in primary antibody at 4°C. Primary antibodies were diluted in the blocking solution, the antibody used was the mouse anti-E6-AP (1:5000; Sigma-Aldrich clone 330). The slices were then washed 3 x 10 minutes in 0.01 M PBS, and incubated for 90 minutes with an anti-mouse secondary

antibody at 1:1000 in blocking solution. Immunohistochemical detection was performed using the Vector Labs 3,3'-diaminobenzidine (DAB) peroxidase substrate kit (SK-4100). The slices were first washed 3 x 10 in 0.01 M PBS and incubated with the Vecotor Labs ABC solution for 1 hour, washed 2 x 5 minutes in 0.01 M PBS, and 3 x 10 minutes in 0.01 M PBS. The DAB was added and allowed to develop for 5 minutes. The development was stopped by addition of 100 μM sodium azide in H_2O. The slices were then washed 2 x 1 minute in 0.01 M PBS and mounted onto coverslips with aquamount.

Tissue homogenization

For total tissue homogenates that were not subsequently fractionated, tissue was homogenized in Kontes glass or Wheaton Teflon tissue grinders in a 2% sodium dodecyl sulfate (SDS) buffer containing 10μg/ml leupeptin and 1 μg/ml pepstatin. A bicinchoninic acid (BCA) protein concentration assay was run on the homogenates, which were then diluted to a final concentration of 0.7-1 mg/ml.

Subcellular fractionation

Tissue was homogenized in homogenization buffer (150 mM KCl, 50 mM Tris-HCl pH 7.5, mM DTT, 0.2 mM PMSF, 1 mM benzamidine, 1 μM pepstatin, 10 μg/ml leupeptin, and 1 μM microcystin-LR) using Wheaton Teflon or Kontes glass tissue grinders at 4°C. Total homogenate was rocked for 30 minutes at 4°C and spun down at 100,000 x g for 1 hour (or 10,000 x g for 10 minutes) yielding an $S1_H$ or ($S1_L$) fraction (soluble cytosolic protein pool) and a P1 pellet (insoluble fraction). Visual comparison of the $S1_H$ and $S1_L$ fractions revealed no difference in protein distribution between fractions,

as well as no change in the fractionation of our proteins of interest. Unless otherwise noted S1 will refer to the low speed (10,000 x g) spin. P1 was resuspended in homogenization buffer containing 1% (v/v) Triton X-100 using a Kontes, rounded tip cone pestle and rocked for 30 minutes at 4°C. The homogenate was then spun down at 10,000 x g for 10 minutes at 4°C yielding an S2 fraction (membrane-associated protein pool) and a P2 pellet (Triton insoluble fraction). The P2 was sonicated at 4°C in homogenization buffer containing 1% (v/v) Triton X-100 and 1% (W/V) sodium deoxycholate and rocked for 30 minutes at 4°C. The homogenate was spun down at 10,000 x g for 10 minutes at 4°C yielding an S3 fraction (PSD-associated fraction) and a P3 pellet (Triton/Deoxycholate-insoluble fraction) (Figures 1 and 2). In some cases, noted in text, after resuspending P2 the homogenate was not spun down so that S3 and P3 were pooled together.

Immunoprecipitation

Homogenates from each fraction were precleared by rocking for 30 minutes at 4ºC in microcentrifuge tubes with a 1:1 slurry of gammabind-G Sepharose beads (Amersham Biosciences) resuspended in IP buffer (150 mM NaCl, 50 mM Tris, and 0.1% Triton in H_2O). After preclearing, the G-Sepharose beads were pelleted by centrifugation and the precleared homogenate was moved into clean microcentrifuge tubes. 2 μg of goat-CaMKII antibody was added to the precleared homogenate and rocked for 1 hour at 4ºC. Gammabind-G-Sepharose was then added to the microfuge tubes and rocked overnight at 4ºC. The goat polyclonal CaMKII antibody was purified off of a CaMKIIα affinity purification column, and it is important to note that this

Figure 1

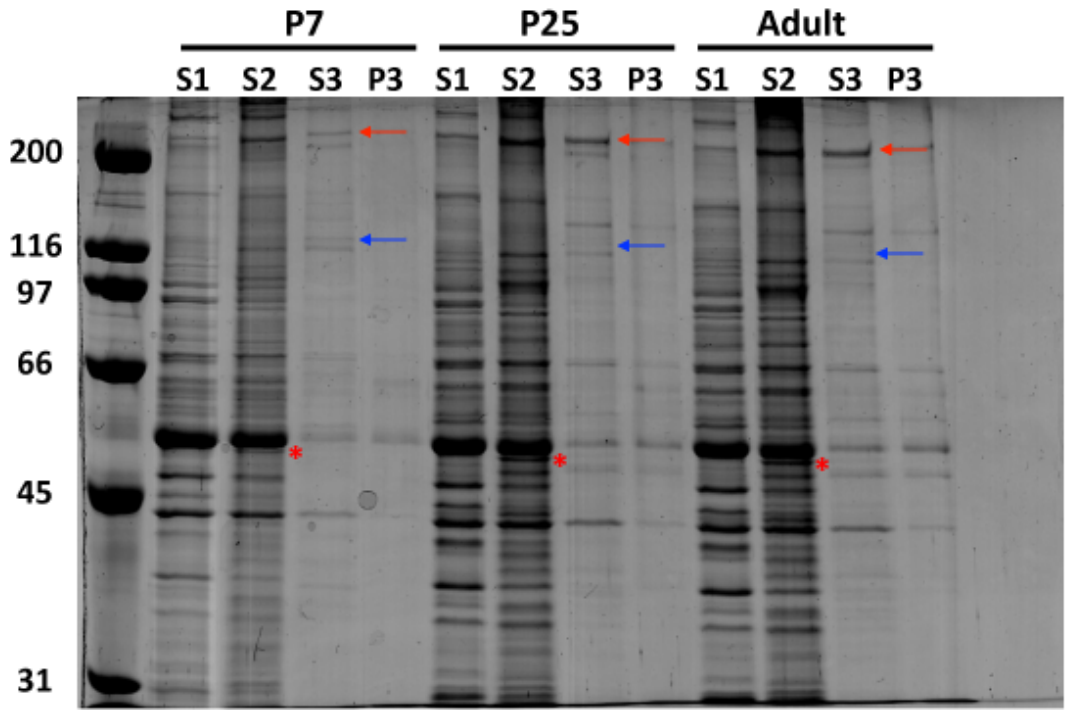

Figure 1. A total protein coomassie stain of the subcellular fractionations (S1, S2, S3, P3) from the hippocampus of WT mice at P7, P25, and P90 loaded by equal volume. Across the developmental timeline there are proteins that increase in expression (Red arrows) as well as proteins that decrease in expression (Blue arrows). The red asterisk is positioned next to CaMKIIα, which can be readily seen in the S2 fraction. Importantly, the S2 (membrane-associated) fractions consists of roughly 60-70% of the total fractionated protein, S1 (cytosolic) fractions contains 25-35% of the total fractionated protein, and the S3/P3 (PSD-associated) fractions consist of <10% of the total fractionated protein. Throughout this dissertation the fractions are loaded by equal volume and western blot analysis uses the total protein stain, Ponceau-S, to normalize for the loading differences.

Figure 2

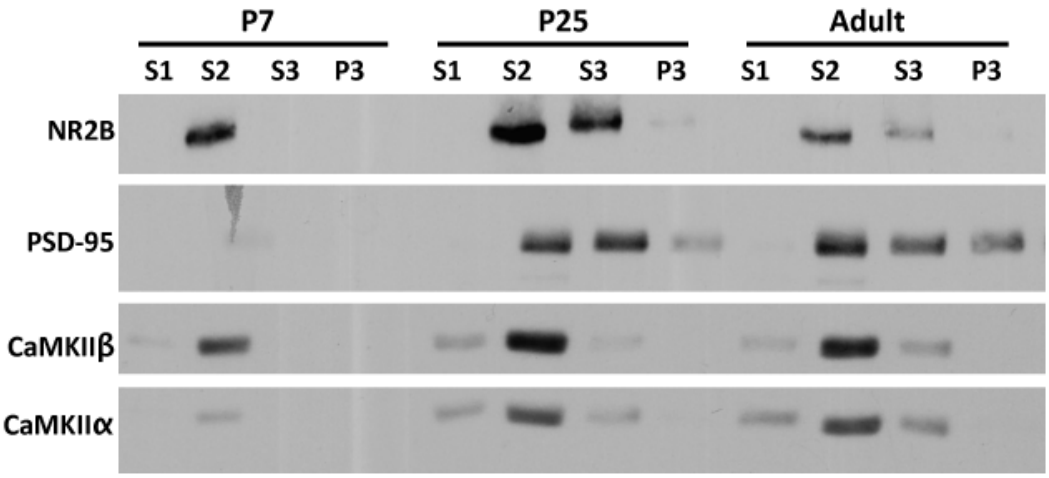

Figure 2. Western blot analysis of hippocampal fractionation of WT mice at P7, P25, and P90. CaMKII and NR2B are exclusively detected in the S2 fraction at P7, but partially translocate to the S3 and P3 fractions at P25 and P90, paralleling the upregulation of PSD-95 expression. These blots were loaded by equal volume so the PSD-95 is enriched in the S3 and P3 fractions due to the fact that there is 9-10-fold more total protein loaded in the S2 versus S3 and P3 (as in Figure 1).

Figure 3

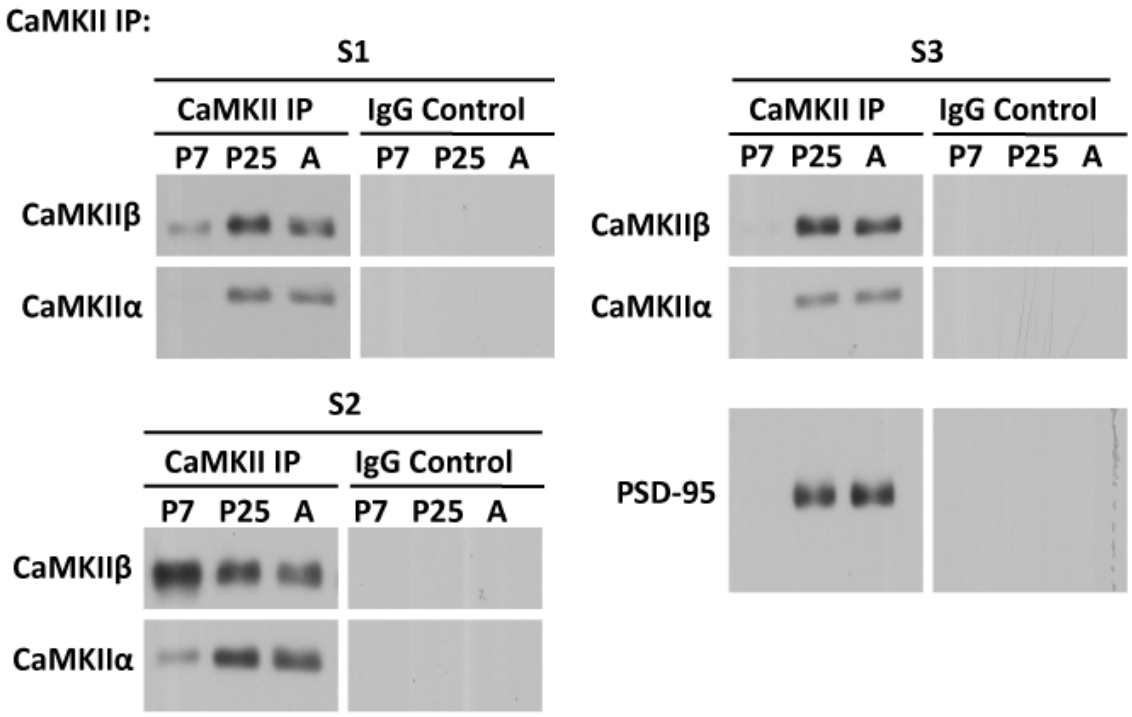

Figure 3. CaMKII immunoprecipitations in S1, S2, and S3 fractions from hippocampus of P7, P25, and P90 mice. CaMKIIβ is readily immunoprecipitated in the S1 and S2 fractions from all ages. CaMKIIα can be immunoprecipitated in the S2 fraction from P7 mice, however the levels of CaMKIIα are significantly lower than that immunoprecipitated from P25 and P90 mice in this same fraction. Both CaMKIIα and CaMKIIβ are immunoprecipitated in the S3 (PSD-associated) fraction from P25 and P90 mice, however no kinase is detected in the S3 fraction from the P7 mice. Co-immunoprecipitation of PSD-95 from the S3 fraction can be detected in both P25 and P90 mice. The IgG controls demonstrate the specificity for the immunoprecipitations, with no CaMKII detected in any fraction, as well as no PSD-95 coming down non-specifically with the IgG control.

Figure 4

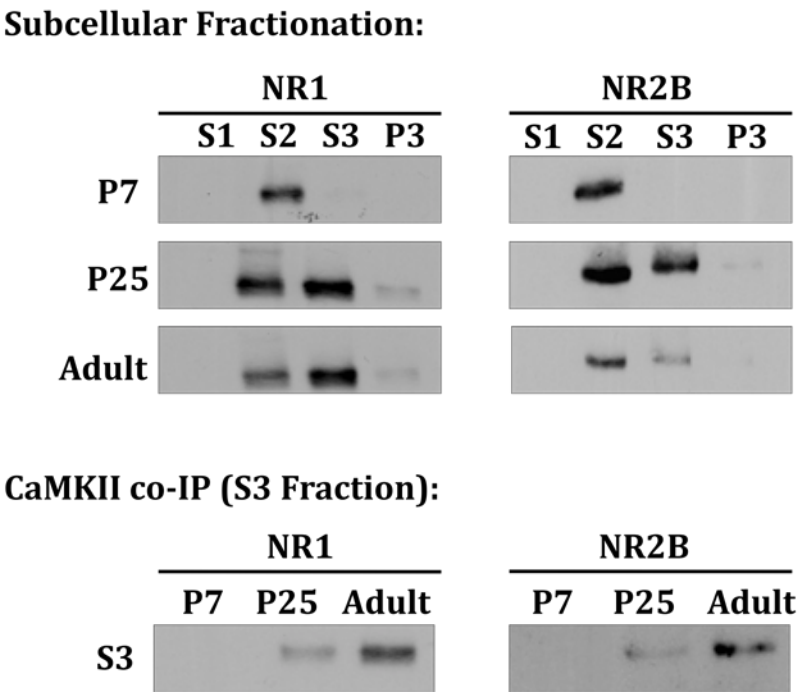

Figure 4. NMDAR subunit fractionation and co-IP with CaMKII throughout development from hippocampus of P7, P25 and P90 mice. Expression of both NR1 and NR2B increases from P7 to P25, when expression is detected in the PSD-associated fractions (S3 and P3). NR1 expression stays consistent into adulthood whereas NR2B expression decrease from P25 to P90 (top panel). The co-immunoprecipitation of NR1 and NR2B with CaMKII (bottom panel) increases with age. The co-immunoprecipitation is first detected at P25 and is increased at P90.

antibody is able to readily detect both CaMKIIα and CaMKIIβ isoforms of the kinase. Control samples were incubated with goat IgG. The samples were pelleted and the supernatant was removed as a depleted input (supernatant from CaMKII IP) or input (supernatant from goat IgG). The beads were washed 3 x 5 minutes in 500 μl of IP buffer and eluted with 2 x SDS loading dye (Figures 3 and 4). Due to the vast differences in expression and subcellular localization of the CaMKII isoforms seen via western blot analysis, I normalized the IPs to: 1) levels of CaMKIIα, 2) levels of CaMKIIβ, and 3) equal loading volume. Additionally, all phospho-proteins were normalized to the respective total protein present in the IPs.

Antibodies

Primary antibodies used for immunoprecipitation and immunoblotting: **CaMKII:** Goat anti-CaMKIIα/β (McNeill and Colbran, 1995), mouse anti-CaMKIIα (ABR), mouse anti-CaMKIIβ (Zymed), mouse anti-phospho-Thr286-CaMKIIα (ABR), rabbit anti-phospho-Thr286-CaMKIIα (Promega), and rabbit anti-phospho-Thr305/306-CaMKIIα (BIOMOL). **NMDAR:** mouse anti-NR1 (BD Pharmingen), mouse anti-NR2B (Transduction Laboratories), rabbit anti-phospho-Ser1303-NR2B (Upstate), and rabbit anti-NR2A (Millipore). **AMPAR:** rabbit anti-GluR1 (Abcam) and rabbit anti-phospho-Ser831-GluR1 (PhosphoSolutions). **Other:** mouse anti-PSD-95 (NeuroMab), mouse anti-E6-AP (Sigma-Aldrich), rabbit anti-E6-AP (Bethyl Labs), mouse anti-GAPDH (Chemicon), mouse anti-synapsin-1 (Santa Cruz), mouse anti-IP3R (NeuroMab), mouse anti-βactin (Santa Cruz), and rabbit anti-AKAP150 (Upstate). Secondary antibodies: All

secondary antibodies used were preabsorbed antibodies from Santa Cruz: Donkey anti-goat, donkey anti-rabbit, donkey anti-mouse, and goat anti-mouse IgG_1.

Behavioral paradigms

Rotarod: Mice were placed on an accelerating rotarod at 4 rpm. Over 5 minutes the rotarod accelerated from 4-40 rpm and the latency to fall was recorded. If the mouse made three consecutive rotations around the rotarod it was recorded as a fall. An individual mouse underwent two trials per day for 5 consecutive days. Each trial was separated by 1 hour. In some instances mice were run for an additional two trials on day 10.

Fear conditioning: Mice were placed in the conditioning chamber under white light and white noise for 2 minutes. At the end of the 2 minutes, the conditioned stimulus (85 dB tone) was administered for 30 seconds. An unconditioned stimulus (0.5 mA, 2 second foot shock) was given at the end of the conditioned stimulus. An additional tone-shock pairing was given 2 minutes following the first pairing. The mice were kept in the chamber for 2 minutes following the training and then placed back in their home cages.

To test context-dependent fear memory, mice were placed back into the conditioned chamber and the amount of freezing was recorded over a 3 minute testing period. Contextual fear was tested 24 hours and 7 days post training.

Cue-dependent fear memory was tested in a novel context (Plexiglas inserts covered the inside of the conditioned chamber and vanilla extract was used as a different odor cue) 24 hours or 7 days post training. Each mouse was placed in the novel context and allowed to explore for 3 minutes. At the end of the three minutes the conditioned cue (85 dB tone) was administered for 3 minutes and the amount of freezing was assayed.

Y-maze: The y-maze was conducted between 10:00 am and 1:00 pm under normal lighting conditions (250-300 lux). For adolescent mice visual cues, construction paper with different patterns, were placed at the end of each arm as well as under each individual arm of the maze. The percentage of spontaneous alternations (the number of times a mouse entered all three arms consecutively without revisiting an arm over the total possible alternations) and the number of total arm entries were manually recorded in a 6-minute test visualized via ANY-maze software (Stoelting) (Figure 5).

Novel object: At weaning (P21), the familiar object (PVC pipe) was placed in the home cage with the weanlings. The mice were housed with the objects until testing at P25-P26. The novel object paradigm was conducted between 10:00 am and 1:00 pm under normal lighting conditions (250-300 lux). 18-24 hours prior to testing the mice were allowed to explore the novel object chamber (empty standard mouse cage) for 20 minutes. On the testing day the mice were placed in the novel object chamber with 2 familiar objects and allowed to explore for 5 minutes. The mice were then placed back into the home cage for 3 minutes. During this time one of the familiar objects in the chamber was replaced with a novel object (50 ml conical tube filled with sand). The mice were placed back in the chamber and allowed to explore for an additional 5 minutes. The amount of time the mouse spent exploring the novel object versus the familiar object was recorded by post-hoc analysis of video collected via ANY-maze software (Stoelting) (Figure 5).

Elevated-plus maze (EPM): The EPM was conducted between 10:00 am and 1:00 pm under normal lighting conditions (250-300 lux). Mice were placed on an open-arm facing the center of the maze. The mouse was allowed to explore the maze for 5

Figure 5

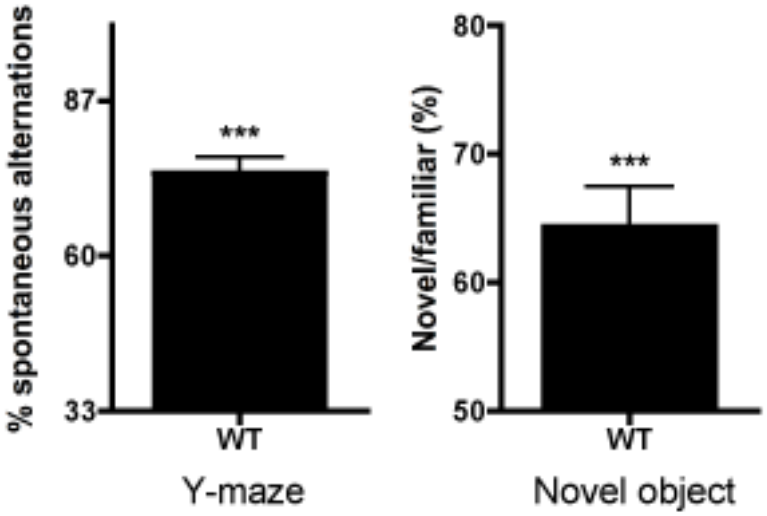

Figure 5. Memory behavioral tasks in adolescent (P24-P26) mice. Due to the limited literature on the success of learning and memory behaviors in adolescent rodents it was first necessary to establish that adolescent mice could perform the tasks. Left panel: WT mice (P24-P25) showed 74% spontaneous alternations in the Y-maze and this was statistically significant over chance (33.3% spontaneous alternations) ($p<0.0001$). Right panel: WT mice showed preference for the novel object over that of the familiar object, spending 64% of the time with the novel object in the novel object recognition task. This was statistically significant from chance (50%) ($p=0.0020$). (N: Y-maze=17; Novel object=9)

minutes. The amount of time spent in the open-arms versus the closed-arms was recorded, along with total arm entries. For control versus stress mice the paradigm was conducted under red light conditions.

Kinase Activity Assay

Hippocampi from WT and AS mice were homogenized in 400 μl of a homogenization buffer (1 M Tris-HCl pH 7.5, 0.5 M EDTA, 0.2 M EGTA, 1 M sucrose, 0.5 M benzamidine, 5 mg/ml aprotinin, 5 mg/ml leupeptin, 1 mM pepstatin, 500 μM NaF, 0.5 M β-glycerophosphate, 200 μM Na pyrophosphate, 500 μM microcystin-LR). 2 μl of homogenate was added to 500 μl of a dilution buffer (50 mM HEPES pH 7.5, 10% (v/v) ethylene glycol, 2 mg/ml bovine serum albumin), 5 μl of sample was then added to 20 μl of ice-cold assay buffer (50 mM HEPES pH 7.5, 10 mM $Mg(Ac)_2$, 0.5 nM $CaCl_2$, 1 mM EGTA, 1 μM CaM, 1 mg/ml BSA, 1 mM DTT, 0.4 mM [γ-^{32}P] ATP, and 10 μM autocamtide). Ca^{2+}/CaM-dependent activity was assayed in buffer without EGTA and Ca^{2+}/CaM-independent activity was assayed in buffer without $CaCl_2$ and CaM. The sample was vortexed and placed at 30°C for 10 minutes. 15 μl of sample was spotted on Whatman phosphocellulose P81 paper squares to stop the reaction. Papers were washed 5 x 15 minutes, rinsed 2 x in 95% EtOH, and dried. The papers were then placed into scintillation vials containing 10 ml of non-aqueous scintillation fluid and counted in the scintillation counter for 2 minutes.

Phosphatase Activity Assay

Hippocampi from WT and AS mice were homogenized as in the kinase assay

(described above). Samples were diluted with or without phosphatase inhibitors (0 inhibitor, 2.5 nM okadaic acid, or 2.5 μM okadaic acid) and incubated on ice for 10 minutes. Samples were then diluted into assay buffer (50 mM Tris-HCl, pH 7.5, 0.1 M NaCl, 20 mM $Mg(Ac)_2$, 10 mg/ml BSA, 0.2 mM EGTA,1mM DTT, [^{32}P]-phosphorylase *a*, and 5mM caffeine) and incubated at 30°C for 30 minutes (Strack et al., 1997b). The assay was stopped with the addition of 40% (w/v) trichloroacetic acid, placed on ice for 10 minutes, and spun down at 10,000 x g for 10 minutes at 4°C. Liquid scintillation counting was used to quantify the ^{32}P-release. [^{32}P]-phosphorylase *a* is a substrate for both PP1 and PP2A (Cohen, 1989). The amount of PP2A activity was determined by the amount of activity inhibited by 2.5 nM okadaic acid. The amount of PP1 activity was determined by the difference in inhibition by 2.5 nM and 2.5 μM of okadaic acid (Cohen, 1991).

Electrophysiology

Field-recordings: Coronal hippocampal slices (300 μm) were cut on a vibratome from P25-P28 control and ES mice in ice-cold sucrose cutting solution (194 mM sucrose, 20 mM NaCl, 4.4 mM KCl, 2 mM $CaCl_2$, 1 mM $MgCl_2$, 1.2 mM NaH_2PO_4, 10 mM glucose, 26 mM $NaHCO_3$, and 1 mM kynurenic acid) bubbled with 95%/5% O_2/CO_2. After dissection, the slices were immediately transferred to an interface recording chamber where they were perfused with heated (30°C) ACSF (124 mM NaCl, 4.4 mM KCl, 2 mM $CaCl_2$, 1.2 mM $MgSO_4$, 1 mM NaH_2PO_4, 10 mM glucose, and 26 mM $NaHCO_3$) that was bubbled with 95%/5% O_2/CO_2. Following a 1-hour recovery period, a stimulating electrode was placed in the Schaffer collaterals with the recoding electrode

placed in the CA1 region of the hippocampus (Chapter 1: Figure 1). An input/output curve was generated to find the maximum fEPSP response. The stimulus intensity that generated the half-maximal slope of the fEPSP was used for LTP experiments. After 20 minutes of stable baseline responses were acquired, a single 100 Hz train was delivered and subsequent responses were recorded for 60 minutes.

Whole-cell patch recordings: These experiments were conducted in collaboration with Dr. Brian Shonesy (postdoctoral researcher in Dr. Roger Colbran's laboratory). Coronal hippocampal slices (300 μm) were generated as previously described. Following a 1-hour recovery period slices were transferred to a submerged recording chamber, and continuously perfused at a rate of 2 ml/min with ACSF bubbled with 95%/5% O_2/CO_2 (28°C). Recording electrodes (3–6 MΩ) were filled with a pipette solution (120 mM Cs-gluconate, 17.5 mM CsCl, 10 mM NaCl, 2 mM $MgCl_2$, 0.2 mM EGTA, 10 mM NaHEPES, 2 mM MgATP, 0.2 mM NaGTP, 1 mM QX-31). The amplitude and frequency of spontaneous EPSCs were recorded. AMPAR mediated responses were generated by holding the membrane potential at -70mV and then the duel AMPAR-NMDAR mediated responses were recoded at +40mV. For AMPAR/NMDAR ratios the duel component responses were subtracted from the AMPAR mediated responses and then expressed as a ratio.

Statistics

Statistical comparisons were made by one-sample *t*-test, unpaired Student *t*-test, one-way ANOVA, or two-way ANOVA followed by Tukey's or Bonforroni post-tests, as appropriate.

CHAPTER III

ANGELMAN SYNDROME

Introduction

Angelman Syndrome (AS) is a neurodevelopmental disorder first described in 1965 by the English physician Dr. Harry Angelman (Angleman, 1965). Over the course of several years Dr. Angelman encountered three young patients, all diagnosed with a different form of mental retardation. The commonalities these patients shared, a distinct gait, lack of speech, and the severity of their mental retardation, led Dr. Angleman to document the new disorder as "Puppet Syndrome," which has since been changed to Angleman Syndrome in dedication to Dr. Angelman.

AS is characterized by a severe mental retardation, movement and balance disorder, language deficiencies, and epilepsy (Laan et al., 1999; Williams et al., 2006). The disorder is caused by the loss of functional E6-Associated Protein (E6-AP), an E3-ubiquitin ligase that is encoded by the *UBE3A* gene. *UBE3A* is a maternally imprinted gene found on chromosome 15q11-13 (Knoll et al., 1989; Kishino et al., 1997; Matsuura et al., 1997; Sutcliffe et al., 1997). 80% of AS cases are due to a large chromosomal deletion on a region of the maternal chromosome encompassing *UBE3A* (Figure 1). Less common causes of AS are *UBE3A* mutations, uniparental paternal disomy (UPD), and imprinting center mutations (Figure 1). Additionally, there are AS patients where the cause has not been determined. Although the genetic cause of AS has been discovered and several E6-AP substrates have been characterized, none of them have been linked to

the pathogenesis of AS (Huibregtse et al., 1991; Kuhne and Banks, 1998; Nuber et al., 1998; Kumar et al., 1999; Reiter et al., 2006). Several mouse models of AS have been developed in attempts to better understand the genetic imprinting and molecular mechanisms underlying AS pathology (Albrecht et al., 1997; Cattanach et al., 1997; Jiang et al., 1998; Miura et al., 2002). These mouse models recapitulate several of the AS phenotypes including an increased seizure susceptibility, motor dysfunction, as well as hippocampal-dependent learning and memory deficits (Jiang et al., 1998; Miura et al., 2002; van Woerden et al., 2007).

The *UBE3A* expression pattern, seen by *in situ* hybridization, suggested maternal imprinting of *UBE3A* was exclusive to the hippocampus, the Purkinje cells of the cerebellum, and the olfactory bulbs, with biallelic expression of *UBE3A* in all other brain regions (Albrecht et al., 1997; Jiang et al., 1998). These initial studies describing *UBE3A* expression guided AS research towards focusing primarily on the hippocampus and cerebellum.

The loss of maternal *UBE3A* gene expression and subsequent E6-AP protein expression leads to several AS-like phenotypes in the mouse. Motor coordination assayed on the rotarod reveals a severe motor deficit in the AS mice (Jiang et al., 1998; Miura et al., 2002). Additionally, gait analysis shows that AS mice have a smaller step length than control mice (Jiang et al., 1998), suggesting that the altered gait is leads to the motor deficits in these mice.

AS mice also display severe hippocampal-dependent learning and memory deficits compared to WT controls. AS mice have an increased latency to find the platform in the Morris water maze task, as well as a decreased time exploring the target

Figure 1

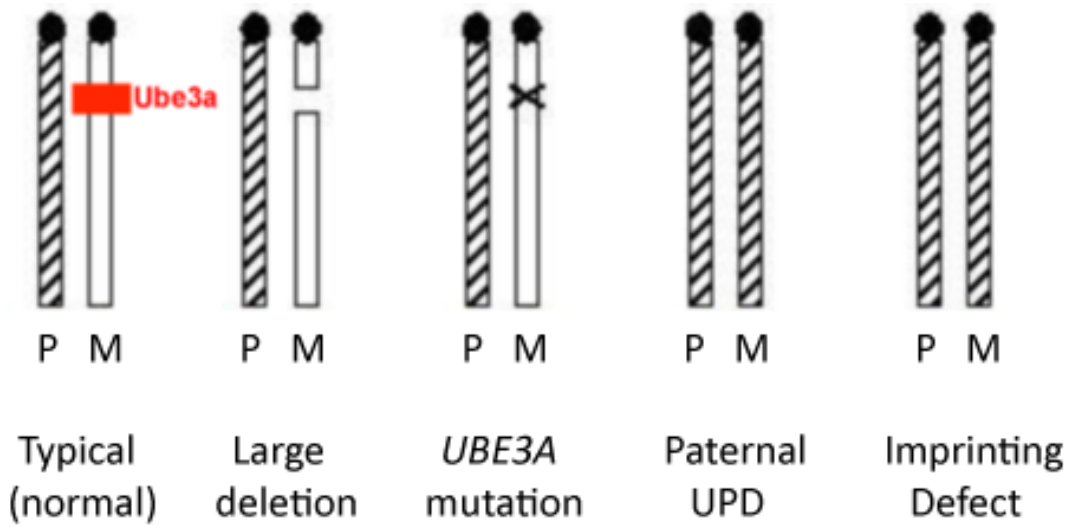

Adapted from Angelman Syndrome Foundation, Inc.

Figure 1. Genetic determinates of Angelman Syndrome. *UBE3A* is normally expressed from the maternal chromosome, 15q11-13. The most common cause of AS is a large chromosomal deletion of the maternal chromosome, occurring in 80% of AS patients. Less common causes of AS are UBE3A mutations, uniparental paternal disomy (UPD), and imprinting center mutations.

quadrant in the probe trial compared to WT mice (Miura et al., 2002). Additionally, AS mice exhibit a significant decrease in the amount of contextual freezing twenty-four hours after training compared to WT mice in a fear conditioning paradigm. There were no differences between the genotypes in the cued portion of the test, suggesting a specific hippocampal-dependent memory deficiency in the AS mice (Jiang et al., 1998). Thus, two separate murine hippocampal-dependent behavioral assays were able to recapitulate intellectual disabilities seen in human patients.

Along with the motor and memory deficits, AS mice show an increase in inducible audiogenic seizure susceptibility (Jiang et al., 1998). The seizure susceptibility in the AS mice is thought to be associated with the increased brain activity seen by EEG analysis in awake non-active animals (Miura et al., 2002). Again mimicking the human disorder by showing a seizure phenotype, one of the most debilitating symptoms of AS that patients and families struggle with day to day (Laan et al., 1999).

With mouse models of AS now available, research efforts turned to identifying the biochemical and physiological mechanisms underlying the phenotypes of AS. In agreement with the behavioral data, generation of LTP is significantly reduced in AS mice (Jiang et al., 1998; Weeber et al., 2003). The loss of LTP in the AS mice is thought to be due to misregulation of CaMKII. In the AS mice there is an increase in both Thr305/306 and Thr286 phosphorylation. This altered phosphorylation leads to a decrease in the total amount of CaMKII associated with the PSD (Weeber et al., 2003). Additionally, the misphosphorylation of CaMKII was linked to a decrease in PP1/PP2A activity in the AS mouse (Weeber et al., 2003).

CaMKII dysfunction in Angelman Syndrome

It has been shown that CaMKIIα phosphorylation at Thr286 and Thr305/306 is elevated in AS compared to WT mice, with no change in total CaMKIIα levels (Weeber et al., 2003). This misphosphorylation of CaMKIIα leads to a decrease of the kinase in PSD-enriched fractions (Weeber et al., 2003), which is thought to be involved in the molecular mechanisms leading to the LTP deficits and learning and memory deficiencies seen in the AS mice (Jiang et al., 1998; Miura et al., 2002; Weeber et al., 2003). We attempted to genetically alter CaMKIIα in attempts to reverse or prevent the AS phenotype from occurring (van Woerden et al., 2007).

Heterozygous CaMKIIα-Thr305Val/Thr306Ala mice (Elgersma et al., 2002) (Table 1) were crossed with AS mice to alter CaMKIIα phosphorylation, function, and location in double mutant AS/CaMKIIαTT305/306VA mice. CaMKIIα-Thr305Val/Thr306Ala mice have been shown to have an increase in total CaMKII in PSD-associated fractions, thought to be due to the decrease in phosphorylated residues 305 and 306. Interestingly the increase in total CaMKII at the PSD was due to an increase in CaMKIIβ, as CaMKIIα levels were not changed in the PSD fraction. Additionally, these mice display enhanced LTP, thought to be caused by a decreased threshold for initiating LTP. The CaMKIIα-Thr305Val/Thr306Ala mice do show memory deficiencies in reversal learning in the Morris water maze and a discrimination deficit in fear conditioning (Elgersma et al., 2002).

Since inhibitory phosphorylation of CaMKII can lead to learning and memory deficiencies (Elgersma et al., 2002; Elgersma et al., 2004), we hypothesized that crossing the AS mice, which have an increased phosphorylation of Thr305 and a decreased

CaMKII associated with the PSD, with heterozygous CaMKIIα-Thr305Val/Thr306Ala mice would decrease the amount of phosphorylation at Thr305/306 in the AS/CaMKII double mutant mice, potentially increasing the amount of CaMKII at the PSD, and prevent behavioral deficits seen in the AS mice (van Woerden et al., 2007).

Double mutant AS/CaMKII mice alter CaMKII phosphorylation and activity

AS mice have increased Thr305 phosphorylation, whereas heterozygous CaMKIIα-Thr305Val/Thr306Ala mice have a decreased Thr305 phosphorylation, compared to WT controls. When crossed, AS/CaMKII mice displayed a similar level of Thr305 phosphorylation as heterozygous CaMKIIα-Thr305Val/Thr306Ala mice, preventing the enhanced Thr305 phosporylation seen in the AS mice. Additionally, AS mice exhibit a 2-fold reduction in CaMKII kinase activity compared to WT controls, which is restored in the AS/CaMKII double mutants (van Woerden et al., 2007).

AS/CaMKII double mutants prevent behavioral deficits seen in AS mice

Mice were assayed for motor deficits using the rotarod. The AS mice displayed a significant rotarod deficiency compared to WT mice. AS/CaMKII double mutants performed equally well as the WT, thus the genetic cross prevents the motor coordination deficits seen in the AS mice. It must be noted that the heterozygous CaMKIIα-Thr305Val/Thr306Ala mice had a significant increase in latency to fall compared to WT mice (van Woerden et al., 2007), presenting the possibility that the AS/CaMKII double mutant did not necessarily prevent the rotarod deficit, but that the AS/CaMKII mice fall

in between the two genetic extremes in this case (i.e. the AS mice and the heterozygous CaMKIIα-Thr305Val/Thr306Ala mice).

One of the most debilitating aspects of AS is the seizure associated with the disorder. Audiogenic seizures were induced by vigorously scratching scissors against the metal grating of the mouse cage lid for twenty seconds or until the mouse begins to seize. Audiogenic seizures were unable to be induced in WT or heterozygous CaMKIIα-Thr305Val/Thr306Ala mice; however in 50% of the AS mice seizure was induced. The number of audiogenic seizures induced in the AS/CaMKII double mutants was reduced 75% from that seen in the AS mice (van Woerden et al., 2007).

The learning and memory deficit in the AS mouse models have been very well characterized (Jiang et al., 1998; Miura et al., 2002). Here we were able to recapitulate the memory deficits in the Morris water maze and fear conditioning paradigms. During the Morris water maze all genotypes were able to decrease their latency to find the hidden platform to the same extent. During the probe trials, both the WT and AS/CaMKII double mutant mice displayed a significantly higher number of platform crosses than the AS mice. Once again demonstrating how the AS/CaMKII double mutant was able to prevent behavioral deficits seen in the AS mice (van Woerden et al., 2007).

In addition to Morris water maze, we assessed hippocampal-dependent learning and memory using the contextual fear conditioning paradigm (Figure 2). In this assay mice were trained to associate a context (shock chamber) with a foot shock. When tested twenty-four hours post training the WT mice displayed roughly 75% freezing, indicating these mice were able to associate the context (shock chamber) with the shock. Consistent with data in the literature, AS mice spent a significantly less time freezing than WT mice

twenty-four hours after training, revealing the memory deficit (Jiang et al., 1998; Miura et al., 2002). The AS/CaMKII double mutant performed as WT mice, significantly better than AS mice. The heterozygous CaMKIIα-Thr305Val/Thr306Ala mice also displayed the same level of freezing as the WT mice; however, knowing that the homozygous CaMKIIα-Thr305Val/Thr306Ala mice have a discrimination deficit seen in the fear conditioning paradigm (Table I) (Elgersma et al., 2002), this may not be normal contextual learning. Similarly, when contextual fear memory was tested seven days post training the same results were obtained with WT, heterozygous CaMKIIα-Thr305Val/Thr306Ala, and AS/CaMKII double mutants freezing to the same extent and AS mice displaying significantly less freezing than that of the WT and AS/CaMKII double mutant mice (van Woerden et al., 2007).

Cued fear conditioning was also assayed to determine if other hippocampal-independent forms of memory may be altered in AS mice. Here mice were trained to associate a cue (tone) with a footshock. Twenty-four hours later the mice were placed into a novel environment, the tone was administered, and the amount of freezing was recorded (Figure 3). All genotypes displayed the same degree of freezing in response to the tone, suggesting that the fear conditioning deficit in the AS mice, that was prevented in the AS/CaMKII double mutant was hippocampal-dependent (van Woerden et al., 2007).

AS/CaMKII double mutant mice prevent the LTP deficits seen in AS mice

Electrophysiological experiments were performed to determine the effects of the AS/CaMKII double mutant mice on the LTP deficit seen in AS mice. A high-frequency

Figure 2

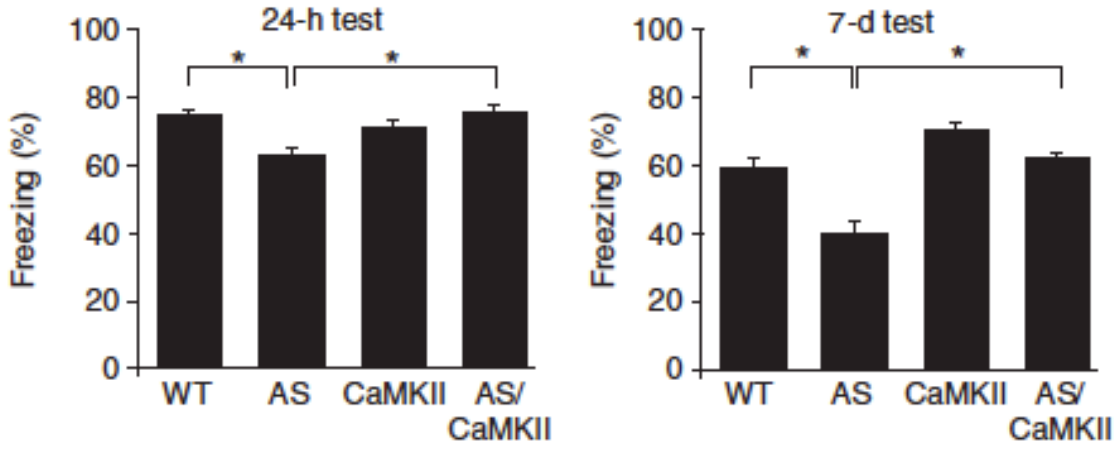

Figure 2. Contextual fear conditioning. We trained mice to associate a context (shock chamber) with a footshock. Hippocampal-dependent memory was assayed by recording the amount of freezing when placed back into the context 24-hr (left panel) or 7-days (right panel) post training. AS mice displayed a significant decrease in the amount of freezing compared to WT and AS/CaMKII double mutants at both time points (van Woerden et al., 2007).

Figure 3

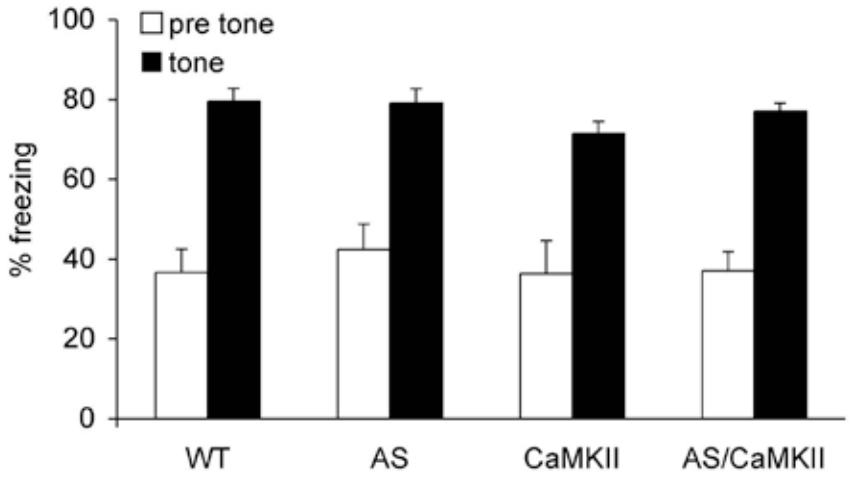

Figure 3. Cued fear conditioning. We trained mice to associate a cue (tone) with a footshock. Hippocampal-independent memory was assayed by the amount of freezing when mice were placed into a novel environment and exposed to the cue. All mice froze to the same extent when tested 24-hrs post training.

100 Hz stimulation was used to induce LTP in hippocampal slices. HFS was able to potentiate fEPSPs in WT slices; however; LTP was not induced in AS slices. This LTP deficit was prevented in the AS/CaMKII double mutant, as HFS was able to induce LTP to similar levels of potentiation as seen in WT slice (van Woerden et al., 2007).

Molecular mechanisms underlying the learning and memory deficits in AS

The discovery of *UBE3A* as the gene responsible for causing AS led to the hunt for the target of E6-AP that was elevated in AS due to the decreased expression of the ubiquitin ligase. To date no such target has been discovered and it is possible that E6-AP functions to alter gene expression at the transcriptional level (Ramamoorthy and Nawaz, 2008). In 2003 a new approach was taken to understand the molecular mechanism underlying AS pathology. Using the current knowledge of normal molecular mechanisms of LTP generation and hippocampal-dependent learning and memory, the laboratory of Dave Sweatt discovered CaMKII had altered phosphorylation and subcellular distribution in AS mice (Weeber et al., 2003). They also showed that PP1/PP2A activity was decreased in these animals, which the authors suggested was the reason for increased CaMKII phosphorylation. The mechanism linking loss of E6-AP expression and/or function to the misregulation of CaMKII has yet to be defined.

Establish baseline behavioral phenotype in an AS mouse model

The goal of my initial project was to uncover the molecular mechanism of how loss of E6-AP leads to the misregulation of CaMKII. I first attempted to reconfirm the behavioral and biochemical data that suggests a role for CaMKII in AS pathology.

To confirm our AS mouse line displayed behavioral deficits characteristic of AS, I used the rotarod to assay for motor coordination and learning deficits that had been previously documented (Jiang et al., 1998; Miura et al., 2002; Weeber et al., 2003; van Woerden et al., 2007). With increasing trials, WT mice were able to display motor learning by an increased latency to fall over the 4 days of testing (Figure 4), which was significantly higher than AS mice (Two-way ANOVA: $F=42.95$, $p<0.0001$). The AS mice were never able to master the rotarod as their latency to fall remained consistent from day 1 to day 4 of training (Figure 4), consistent with the motor coordination and learning deficits reported in these mice.

Expression of CaMKII in AS mice

Previous evaluation of total hippocampal homogenates from WT and AS revealed no change in total levels of several proteins, including CaMKIIα, known to be involved in LTP and learning and memory (Weeber et al., 2003). Closer inspection of CaMKIIα did show that there was a 60% increase in phospho-Thr286 CaMKIIα levels and a 33% increase in phospho-Thr305/306 CaMKIIα levels in total hippocampal homogenates in AS compared to WT animals (Weeber et al., 2003). Moreover, this misphosphorylation altered the subcellular localization of the kinase, causing a 50% reduction in PSD-associated CaMKIIα in the AS mice. Interestingly, the PSD-associated CaMKIIα in the AS mice displayed 2.5-fold higher levels of phospho-Thr286 levels with no change in phospho-Thr305/306 levels (Weeber et al., 2003). This is counterintuitive due to the large literature demonstrating CaMKIIα phosphorylated at Thr286 has increased affinity for PSDs (Strack et al., 1997a; Strack and Colbran, 1998; Dosemeci et al., 2001).

Figure 4

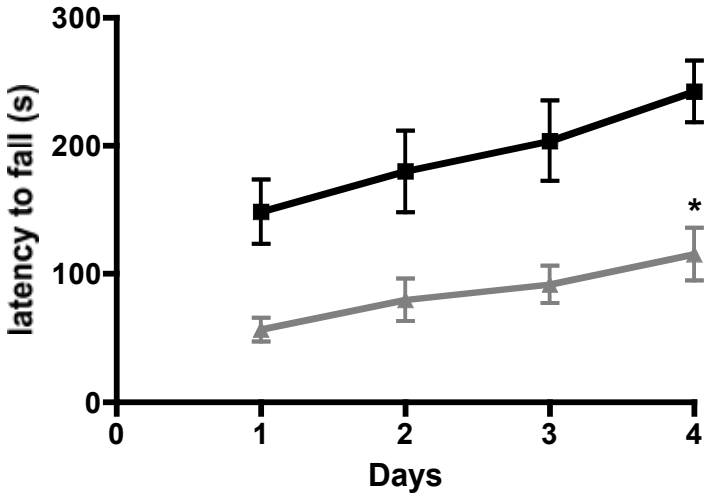

Figure 4. Rotarod analysis of WT and AS mice. Over 4 days of training (2-trails/day) WT mice displayed motor memory with an increase in their latency to fall from day 1 to day 4. AS mice were never able to master the apparatus and had a significant decrease in latency to fall compared to WT animals. (WT= 6 AS= 6; Two-way ANOVA: $F=42.95$, $p<0.0001$)

Figure 5

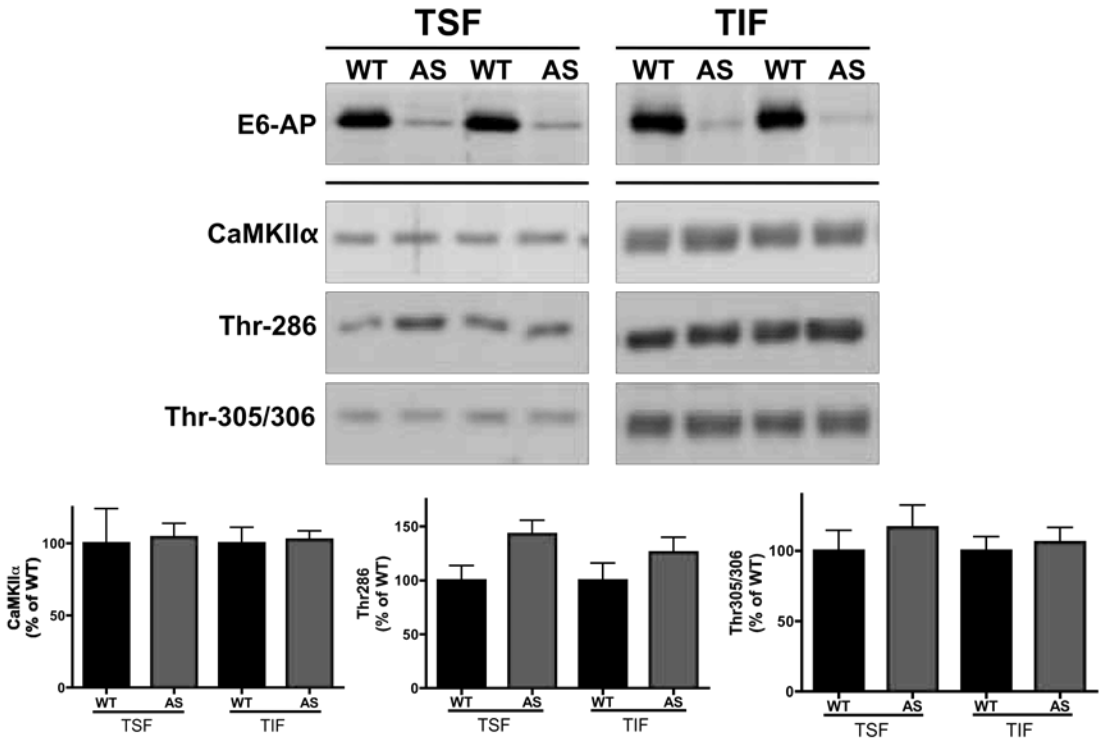

Figure 5. Western blot analysis comparing hippocampal homogenates from WT and AS mice confirmed the genotypes with ~90-95% reduction in E6-AP levels in both the TSF and TIF. There was no change CaMKIIα subcellular localization, nor was there a change in CaMKIIα phosphorylation (Thr286 or Thr305/306) in AS compared to WT mice**.** Quantification below western blots; total CaMKIIα (left panel), Thr286 (middle panel), and Thr305/306 (right panel). (WT= 5 AS= 7)

I used western blot analysis to confirm the changes in CaMKII phosphorylation and subcellular localization in hippocampi from 2-3 month old AS mice. Here I used a modified fractionation protocol to isolate a Triton-soluble fraction (TSF) (cytosolic-membrane protein pool) and a Triton-insoluble fraction (TIF) (PSD-fraction) (Brown et al., 2005). To confirm the genotypes of WT and AS mice in both the TSF and the TIF I performed western blot analysis using an E6-AP antibody. AS mice showed roughly a 90% reduction of E6-AP in both the TSF and TIF (Figure 5).

Western blot analysis of CaMKIIα showed no difference in total levels in the TSF (Figure 5). In contrast to what was reported by Weeber et al., 2003, I was unable to detect a change in the amount of CaMKIIα in the PSD-fraction (TIF) (Figure 5). Additionally, although I detected a trend for an increase in levels of phospho-Thr286 in both fractions from AS mice (Figure 5), this never reached statistical significance in repeated assays across a range of ages (P10, P21, and 2-3 month) (data not shown). As with the phospho-Thr286, using western blot analysis, I was unable to detect the previously reported change in levels of phospho-Thr305/306 (Figure 5).

Altered CaMKII activity in AS mice

Due to the inability to detect significant changes in phosphorylated CaMKIIα in our AS mouse model, we turned to a kinase assay to evaluate potential changes in the kinase activity of CaMKII in AS mice. Moreover, we wanted to see if CaMKII was indeed playing a role in AS pathology.

Once again a previous report had documented a decrease CaMKII activity in homogenates from adult AS compared to WT mice (Weeber et al., 2003). Using

autocamtide, a peptide substrate mimicking the Thr286 autophosporylation site of CaMKII, we assayed the Ca^{2+}/calmodulin dependent and Ca^{2+}/calmodulin independent activity in hippocampal homogenates from AS and WT mice at P10 and P21. Interestingly, hippocampal homogenates from P10 AS mice showed a 23% decrease in Ca^{2+}/calmodulin dependent CaMKII activity compared to that of WT, with no change in Ca^{2+}/calmodulin independent activity (Figure 6). No changes in CaMKII activity were detected at the P21 time point (Figure 6). Our data suggests that developmental regulation of CaMKII may be altered in AS mice, even though we were unable to detect CaMKII expression or phosphorylation changes via western blot analysis. It may be interesting to evaluate CaMKIIα as well as CaMKIIβ expression profiles early on in development (P5-P10) to determine if the severity of AS pathology may be linked to developmental regulation of CaMKII.

Phosphatase activity in AS hippocampus

The reported increase in CaMKII phosphorylation and activity in adult AS mice has been linked to a non-specific decrease in PP2A/PP1 activity (Weeber et al., 2003). We were interested if we could confirm the phosphatase activity decrease in AS mice as well as identify what phosphatase (PP2A or PP1) was responsible for the decreased activity. To this end we took advantage of the PP1/PP2A substrate, [^{32}P]-phosphorylase *a* (Cohen, 1989). Using 2.5 nM or 2.5 μM okadaic acid to block PP2A or both PP2A/PP1, respectively (Cohen, 1991), we determined that there was no change in the activity of PP2A or PP1 in the adult hippocampus of AS mice (Figure 7).

Figure 6

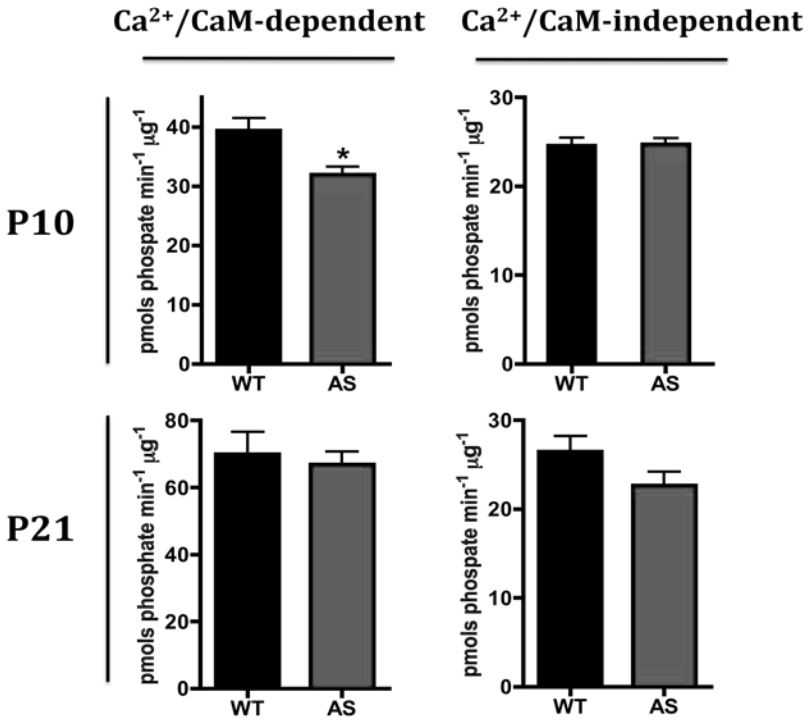

Figure 6. CaMKII kinase activity assay. Ca^{2+}/calmodulin-dependent CaMKII activity was significantly decrease in AS versus WT mice in P10, but not P21, hippocampal homogenates. Ca^{2+}/calmodulin-independent CaMKII activity was unchanged at either time point between genotypes. (* p= 0.0174, WT P10= 5; AS P10= 5; WT P21= 4; AS P21=6)

Figure 7

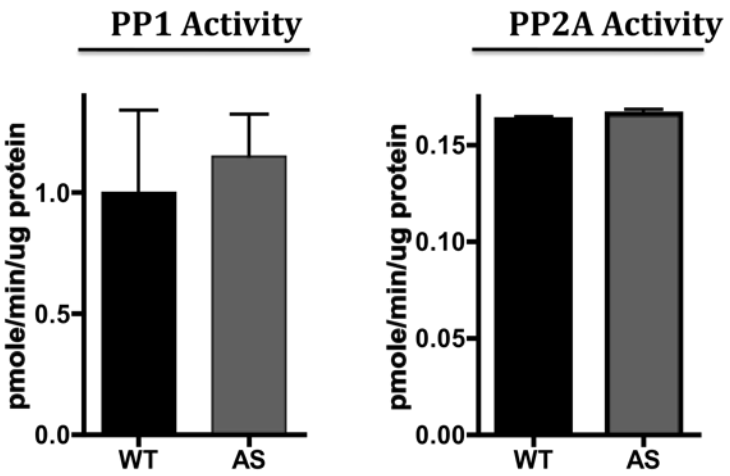

Figure 7. PP1/PP2A phosphatase activity. No differences in PP1 activity or PP2A activity were detected between WT and AS mouse hippocampal homogenates. (Adult mice 3-4 months, WT= 3; AS= 3)

Results

E6-AP expression is significantly reduced throughout the brain of the AS mouse

In situ hybridization data suggested that *UBE3A* is maternally imprinted in the hippocampus, cerebellum, and olfactory bulbs, with biallelic expression throughout the rest of the brain (Albrecht et al., 1997; Cattanach et al., 1997; Jiang et al., 1998). This has led the AS field to assume that protein expression of E6-AP follows the identical pattern, with E6-AP expression deficient in the hippocampus, cerebellum, and olfactory bulbs in the AS mouse, and more importantly no change in E6-AP levels in other brain regions. Using western blot analysis of E6-AP on several brain regions of WT and AS to confirm the genotypes of the mice, we noticed that the lack of E6-AP expression is not isolated to hippocampus, cerebellum, and olfactory bulbs. Additionally, recent data looking at E6-AP protein levels suggests that the loss of E6-AP in the AS brain may be more global than previously thought (Dindot et al., 2008; Yashiro et al., 2009). This underscores the importance for better characterization of E6-AP expression patterns in the AS mouse. Here we use western blot and immunocytochemical/immunohistochemical analysis to determine the effects of maternal imprinting of *UBE3A* on E6-AP expression across multiple brain regions as well as peripheral tissues.

To begin to understand the extent of the effects of maternal imprinting on E6-AP expression we performed western blot analysis on several brain regions microdissected from WT and AS mice (Figure 8). Total homogenates from the hippocampus, striatum, hypothalamus, thalamus, cortex, cerebellum, midbrain, and olfactory bulbs were prepared

form WT and AS mice. The western blot analysis shows expression of E6-AP in all brain regions assayed from WT mice, with the highest relative expression in the cortex, thalamus, and olfactory bulbs (Figure 8). Comparison of E6-AP levels across WT brain regions revealed a significant 2.5-fold variation (one-way ANOVA; $p=0.0017$). Post-hoc Tukey's multiple comparison test showed E6-AP expression in the striatum was lower than that of the thalamus (2.2-fold; $p<0.05$), cortex (2.2-fold; $p<0.05$), and olfactory bulbs (2.5-fold; $p<0.01$). Additionally, E6-AP expression was lower in the hypothalamus (1.7-fold; $p<0.05$) and the cerebellum (1.9-fold; $p<0.05$) when compared to the olfactory bulbs.

In comparison, all brain regions assayed from the AS mice showed a marked reduction in E6-AP expression (Figure 8). Longer film exposure times revealed low levels of E6-AP in all AS brain regions, and we estimated that E6-AP levels were reduced by at least 90-95% in all brain regions of AS mice relative to WT brain regions.

To more completely evaluate the cell-type specificity of E6-AP expression in the brain we performed immunohistochemical analysis in 40 μm coronal slices from WT and AS animals. In slices from WT animals, E6-AP specific staining was seen throughout the pyramidal cell layers and the dentate gyrus of the hippocampus, as well as cells spotted throughout the stratum moleculare in a pattern consistent with interneuron staining. Notably there was no specific E6-AP staining in slices from the AS mice in any of the brain regions tested (Figure 9 and Gustin et al., 2010). The pattern of E6-AP staining in the hippocampus suggested that both pyramidal cells as well as interneurons expressed E6-AP (Figure 9 and Gustin et al., 2010). In order to confirm interneuron E6-AP expression, co-staining experiments using the interneuron specific markers parvalbumin

Figure 8

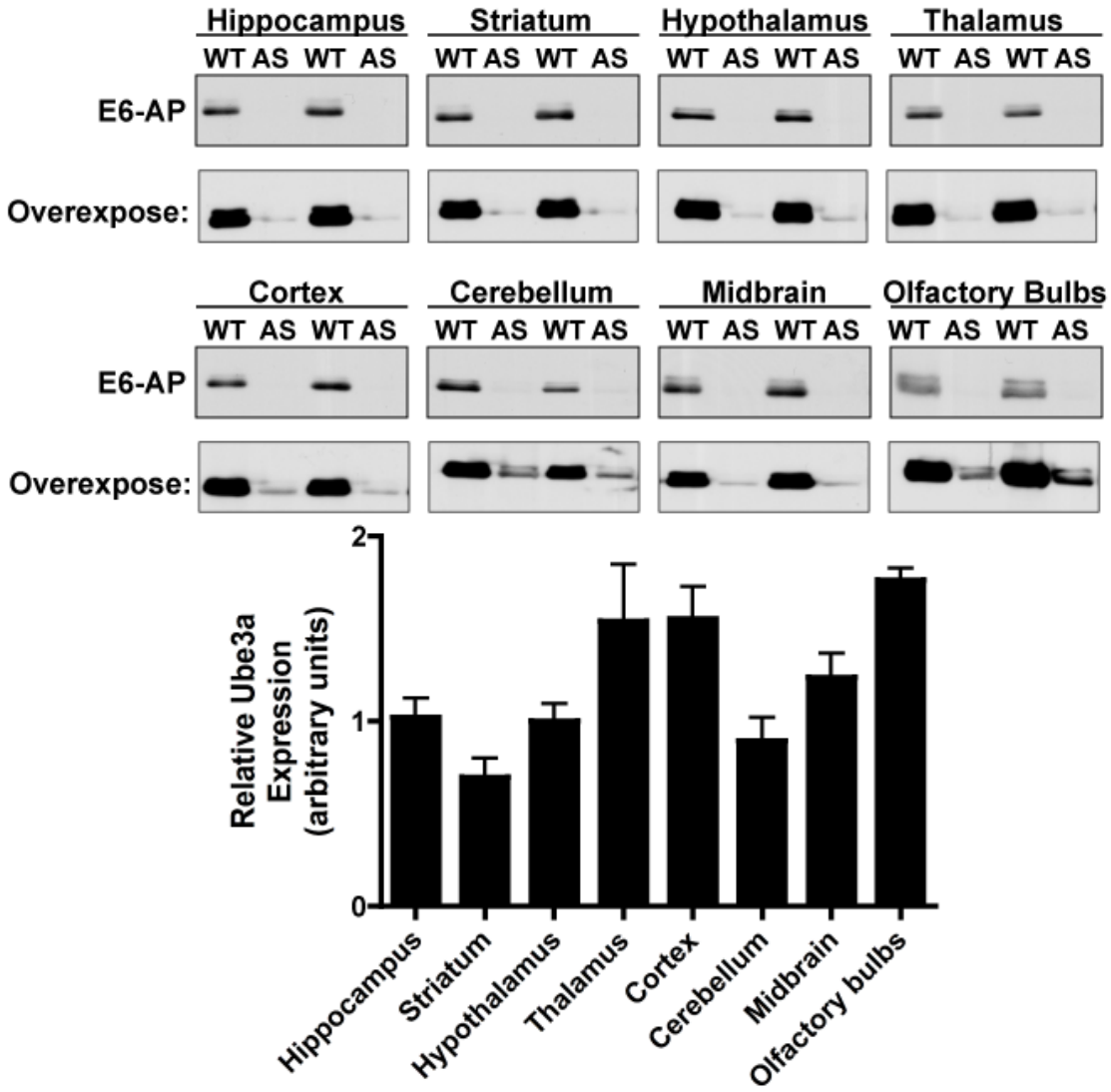

Figure 8. Western blot analysis of WT and AS mouse brain regions. Top: Western blot analysis of total homogenates from hippocampus, striatum, hypothalamus, thalamus, cortex, cerebellum, midbrain, and olfactory bulbs shows an estimated 90-95% loss of E6-AP in AS mice compared to WT mice. Film overexposure reveals the presence of E6-AP in AS all brain regions tested. Bottom: Quantification of the relative E6-AP levels across WT mouse brain regions reveals a significant 2.5-fold variation between brain regions (one-way ANOVA p=0.0017; N=4). (Gustin et al., 2010)

Figure 9

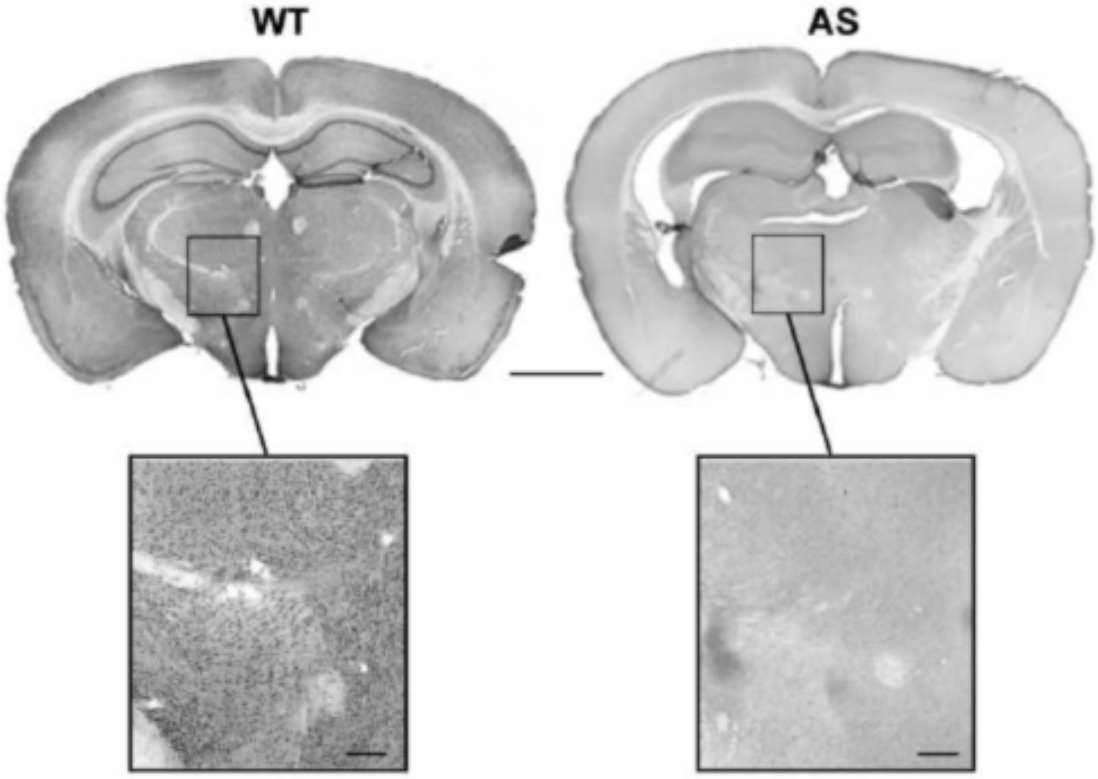

Figure 9. Immunohistochemical analysis comparing brain slices of coronal slices from WT and AS mice. E6-AP staining was detected throughout brain slices from WT mice. Intense staining in the pyramidal cell layer of the hippocampus of WT mice was observed. Strikingly, no E6-AP could be detected in slices from AS mice (Figure courtesy of Dr. Ariel Deutch, Gustin et al., 2010)

(PV) and calretinin (CR) were performed. E6-AP specific staining was seen in interneurons expressing PV and CR, respectively (Figure 10). E6-AP was detected in interneurons present in the globus palidus and the reticular nucleus of the thalamus. Additionally, E6-AP was detected in the majority of PV and CR positive interneurons of the neocotex. Co-staining experiments of E6-AP and glial fibrillary acidic protein (GFAP), a glial cell marker, revealed no E6-AP staining in glial cells, confirming the neuronal specificity of E6-AP staining in the brain (Figure 10).

Subcellular E6-AP expression profile

To determine the subcellular distribution of E6-AP, immunocytochemical and subcellular fractionation studies were performed. Using WT rat hippocampal dissociated cultures we were able to show E6-AP was ubiquitously expressed throughout the neuron with most intense staining in the nucleus; however, staining in the soma and dendritic arbors was also readily detectable (Figure 11). E6-AP synaptic expression was evaluated using co-staining experiments with synapsin-1 (presynaptic marker) and PSD-95 (postsynaptic marker) antibodies, respectively. The co-localization of E6-AP with synapsin-1 and PSD-95 suggests the presence of E6-AP in both presynaptic and postsynaptic neurons (Figure 11).

Biochemical subcellular fractionation on WT mouse hippocampi was performed to further examine the subcellular localization of E6-AP. The subcellular fractionation protocol uses homogenization buffers containing detergents with increasing harshness to isolate different pools of proteins from different subcellular compartments. Our protocol yields an S1 fraction (soluble protein pool), S2 fraction (membrane-associated protein

Figure 10

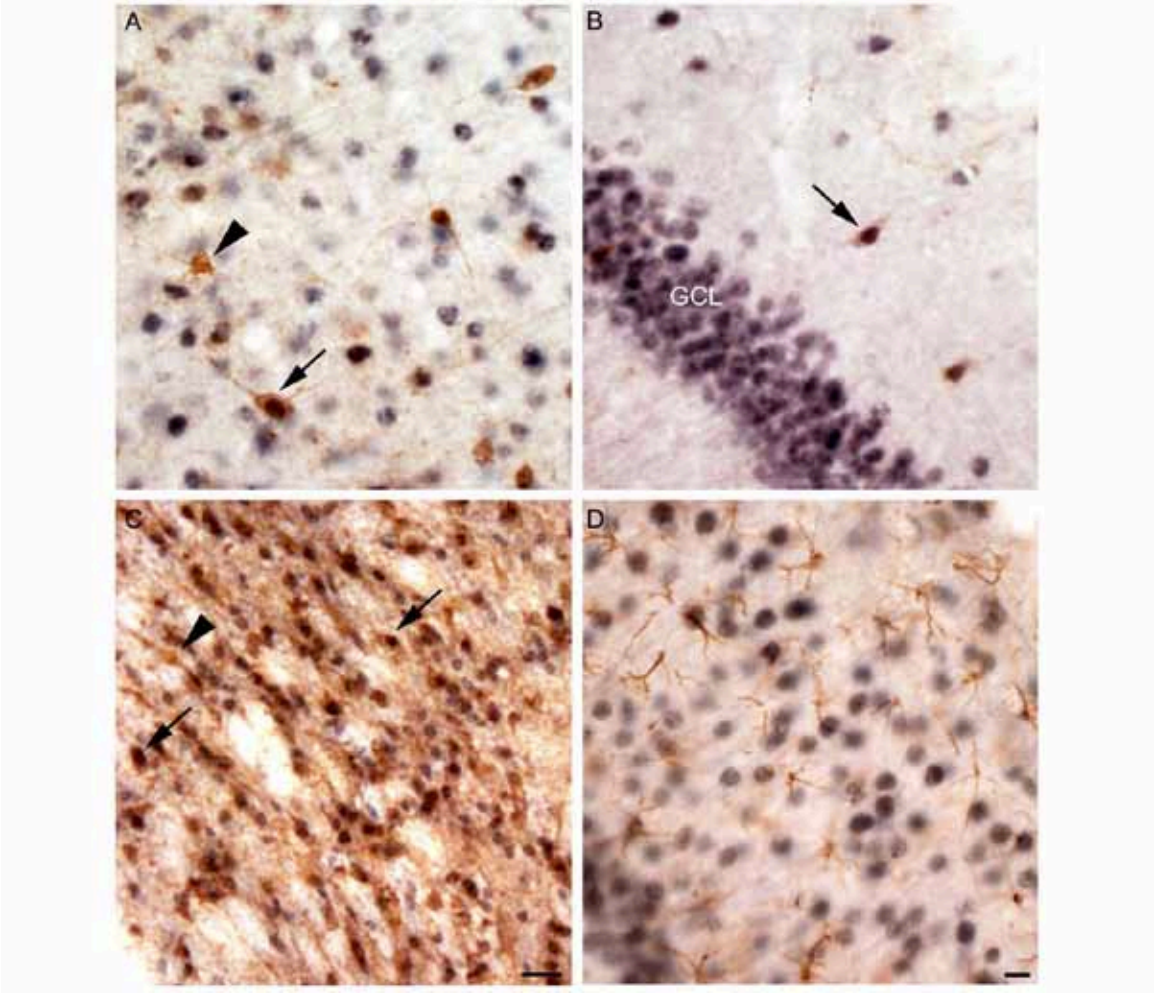

Figure 10: E6-AP was found to be expressed in interneurons but not astrocytes. **A.** E6-AP co-localized with a fraction of parvalbumin (PV) expressing interneurons in the neocortex (arrow). **B.** In the hippocampus E6-AP was found to co-localize to interneurons expressing calretinin. **C.** The majority of PV-positive interneurons in the thalamic reticular nucleus co-localized with E6-AP. **D.** In the hippocampus, astrocytes, stained with GFAP, did not express E6-AP. Scale bars are 25 μm in panel C and 10 μm in panel D; the scale bar in panel D applies also to panels A and B. (Figure courtesy of Dr. Ariel Deutch, Gustin et al., 2010)

Figure 11

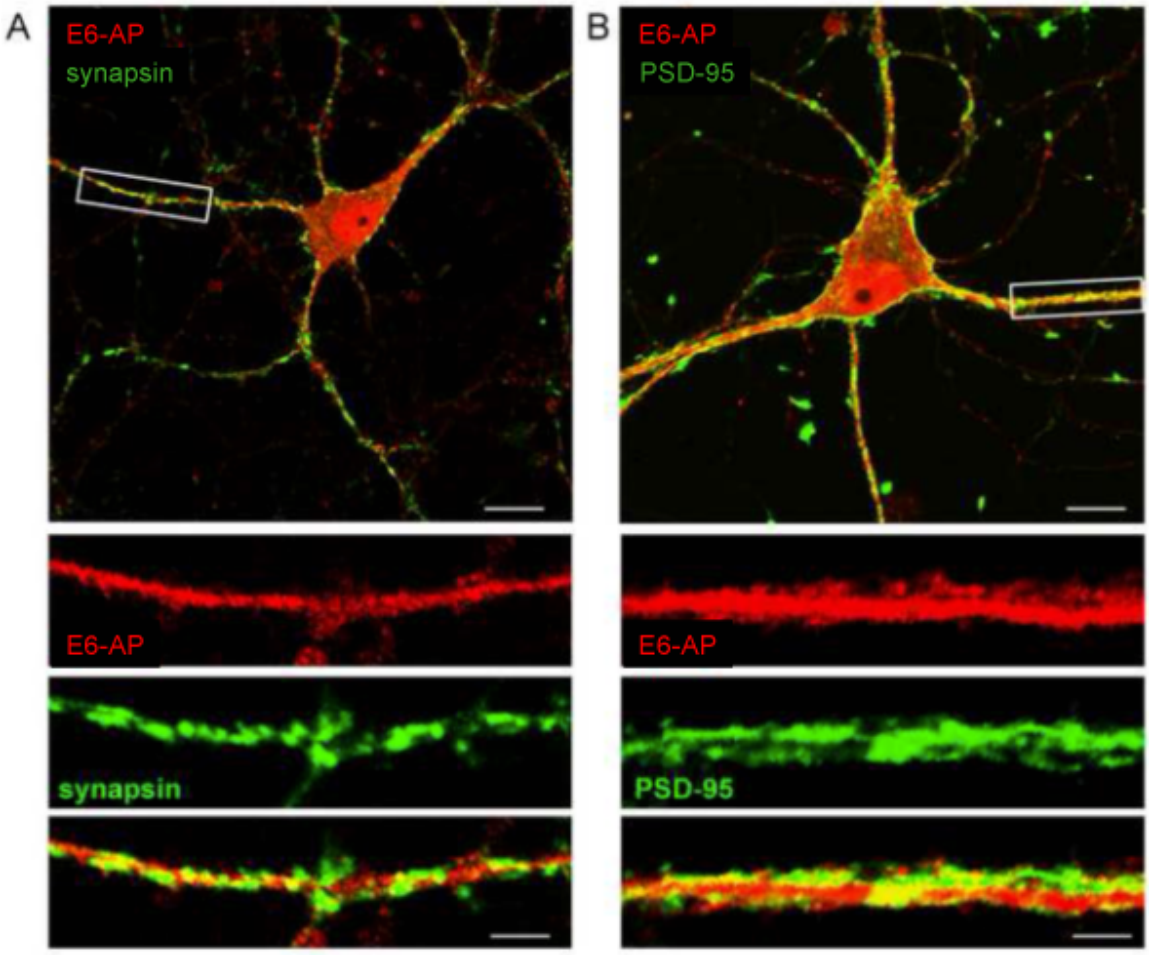

Figure 11. Immunocytochemical analysis of rat hippocampal dissociated neuronal culture. E6-AP staining is ubiquitous throughout neurons, with the most intense staining seen in the nucleus; however staining is visible in soma and dendrites (Red images in A and B). Partial co-localization of E6-AP with synapsin (A) and PSD-95 (B) suggests E6-AP is expressed at the synapse and potentially at both pre- and postsynaptic sites. (Scale bars: Upper panels 20 μm; lower panel 5 μm) (Figure courtesy of Dr. Kevin Haas, Gustin et al., 2010).

pool), S3 fraction (PSD-associated pool), and a P3 pellet (insoluble fraction). (See Chapter 2: Methods for a detailed description of the biochemical fractionation protocol) Equal amounts of protein from each fraction were loaded into a 7.5% acrylamide gel for SDS-PAGE and western blot analysis. The majority of E6-AP co-fractionated with the cytosolic protein GAPDH in the S1 fraction (soluble protein pool). Lower levels of E6-AP co-fractionated with the IP3R, an endoplasmic reticulum marker, in the S2 fraction (membrane-associated protein pool). E6-AP was also detected in the S3 fraction (PSD-associated protein pool) and P3 pellet (insoluble fraction), where the majority of PSD-95 fractionates (Figure 12). These data are consistent with a broad distribution of E6-AP throughout the neuron, with the highest abundance in soluble pools.

Maternal imprinting of *UBE3A* and E6-AP expression in peripheral tissues

Little is known about E6-AP expression in peripheral tissues, or whether a lack of maternally expressed E6-AP in the periphery could contribute to associated symptoms in AS. To begin to evaluate E6-AP expression in peripheral tissues, we compared E6-AP levels in total homogenates of the heart, liver, and kidney from WT and AS mice. E6-AP was readily detected in WT tissues via western blot analysis (Figure 13). Interestingly, E6-AP levels in heart, liver, and kidney from AS mice were reduced by 73±14%, 68±7%, and 64±18% respectively, compared to levels seen in WT tissues (Figure 13). Equal biallelic gene expression of the maternal and paternal genes would contribute ~50% of protein expression. Therefore we tested whether the total tissue levels of E6-AP in AS mice were significantly less than the predicted 50% of WT levels. A one-sample *t*-test revealed that reduction in E6-AP levels in AS heart ($p=0.006$) and AS liver ($p=0.01$)

Figure 12

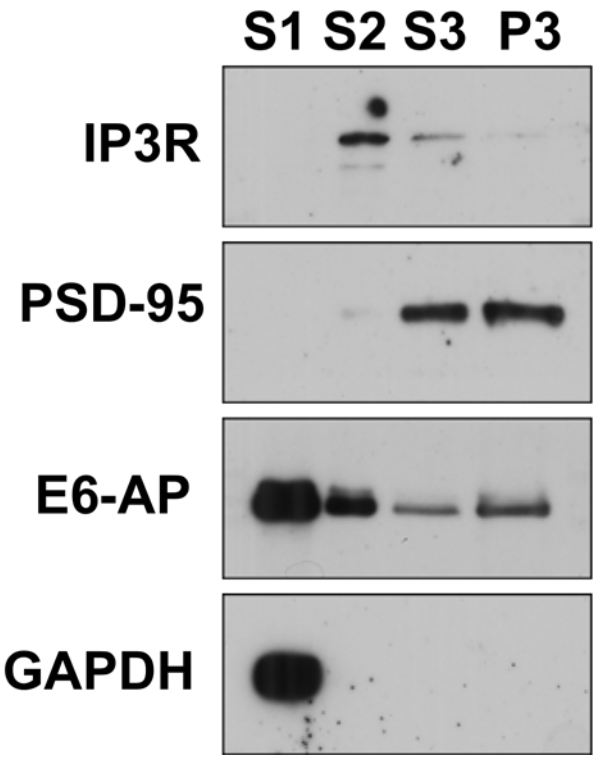

Figure 12. Biochemical subcellular fractionation of WT hippocampus. E6-AP is detected in the soluble protein pool (S1), membrane-associated protein pool (S2), PSD-associated protein pool (S3), and the insoluble fraction (P3). The majority of E6-AP is soluble, fractionating with the cytosolic protein, GAPDH (S1). E6-AP also co-fractionates with the ER protein , IP3R (S2), and with PSD-95, a marker of PSD (S3 and P3). (Gustin et al., 2010)

Figure 13

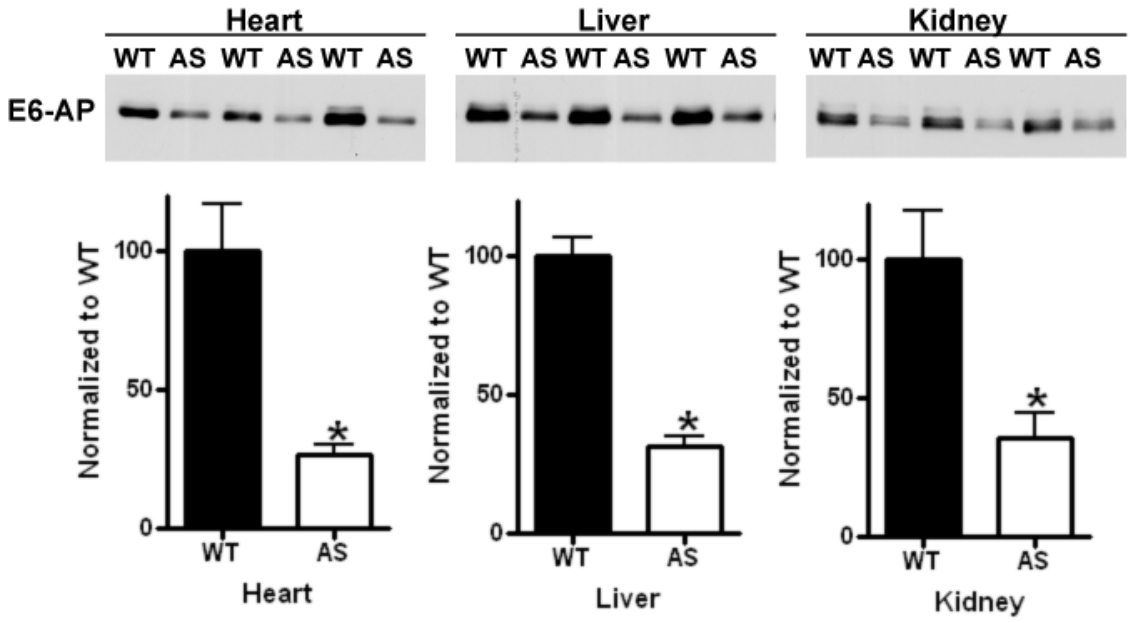

Figure 13. Peripheral expression of E6-AP. E6-AP was readily detected in total homogenates of heart, liver, and kidney from WT and AS mice. The relative expression of E6-AP in AS mice was significantly decreased from WT in all peripheral tissues (heart 73±14%, p=0.0038; liver 68±7%, p=0.0001; and kidney 64±18%, p=0.0165). The decrease in all peripheral tissues was greater than 50%, suggesting maternal imprinting may be playing a role in the periphery. (Animals WT=4; AS=3) (Gustin et al., 2010)

were reduced by significantly more than 50% of the WT; however, in the kidney there was only a trend for loss of E6-AP expression to be significantly greater than 50% of the WT ($p=0.21$). This suggests that reduced levels of *UBE3A* in peripheral tissues could potentially contribute to symptoms of AS.

Discussion

AS research has centered around hippocampal and cerebellar dysfunction due to the initial *in situ* hybridization studies describing the maternal imprinting of *UBE3A* (Albrecht et al., 1997; Jiang et al., 1998). However, until recently there were no studies evaluating the expression profile of the *UBE3A* protein product, E6-AP. Through western blot and immunohistochemical analysis we were able to show that the loss of E6-AP in AS mice is not limited to the hippocampus and cerebellum, but in fact there is a global loss of E6-AP throughout the brain of AS mice. These results highlight the importance of evaluating protein expression changes in addition to transcript levels.

These results have changed the way we think about the mechanisms underlying AS pathology, and underscore the need for research efforts to extend beyond the hippocampus and cerebellum to more global approaches. These new data are consistent with previous RT-PCR studies evaluating human AS brain samples, which showed UBE3A transcript was reduced to 10% of control levels in the frontal cortex (Rougeulle et al., 1997). Our E6-AP expression data also extends work done on *UBE3A*-YFP reporter mouse that shows loss of E6-AP expression is not limited to the hippocampus and cerebellum (Dindot et al., 2008), and a recent report showing the E6-AP levels are dramatically down in neocortical areas in AS mice (Yashiro et al., 2009).

The roughly 90-95% global loss of E6-AP across all brain regions in the AS mouse is not surprising due to the broad pathological phenotypes displayed by these mice. As we move away from thinking of AS pathology strictly stemming from hippocampal and cerebellar dysfunction, a more global mechanism of AS pathology can potentially be revealed. The movement disorder associated with AS suggests dysfunction in basal ganglia circuitry (Beckung et al., 2004), while the severe impairment of speech may be linked to deficiencies in cortical circuitry development (Catani et al., 2005). Additionally, the seizure phenotype, EEG abnormalities, and sleep disturbances may be the outcome of thalamocortical dysfunction (Lossie et al., 2001; Colas et al., 2005; Miano et al., 2005).

A closer look at the subcellular localization of E6-AP, using immunocytochemistry and biochemical subcellular fractionation, revealed a ubiquitous expression pattern throughout the neurons. The highest levels of E6-AP were detected in nuclear and cystosolic pools of protein; however, E6-AP was readily detectible in membrane-associated as well as PSD-associated pools of protein. Partial co-localization with synapsin and PSD-95 showed that E6-AP is possibly both pre- and post-synaptic. Others have also recently reported that E6-AP localizes to dendrites and spines (Dindot et al., 2008; Yashiro et al., 2009). Additional immunocytochemical analysis showed that E6-AP expression is not restricted to excitatory neurons, as co-staining with GABAergic interneuron markers revealed the presence of E6-AP in both PV and CR positive interneurons.

Extending our studies into peripheral tissues, we documented a significant decrease in E6-AP levels in the heart, liver, and kidney of AS mice. Generally,

genes/proteins are expressed equally from both alleles, and a typical heterozygote will show a 50% reduction in protein levels. In the AS mice we detected a ~75% reduction in the peripheral tissues assayed, below the 50% reduction expected if there was equal biallelic expression. One report suggested that *UBE3A* is preferentially maternally imprinted in human fibroblast cells (Herzing et al., 2002), but no study has shown that maternal imprinting of *UBE3A* in peripheral tissues extends to the E6-AP protein level. Although clinical significance of maternal imprinting of *UBE3A* and subsequent loss of E6-AP in the periphery is unclear, it is known that AS patients suffer from disturbances in gastrointestinal function (Laan et al., 1999; Williams et al., 2006). These findings demonstrate the importance of evaluating the role of E6-AP deficiency in these symptoms, as well as taking a closer look at other potential adverse symptoms of AS that my be due to a loss of peripheral E6-AP protein. These expression studies have revealed a global E6-AP deficit in AS mice that extend, not just throughout the brain, but into peripheral tissues as well. This provides a foundation for further exploration into how E6-AP deficiency leads to the vast number of symptoms seen in AS.

The documented CaMKII misregulation in AS mice (Weeber et al., 2003) and the prevention of several of the AS behavioral phenotypes when AS mice are crossed with CaMKIIα-Thr286Ala heterozygous mice (van Woerden et al., 2007), suggested CaMKII may be playing a direct role in AS pathology. Unfortunately, our attempts to recapitulate the CaMKII altered phosphorylation and activity were unsuccessful. Additionally, we did not see the change in phosphatase activity that had been previously reported in the AS mice (Weeber et al., 2003). Although we were unable to confirm the alterations in

CaMKII previously seen, genotyping and western blot analysis, along with rotarod behavioral data, confirmed that we were assaying AS mice.

Our biochemical analysis of P10 AS mice did reveal a significant decrease in CaMKII activity that returned to WT levels by P21. This suggests that there may be a time window, early in development, that E6-AP deficiency may alter CaMKII regulation in AS mice. CaMKII is known to play an important role in synaptogenesis during this time period. Alteration in CaMKII expression, phosphorylation, activity, protein/protein interactions, and/or subcellular localization could have deleterious effects on synapse development. This becomes more interesting as we know that E6-AP is localized to both pre- and post- synaptic neurons in PSD-enriched pools, areas where CaMKII is expressed. A closer look at the expression pattern of E6-AP throughout development is necessary for complete understanding of how E6-AP may be functioning. Furthermore E6-AP substrates that may be expressed early on in development may have been overlooked due to the time points during which AS research has focused. It would also be interesting to evaluate CaMKIIα and CaMKIIβ expression, phosphorylation state, and activity in AS mice earlier in development to see if misregulation of CaMKII during development could be causing the AS phenotype. There is evidence that AS mice do have abnormal spine morphology (Dindot et al., 2008). It is possible that CaMKII misregulation during critical time points during development could lead to the phenotypes seen in AS.

A recent report in the literature was able to show that neuronal activity induces *UBE3A* transcription and that this leads to the degradation of Arc (Greer et al., 2010). Arc is a synaptic protein important for the internalization of AMPARs (Chowdhury et al.,

2006; Rial Verde et al., 2006; Shepherd et al., 2006). In neurons cultured from *UBE3A* KO mice the increase in Arc was shown to increase AMPAR internalization leading to a decrease in the AMPA/NMDA ratio, along with a decrease in mESPC frequency, when compared to WT neurons (Greer et al., 2010). The authors go on to posit, that when the AS mice were crossed with the CaMKIIα-Thr305Val/Thr306Ala heterozygous mice (van Woerden et al., 2007), the increase in CaMKII activity increased AMPAR insertion into the synapse, allowing for a rescue of the deficits in the double mutants. This suggests that the CaMKII role in AS is more indirect rather than causative. Therefore, the rescued behavioral deficits may be due to a generalized AMPAR insertion rather than a direct CaMKII effect. The one major caveat to the Arc hypothesis is that all experiments were conducted in *UBE3A* KO neurons. It may be the case that the ~5-10% of E6-AP protein that is expressed from the paternal *UBE3A* gene (Gustin et al., 2010) is enough to control Arc levels at the synapse and that Arc is not playing a major role in the AS phenotype.

In considering possible explanations for the loss of CaMKII phenotypes from the AS mice used in these studies, I became concerned about the breeding strategies currently in use. Traditionally, breeding of AS mice has been done by crossing WT males with AS females, such that all pups are reared by AS females. This raises the possibility that the broad AS phenotype of the dams may compromise normal maternal care in some way, producing a chronic early-life stress in the pups. As will be discussed in Chapter 4, transient early-life stress can have a prolonged impact on future brain function. Thus, early-life stress in our AS mice (raised by AS dams) may contribute to some aspects of the phenotype displayed by the pups in adulthood. It is unknown what effects this early-life stress may be playing in the misregulation of CaMKII, and it is also unknown what

additional epigenetic factors are being altered, specifically due to the early-life stress, and not the AS phenotype itself.

I suggest that a different breeding strategy be developed for the maintenance of AS colonies and generation of experimental mice. Human AS patients inherit the *UBE3A* mutation from their mothers. However, the mothers are almost always asymptomatic because they inherit the mutation paternally. In contrast, the current mouse breeding strategy raises experimental animals using symptomatic dams, which are lacking 90-95% of the E6-AP protein across all brain regions, perpetuating an early-life stress throughout the colony via the epigenetic factors and enhancing sensitivity to other environmental factors. I suggest that the AS mouse model should be maintained as a paternal deficient mouse, more closely mimicking the propagation of AS in the human population. Experimental mice should be generated by crossing asymptomatic females (paternal *UBE3A* deficient mice) with WT male mice to yield WT and AS littermates with no potential for external stress issues to confound the interpretation.

CHAPTER IV

EARLY-LIFE CHRONIC STRESS AND LEARNING AND MEMORY

Introduction

The potential confound of AS phenotypes by environmental factors begged the question, does CaMKII play a role in the molecular mechanisms underlying the negative effects propagated through chronic early-life environmental stressors? Stress in different forms is known to affect both synaptic plasticity and performance on a number of behavioral paradigms in the rodent (Table 1). Depending on the type and duration of stress, as well as the age of the animal during exposure, a variety of biochemical, electrophysiological, and behavioral outcomes have been reported.

The effects of stress on CaMKII are not well understood. A number of biochemical, morphological, electrophysiological, and behavioral effects due to different stressors can be linked to CaMKII and CaMKII dysfunction or misregulation. However, the effects on CaMKII vary with the time, duration, and type of stressor (Table 1). For example, acute stress leads to an increase in Thr286 phosphorylation (Suenaga et al., 2004; Ahmed et al., 2006), whereas chronic stress leads to a decrease in Thr286 phosphorylation (Gerges et al., 2004; Fumagalli et al., 2009). At a biochemical level, this is consistent with the idea that acute stress can enhance cognitive ability, whereas chronic stress is detrimental to cognition.

Chronic and acute stress have both been shown to effect synaptic plasticity. Acute restraint stress in adult rats has been shown to enhance LTP (Suenaga et al., 2004).

Table 1

Stress Paradigm	Age/Duration	CaMKII Effects	LTP/LTD	Behavior	Reference
Chronic Stress					
Intruder psychosocial stress	Adult/ 1 month	↓ P286/↓ CaMKIIα (no change in ratio) in CA1	↓ LTD	?	Gerges et al., 2004
Restraint Stress *see pharmacological stress mimic	Adult/ 6 hr/day 21 days	?	?	MWM deficit	Xu et al., 2009
Neonatal isolation	P1-P7/ 1 hr/day	?	↑ LTD (P27-P43)	?	Yun et al., 2008
Dam restraint stress (prenatal)	E14-delivery/ 3x/day for 45 minutes	↓ P286 in PFC ↓ P286 trend in Hippocampus	?	?	Fumagalli et al., 2009
Maternal separation	P1-P14/ 3 hr/day	?	?	Anxiety/fear in open field and EPM (P60)	Romeo et al., 2004
Maternal separation	P4-P21/ 3 hr/day	?	?	FST deficit (P61)	MacQueen et al., 2003
Acute Stress					
Restraint stress	Adult/ 45 minutes, 90 minutes, or 4 days	↑ P286 (no change total CaMKIIα) in Hippocampus	↑ LTP	?	Suenaga et al., 2004
Swim Stress	Adult/ 2 minutes	↑ P286 in DG and CA1	?	?	Ahmed et al, 2006
REM deprivation	Young(P11-P25) or Adolescent(P39-53)/ 3 consecutive nights	No change in total CaMKIIα ↑ P286 trend in young hippocampus	?	?	Lopez et al., 2008
Pharmacological Stress Mimetic					
Dexamethasone-tappering dose (0.5 mg/kg day1, 0.3 mg/kg day2, 0.1 mg/kg day3)	P4-P6 (Acute)	↑ P286 in CA1, PFC, and Amygdala	↓ LTP ↑ LTD	Passive avoidance deficit	Huang et al., 2007 and Lin et al., 2006
Cortiosterone (0.1mM) *see chronic stress	Acute hippocampal slices/ 24 hrs	↑ P286	?	?	Xu et al., 2009

Table Legend: - (no change), ↑ (increase), ↓ (decrease), **?** (unknown), **PFC** (prefrontal cortex), **DG** (dentate gyrus), **MWM** (Morris water maze), **EPM** (elevated-plus maze), **FST** (forced swim test)

Conversely, chronic psychosocial stress using an intruder stress paradigm for one month in adult rats causes a reduction in LTP (Gerges et al., 2004). Interestingly, maternal separation of rat pups for one hour a day from P0-P7 leads to an increase in LTD in later adolescent time points at which LTD is absent in control animals (Ku et al., 2008). When elevation of corticosterone levels is mimicked by dexamethasone administration in rats from P1-P3 and then assayed at 5-weeks of age, there is a decrease in LTP along with an increase in LTD (Lin et al., 2006; Huang et al., 2007). This could potentially be due to a developmental delay that shifts a sliding threshold for LTP/LTD induction.

Chronic environmental stressors can also affect performance on a number of behavioral paradigms. Chronic stress in adult rats can lead to deficits in Morris water maze performance (Xu et al., 2009). Additionally, early-life stressors can lead to behavioral deficits later in life. These include deficits in passive avoidance tests, novel object recognition, Morris water maze, elevated-plus maze, as well as forced swim test (MacQueen et al., 2003; Romeo et al., 2003; Lin et al., 2006; Huang et al., 2007; Rice et al., 2008).

Taken together, the evidence suggests that early-life stressors are leading to CaMKII misphosphorylation and mislocalization. These changes in CaMKII can affect the proper regulation and activity of the kinase, and it has been shown in a variety of experimental paradigms that this leads to alterations in synaptic plasticity. Furthermore, misregulation of CaMKII has dramatic effects on learning and memory behavioral paradigms. This led to the hypothesis that early-life stress is altering the phosphorylation, subcellular localization, and protein/protein interactions of CaMKII, which is leading to the physiological and behavioral deficits seen later in life.

A new mouse model of early-life stress

To test if misregulation of CaMKII could be playing a role in the development of learning and memory deficits associated with early-life stress, we adopted a behavioral paradigm of chronic early-life stress first described in the Baram laboratory (Rice et al., 2008). The chronic early-life stress paradigm we used, introduced an environmental stressor between P2-P9 in C57BL/6J mice (Figure 1). The success of the ES is determined by tracking the weight of Control versus ES mice at P9, additionally weights are taken at P25 and P90 (Figure 2). The decrease in weight is due to fractured maternal care due to the dams leaving their litters to search for nesting material (Rice et al., 2008). The pups are thought to be affected not only by the uncomfortable environment, but also suffer from a temperature stress, as well as decreased time feeding. We also speculate that stress may affect lactation in the dams compromising milk production and adding to the feeding deficits in the ES pups.

Mice undergoing this chronic early-life stress paradigm have been shown to have a ~4-fold increase in basal plasma cortocosterone (CORT) levels compared to control mice at P9 persisting into adult mice (Rice et al., 2008). Along with the change in plasma CORT levels, ES mice show a 75% decrease in corticotrophin releasing hormone (CRH) mRNA levels in the hypothalamic paraventricular nucleus (PVN) at P9, again persisting into the adult (Rice et al., 2008).

The ES mice are deficient in hippocampal-dependent learning and memory behavioral tasks at adult time points. In the Morris water maze, ES mice show an increased latency to escape on the second day of training compared to the control mice, revealing a subtle learning and memory deficiency in the ES mice (Rice et al., 2008). To

Figure 1

Figure 1. Early-life stress paradigm. At P2 litters are culled to 5 pups and moved with Dam into new home cages. Control mice are placed in a standard cage with a 5cm x 5cm nesting square. Early-life stress mice are placed on a wire mesh floor suspended 2-2.5cm from the bottom of the cage containing 10% of the normal corncob bedding material. The early-life stress mice receive reduced nesting material (2.5cm x 5cm nesting square). At P9 all mice are moved to a standard mouse cage and weaned at P21 as per normal procedure.

Figure 2

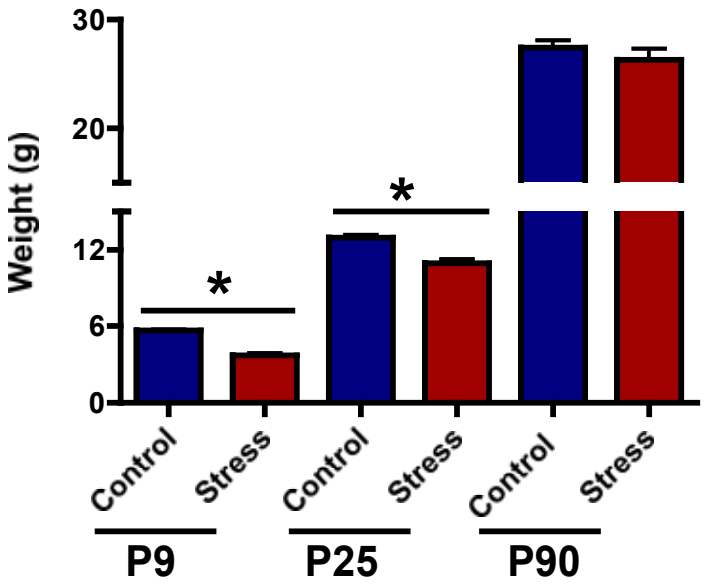

Figure 2. Weight (g) of Control and ES mice. Weight of control and ES mice was determined on P9 at the end of the stress paradigm. Control mice were significantly heavier than stress mice ($p<0.0001$). The difference in weight was maintained at P25 ($p<0.0001$), and at P90 there was no longer a weight difference between control and stress mice (P9: Con=5.6g, N=25; Str=3.7g, N=23. P25: Con=12.9g, N=24; Str=10.9g, N=18. P90: Con=27.46, N=5; Str=26.32, N=5).

confirm there was a learning and memory deficit in the ES mice, the novel object assay was used. The ES mice spent significantly less time exploring the novel object versus the familiar object than that of the control mice (Rice et al., 2008). This confirms the memory deficit seen in the Morris water maze. It is important to reiterate that these learning and memory tasks are being conducted on adult animals where the stress was performed in a very specific time-window in early postnatal development. Thus, these deficits reveal a long-lasting change in developmental programming.

In mice, exposure to novel objects are anxiogenic events, which could account for the decrease in time spent with the novel object seen in the ES mice. However, open-field activity tasks revealed no effect of early-life stress on anxiety, as evidence by no differences in center time between control and ES mice. However, more appropriate anxiety behavioral assays must be completed to make definitive conclusions on the anxiety of these animals.

Results

Early-life stress effects on CaMKII

As an initial test of the hypothesis that the effects of early-life stress may be in part mediated by long-term disruptions in CaMKII signaling, we analyzed hippocampal homogenates from P25 control or ES mice by western blotting.

Total hippocampal homogenates from P25 control and ES mice did not reveal any major differences in the expression levels of CaMKIIα or CaMKIIβ, however there was a trend for a decrease in the CaMKIIα Thr286 phosphorylation in the ES mice compared to

the controls (Figure 3). This suggests that there could be a shift in the subcellular localization of CaMKII due to the fact that Thr286 increases the affinity of the kinase for the PSD. Additionally, there was no change in total levels of PSD-95, NR1, NR2A, NR2B, Ser1303 phosphorylation, GluR1, or Ser831 phosphorylation in control versus ES mice (data not shown).

Subcellular fractionation to isolate an S1 (cytosolic protein pool), S2 (membrane-associated protein pool), S3 (PSD-associated protein pool), and P3 (insoluble pellet) was performed to determine if early-life stress caused a shift in CaMKII distribution in P25 mice. CaMKIIα levels were reduced in the PSD-associated S3 and P3 fractions, as well as the S1 fraction with no change in the S2 fraction (Figure 4). It may be counterintuitive that there is no change in the amount of CaMKIIα from the total homogenates and a decrease in the S1, S3, and P3 fractions from the ES mice. However, this is potentially due to how the protein is distributed in the fractions. The majority of protein is isolated in the S2 fraction with less than 10% of the protein in the S3 and P3 fractions, so the S2 fraction is more representative of the total homogenate (see Chapter 2: Methods, figures 1 and 2). There was also a strong trend for a reduction of CaMKIIα Thr286 phosphorylation in the S2 and S3 fractions (Figure 4). CaMKIIβ levels were unchanged in the S2 fraction; however, CaMKIIβ was not detected in the other fractions (Figure 4).

We looked at the distribution of several other PSD-associated proteins known to be important in learning and memory, and that may interact either directly or indirectly with CaMKII (Figure 5). PSD-95, a scaffolding protein and the prototypical PSD marker, was reduced in the P3 fraction of ES mice compared to controls (Figure 5). We

Figure 3

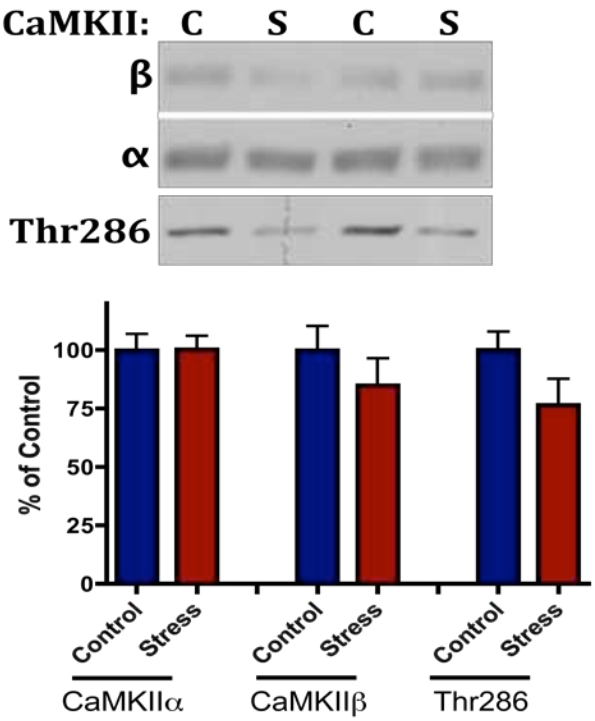

Figure 3. Western blot analysis of total hippocampal homogenates from P25 control and ES mice revealed no change in the total amount of CaMKIIα or CaMKIIβ normalized to total protein loaded. There was a non-significant 25% decrease in CaMKIIα-Thr286 phosphorylation when normalized to total CaMKIIα ($p=0.12$). (Control=5; Stress=5)

Figure 4

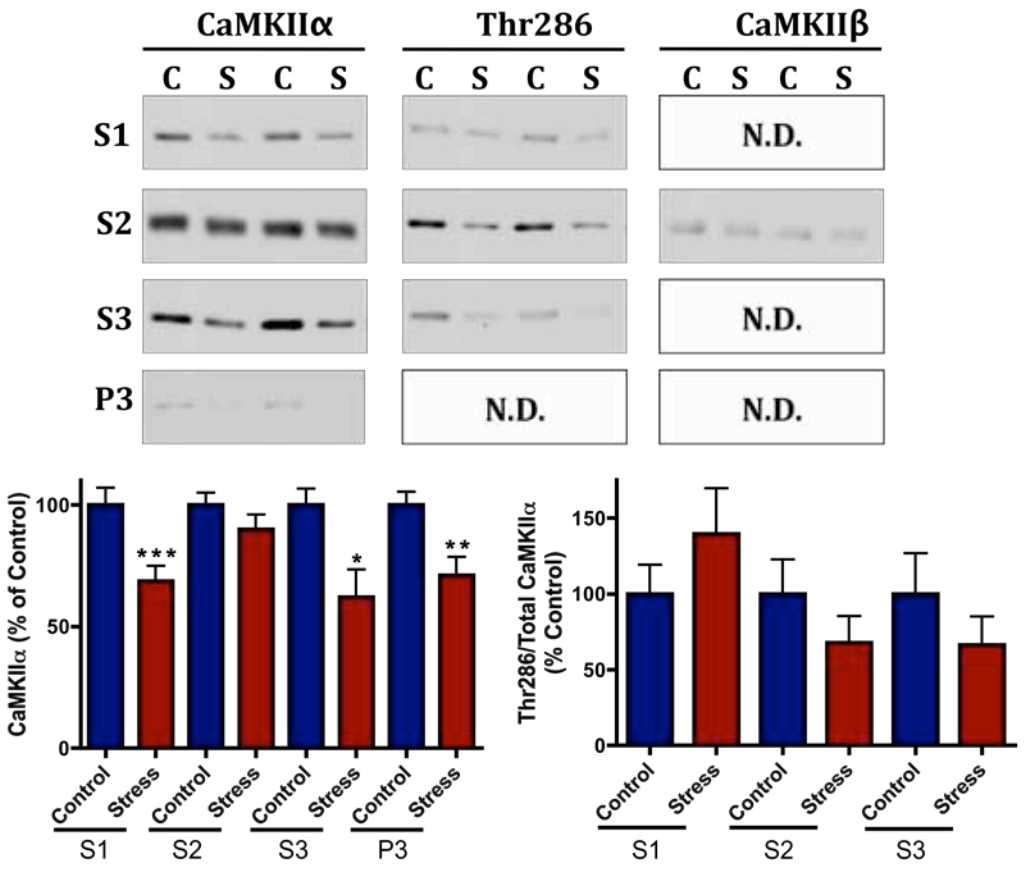

Figure 4. Western blot analysis of subcellular fractionation of total hippocampal homogenates from P25 control and ES mice. CaMKIIα levels were decreased in S1 ($p=0.01$), S3 ($p=0.02$), and P3 ($p=0.0128$) from ES mice. There was no change in the levels of CaMKIIα or CaMKIIβ in the S2 fractions of control and ES mice. When normalized to total CaMKIIα, there was a non-significant trend for a 40% decrease in Thr286 phosphorylation in S2 and S3 fractions from ES compared to control mice. (Control=5; Stress=5)

also wanted to determine if there was a redistribution of the subcellular localization of NMDAR and AMPAR subunits, due to the role these receptors play in synaptic plasticity and learning and memory. The NR1 subunit was significantly reduced in the P3 fraction of ES mice compared to controls (Figure 5). Though not significant, the P3 fraction of the ES mice showed a strong trend for a reduction in NR2A levels and lesser so for NR2B levels (Figure 5). Again this fits with the reduction in PSD-95 and the possibility that there is a decrease in the number of PSDs in the ES mice. The GluR1 subunit of the AMPAR was not detected in the P3 fraction; however, no change in GluR1 levels was detected in the S2 or S3 fractions of the ES mice compared to that of control (Figure 5). Interestingly, there was a strong trend for a decrease in GluR1 Ser831 phosphorylation in the S3 fraction as well as an increase in Ser831 in the S2 fraction in the ES mice when normalized to total GluR1 (Figure 5). This suggests that CaMKII function may be altered in the PSD-associated fractions, which is leading to a decrease in phosphorylation of Ser831 of the GluR1 AMPAR subunit, a substrate of CaMKII that modulates of AMPAR function.

Changes in the phosphorylation state of CaMKII, as well as changes in the distribution of the kinase and several of its known interacting partners could affect the interaction of CaMKII with these other proteins. Immunoprecipitation (IP) studies were performed to determine how early-life stress could affect CaMKII's interaction with PSD-associated proteins. We first assayed for differences in the amount of CaMKII precipitated from control versus ES fractions (Figure 6). In all fractions there was a significant decrease in the amount of CaMKIIα coming down in the IPs from ES mice compared to controls, with a 50% reduction in the S3 (PSD-associated fraction) (Figure

Figure 5

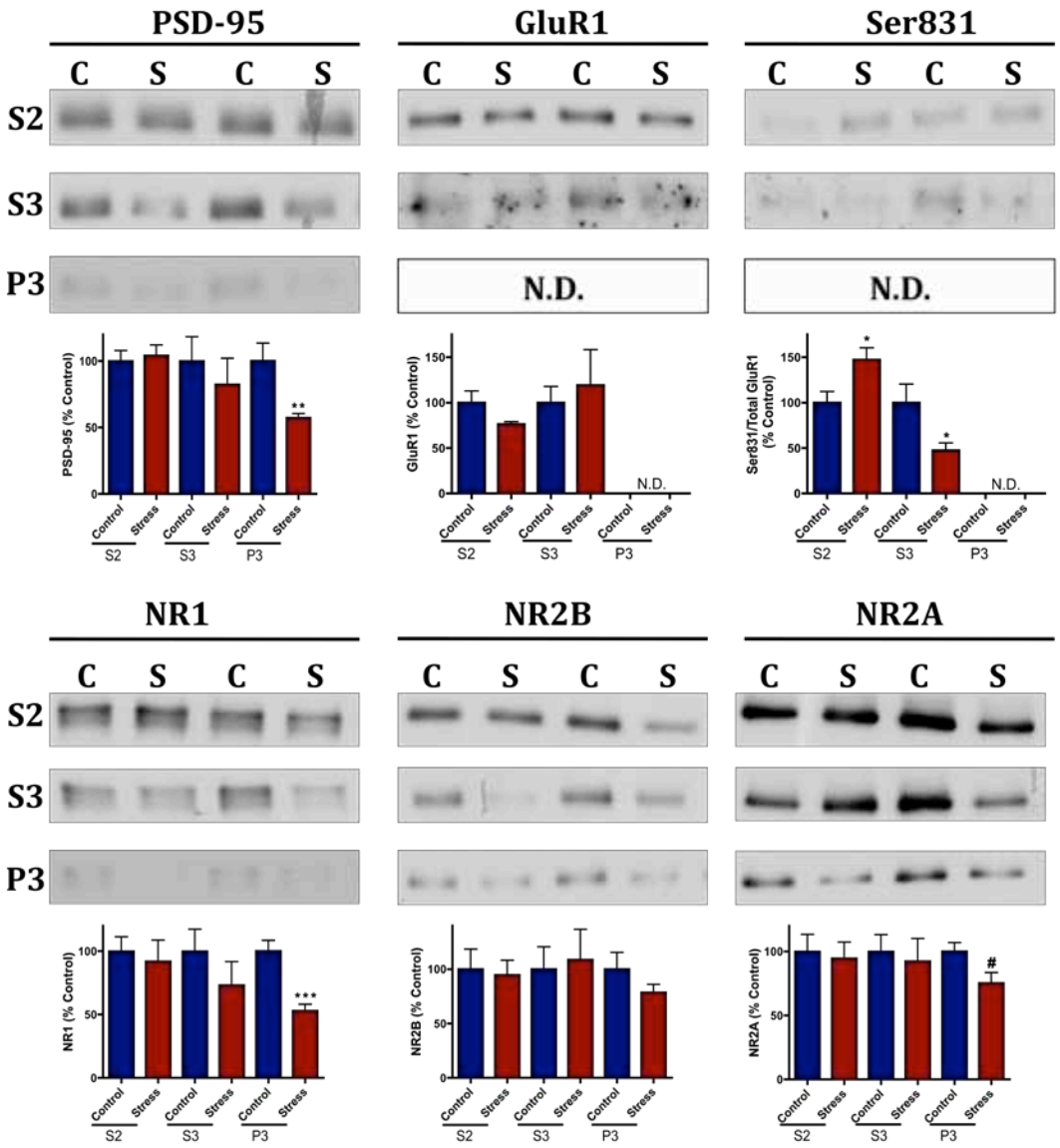

Figure 5. Distribution of several PSD-associated proteins in the subcellular fractions of hippocampal homogenates from P25 control and ES mice. PSD-95 was significantly reduced in P3 fractions from ES mice (p=0.0156). Although there was no change in the amount of total GluR1 detected in the S2 or S3 fraction, there was a trend for an increase in S2 (p=0.03) and a decrease in S3 (p=0.04) of phosphorylated Ser831 when normalized to total GluR1 in the respective fractions. The NR1 subunit of the NMDAR was significantly decreased in the P3 fraction from ES compared to control mice (p=0.0015). There were no differences in the amount of NR2B or NR2A subunits in any of the fractions when normalized to total protein loaded; however there was a trend for a decrease in the amount of NR2A in the P3 fraction from ES mice (p=0.051). (Control=5; Stress=5)

6). This is consistent with the total levels in each fraction shown in Figure 3, where there was reduced CaMKIIα in S1, S3, and P3. In the S2 fraction, the significant 13% reduction of CaMKIIα levels in the IPs from ES samples is similar to the ~12% decrease in the amount of CaMKIIα in the ES S2 fraction (figure 3). Thus, the IPs recapitulate the reductions in CaMKIIα levels detected in the ES fractions (Figure 3 and 6). Moreover, levels of Thr286 phosphorylation in IPs from the ES S3 fraction are significantly reduced; however, the ratio of phospho-Thr286 to total CaMKIIα is not different between the control and stress groups (Figure 6). Together this shows that ES mice have a reduced level of CaMKIIα in PSD-associated fractions compared to control mice, and that the ES mice also have a decrease total amount of CaMKIIα phosphorylated at Thr286 in these same fractions. This does not change the ratio of the CaMKIIα:Thr286 phosporylation in the PSD-associated fractions.

CaMKIIβ was only detected in the S2 fraction homogenates (Figure 3), but was detected in all IP complexes (Figure 6). In agreement with the western blot data from the S2 fraction total homogenate, CaMKIIβ was unchanged in the ES mouse IP from the same fraction. Interestingly, CaMKIIβ levels were significantly reduced in the IP from the S1 fraction of ES mice when normalized to CaMKIIα (Figure 6). These changes in CaMKIIα and CaMKIIβ levels in the different fractions of the ES mice alter the ratios of CaMKIIα and CaMKIIβ in the holoenzyme, potentially altering protein/protein interactions (Figure 6).

In order to look more specifically at potential changes in CaMKII's interaction with its known interacting proteins, we analyzed CaMKII IPs from the different fractions of control and ES mice by western blot. Total levels of PSD-95 in the S2 and the S3

Figure 6

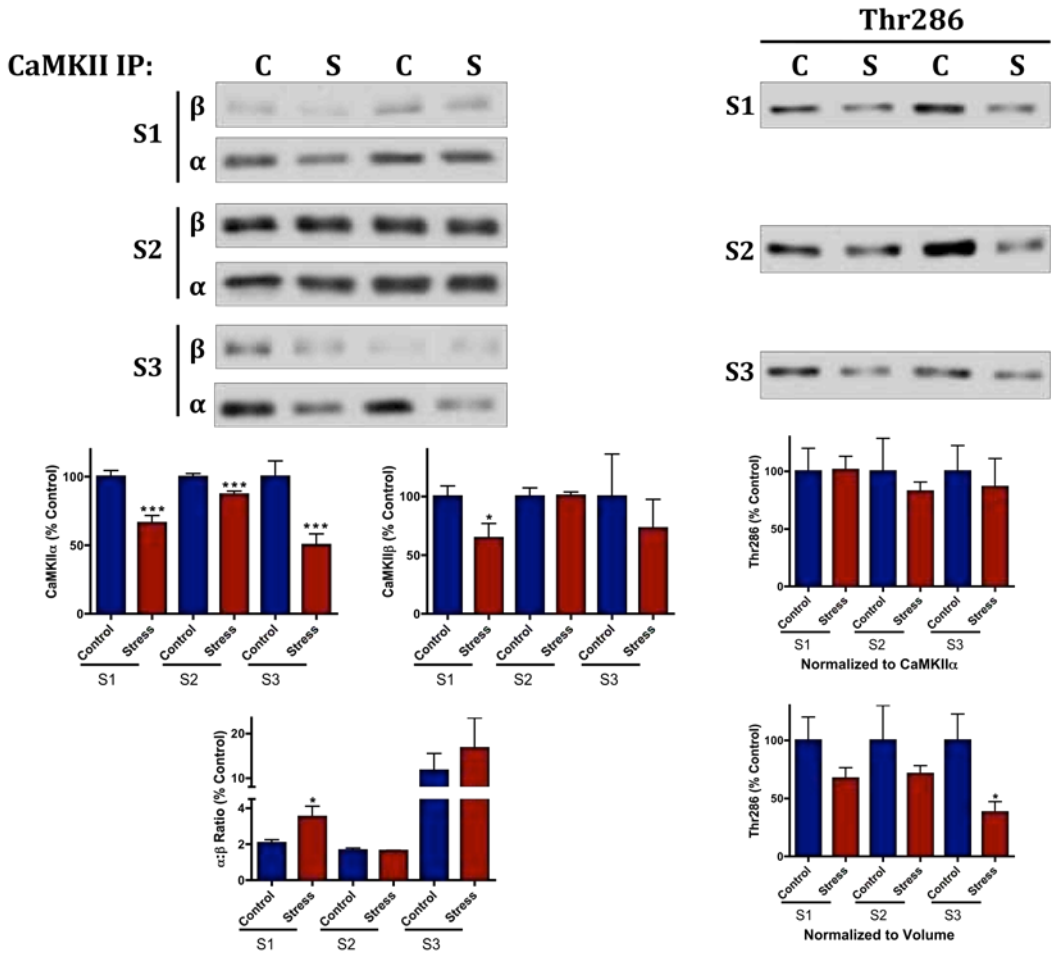

Figure 6. CaMKII immunoprecipitations on fractions isolated from P25 control and ES mice. The amount of CaMKIIα precipitated from ES mice was significantly decreased in all fractions (S1: p=0.0015; S2: p=0.0055; S3: p=0.0077). CaMKIIβ was only decreased in the S1 fraction from ES compared to WT mice when normalized to CaMKIIα (p=0.0487), revealing a shift in the CaMKIIα:CaMKIIβ ratio in the S1 fraction (p=0.04). When normalized to total CaMKIIα, phosphorylated Thr286 was unchanged. Alternatively, when normalized to volume there was a decrease in Thr286 phosphorylation in the IP from the S3 fraction (p=0.03), meaning there is an overall lose of CaMKIIα phosphorylated at Thr286 in the PSD-enriched fraction. (Control=5; Stress=5)

fractions from the control and ES mice were not significantly different (Figure 5). However, levels of PSD-95 in CaMKII IPs were increased by ~63% when normalized to the total amount of CaMKIIα in the IPs. In contrast, there was no difference in the interaction of CaMKII and PSD-95 in the S2 fraction (Figure 7). This means that although there is 50% less CaMKIIα in the S3 IP in the ES mice there is 63% more PSD-95 associated with the CaMKIIα that is present. Although not significant, there appears to be a 40% decrease in the CaMKIIα:CaMKIIβ ratio, suggesting that the stress is causing a shift in holoenzyme composition that may be altering CaMKII's interaction with PSD-95.

We also wanted to determine if there was a difference in the amount of NMDAR subunits that were interacting with CaMKII in the ES mice. The NR1 subunits were shown to have an increased association with CaMKII in both the S2 and S3 fractions of the ES mice when normalized to CaMKIIα (Figure 7). Co-IP of NR2A and NR2B with CaMKII were both increased in the S3 fraction of ES mice, but showed no change in the S2 fraction between groups (Figure 7). None of these increases are statistically significant, and additional studies to increase the N need to be performed.

To this point, all proteins evaluated showed increased interaction when normalized to CaMKIIα. To show the specificity for these increased interactions, we probed the fractions and IPs for A-Kinase Associated Protein 150 (AKAP150), a protein thought to indirectly complex with CaMKII via SAP97 (Nikandrova et al., 2010) (Figure 8). The expression of AKAP150 mirrored that of CaMKIIα throughout the fractions (Figure 8). More importantly, there was no change in the amount of AKAP150 associated with CaMKII when normalized to CaMKIIα in the IP in the S2 or S3 fraction

Figure 7

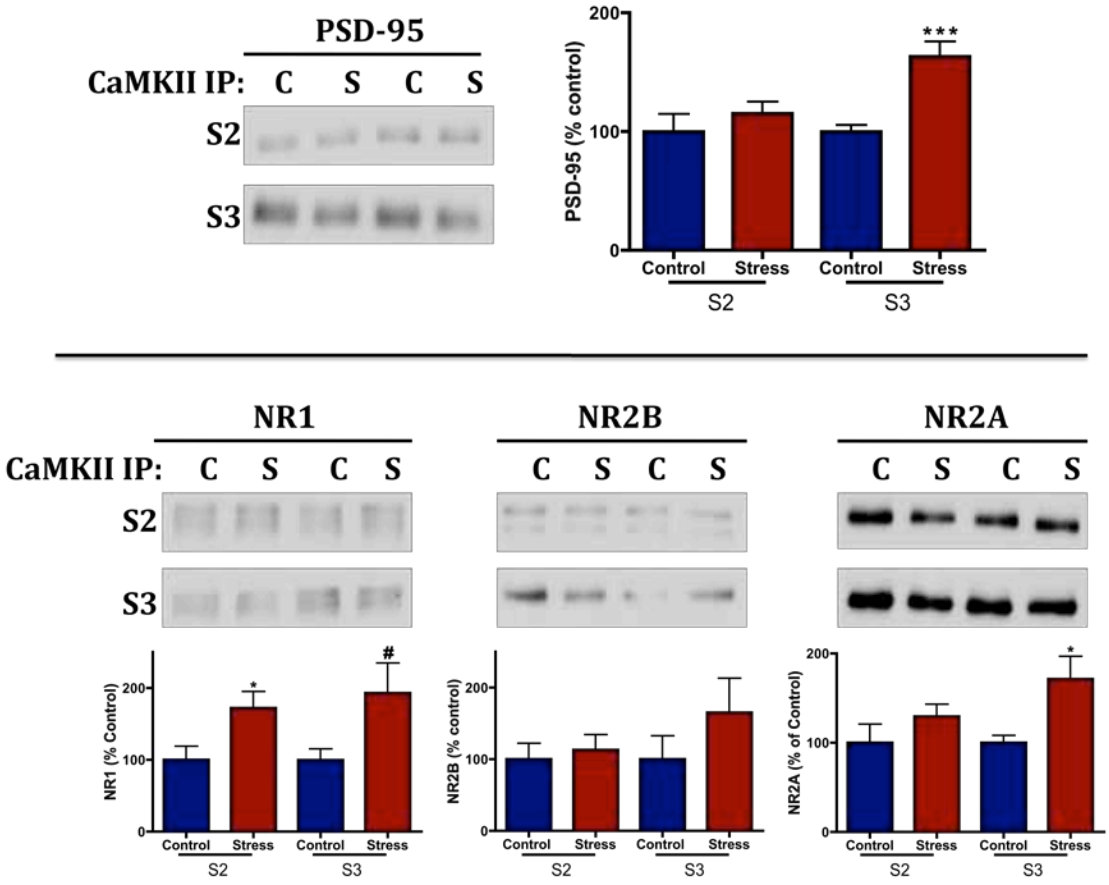

Figure 7. CaMKII co-IPs in S2 and S3 hippocampal fractions from P25 control and ES mice. Top panel: There is an increase in the amount of PSD-95 co-precipitated in S3 fractions from ES mice (p=0.0017). Bottom panel: CaMKII co-IP of NMDAR subunits. The amount of NR1 in the CaMKII IPs in S2 fractions from ES mice was increased compared to controls (p=0.04), with a trend for an increase in S3 fractions (p=0.06). NR2A showed a similar increase in CaMKII IPs from the S3 fractions in ES mice (p=0.02). NR2B co-IPs were unchanged in S2 fractions with a trend for an increase in the S3 fractions comparing control and ES mice. (Control=5; Stress=5)

of control versus ES animals (Figure 8).

Early-life stress induced electrophysiological changes

The mislocalization of CaMKII and the altered protein interactions, along with the decrease in PSD-95 that suggests a potential loss of dendritic spines in the ES mice, lead us to hypothesize that these mice would have altered electrophysiological properties associated with early-life stress. LTP experiments were performed as a cellular correlate to learning and memory. In slices from control mice there was a 187% potentiation of the slope of the fEPSP 60 minutes post LTP induction (Figure 9). Slices from the ES mice also showed LTP, but the extent of potentiation was reduced to 154% (Figure 9). The difference in LTP generation between control and ES mice was significant using the two-way repeated measures ANOVA statistical analysis ($p=0.0428$).

We wanted to identify if there are any changes in synaptic transmission that could lead to the reduction of LTP seen in the ES mice. To achieve this, we performed whole cell patch clamp recordings in CA1 pyramidal neurons from control and ES mice. By including Cs and TEA in the patch pipette to block K channels, we isolated AMPAR-mediated spontaneous-EPSCs (sEPSCs) while voltage-clamping the membrane at -70 mV. These events are action potential dependent, and are thought to be the result of multivesicular release events. The amplitude of the sEPSC, which is a function of the number of receptors present on the postsynaptic terminal as well as the function of individual AMPAR channels, is reduced 36% in ES slices compared to control slices (Figure 10). Additionally, the frequency of events, which can be altered by changes in the probability of release or the number of synapses, was decreased by 51% in ES slices

Figure 8

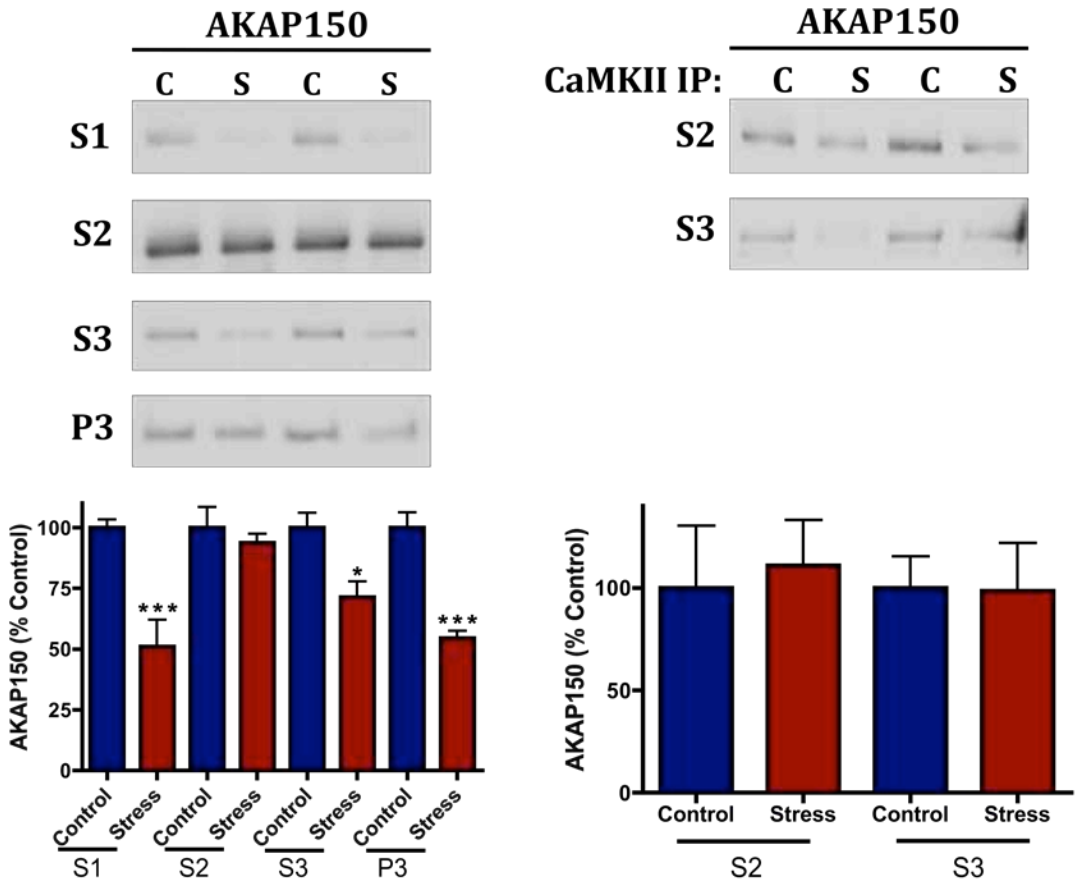

Figure 8. AKAP150 subcellular localization and co-IP with CaMKII in control and stress mice. Left panel: AKAP150 levels were decreased in S1 ($p=0.0028$), S3 ($p=0.0113$), and P3 ($p=0.0002$), paralleling the expression pattern of CaMKIIα. Right panel: The CaMKII co-IP of AKAP150 in S2 and S3 fractions from ES mice were unchanged from that of controls when normalized to the amount of total CaMKIIα in the respective IPs. (Control=5; Stress=5)

Figure 9

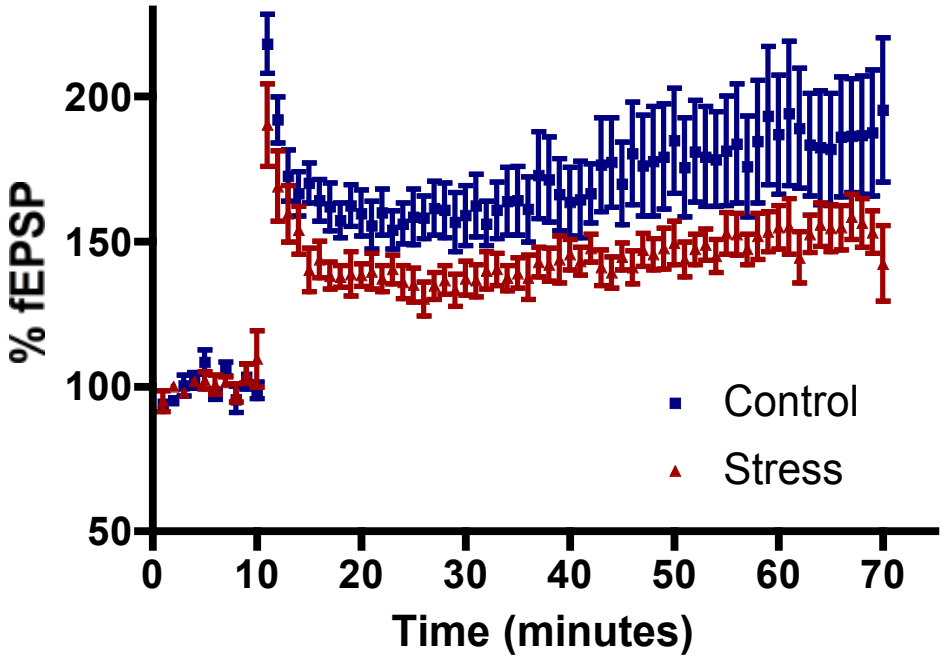

Figure 9. LTP recordings in P25-P28 control versus ES mice. A single-train, 100 Hz HFS was used to induce LTP in hippocampal slices from control and ES mice. 60 minutes post stimulation control slices had potentiated 187%, whereas ES slices had only potentiated 154%, a greater than 30% reduction in LTP due to early-life stress. (Control=6 slices, 4 mice; Stress=8 slices, 4 mice)

(Figure 10).

To understand if there is a developmental delay that may have altered the AMPA/NMDA receptor ratio that could account for the change in sEPSC responses, we again turned to whole-cell patch clamp. AMPAR mediated responses were generated by holding the cell at -70 mV, at which AMPAR-mediated evoked EPSCs can be isolated as NMDARs will be inactive due the Mg-blockade. After AMPAR responses were recorded the cell was stepped to +40 mV to relieve the Mg^{2+} block of the NMDAR, we measured 50 ms after the peak of the dual component eEPSC to identify the NMDAR component. There was no change in the AMPA/NMDA receptor ratios comparing control and ES slices (data not shown).

Long-term Effects of early-life stress

To understand the long-term effects of the early-life stress in adulthood, biochemical and electrophysiological analysis was also performed on 3-month old mice. Western blots of total hippocampal homogenates revealed a trend for a decrease in CaMKIIα expression following ES compared to control mice (Figure 11). CaMKIIβ expression in the same samples was unchanged, leading to a trend for a decrease in the CaMKIIα:CaMKIIβ ratio (Figure 11). However, there was no difference in Thr286 phosphorylation in the total homogenates of control and ES mice (Figure 11). GluR1 levels in total homogenates of control compared to the ES mice were unchanged; however, Ser831 levels were decreased in the ES mice when normalized to total GluR1 (Figure 11). Protein expression of all other proteins analyzed in the total homogenates was unchanged (data not shown).

Figure 10

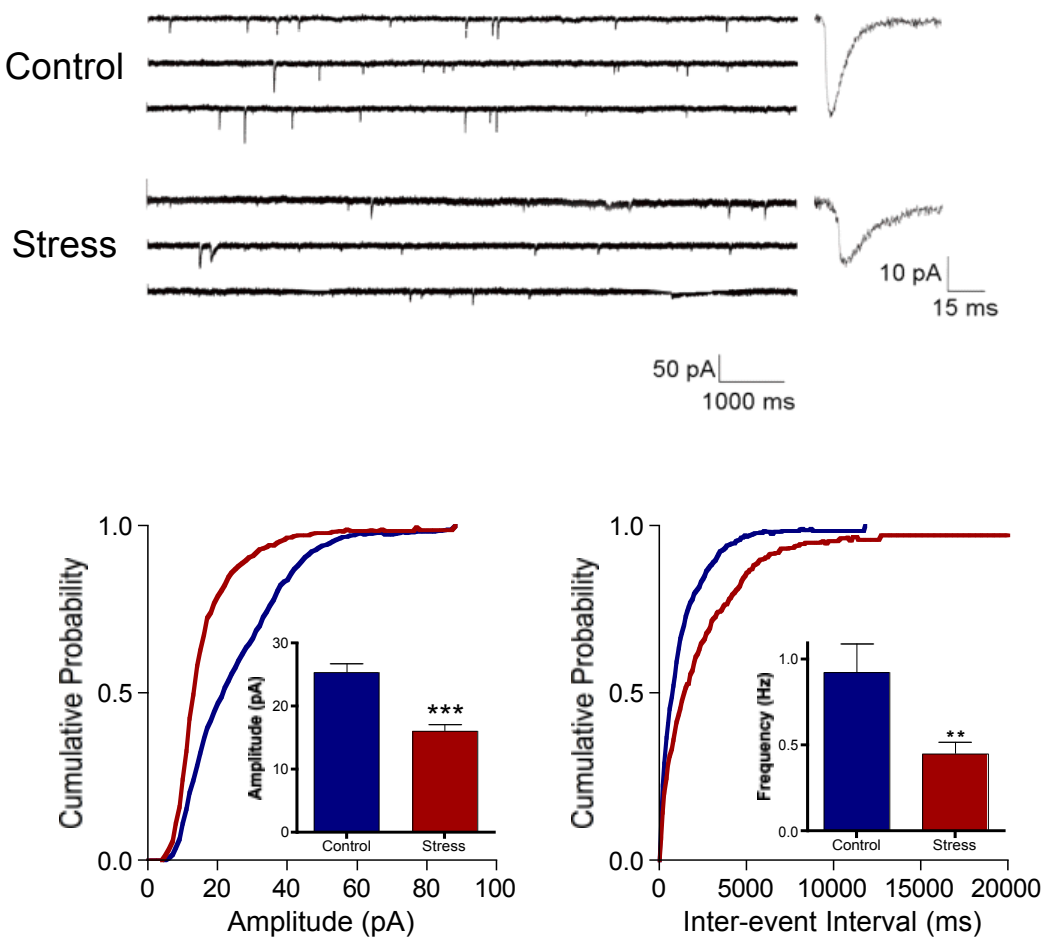

Figure 10. Spontaneous EPSCs from whole-cell voltage clamp recordings (Vh = -70 mV) revealed a decrease in both the amplitude (p=0.0001) and frequency (p=0.0117) of responses in ES compared to control mice. (Control=7 slices, 5 mice; Stress=9 slices, 5 mice)
(Figure courtesy of Brian Shonesy)

To take a closer look at protein distribution, subcellular fractionation was performed as previously described. CaMKIIα was unchanged throughout all fractions assayed. There were trends for a decrease in both S3 and P3 fractions (the PSD-associated fractions) where the majority of CaMKII localizes, fitting with the global decrease in CaMKIIα seen in the total homogenates (Figure 12). CaMKIIβ was unchanged in all fractions, which led to a trend for a decrease in the CaMKIIα:CaMKIIβ ratio in the ES mice in the P3 PSD-associated fraction (Figure 12).

We also wanted to determine the changes in subcellular localization of several other proteins important in learning and memory, especially their expression in the synaptic (S3 and P3) and extrasynaptic (S2) pools of protein. PSD-95 levels were significantly reduced in the adult ES P3 fraction compared to control (Figure 13). The trend for a decrease in the NR2B subunit of the NMDAR in the P3 fraction of adolescent ES mice (Figure 5) was also maintained into adulthood (Figure 13). Interestingly, NR2A levels in the P3 fraction were normal in adult ES animals (Figure 13), where there was a strong trend for a decrease in the adolescent ES animals (Figure 5). The early-life stress may be leading to a switch in the NR2B:NR2A ratio, which would potentially alter NMDAR function. The CaMKII dependent Ser1303 phosphorylation of the NR2B subunit can also affect NMDAR function. Interestingly, there was no change in the total levels of phospho-Ser1303 in the total homogenates in adult ES mice. However, there was a strong trend for an increase of Ser1303 phosphorylation in the S3 fraction, with a decrease of Ser1303 phosporylation in the P3 fraction in the ES mice (Figure 13), suggesting a shift in subcellular localization of NR2B containing NMDARs that are phosphorylated at Ser1303. This could drastically alter normal NMDAR function if there

Figure 11

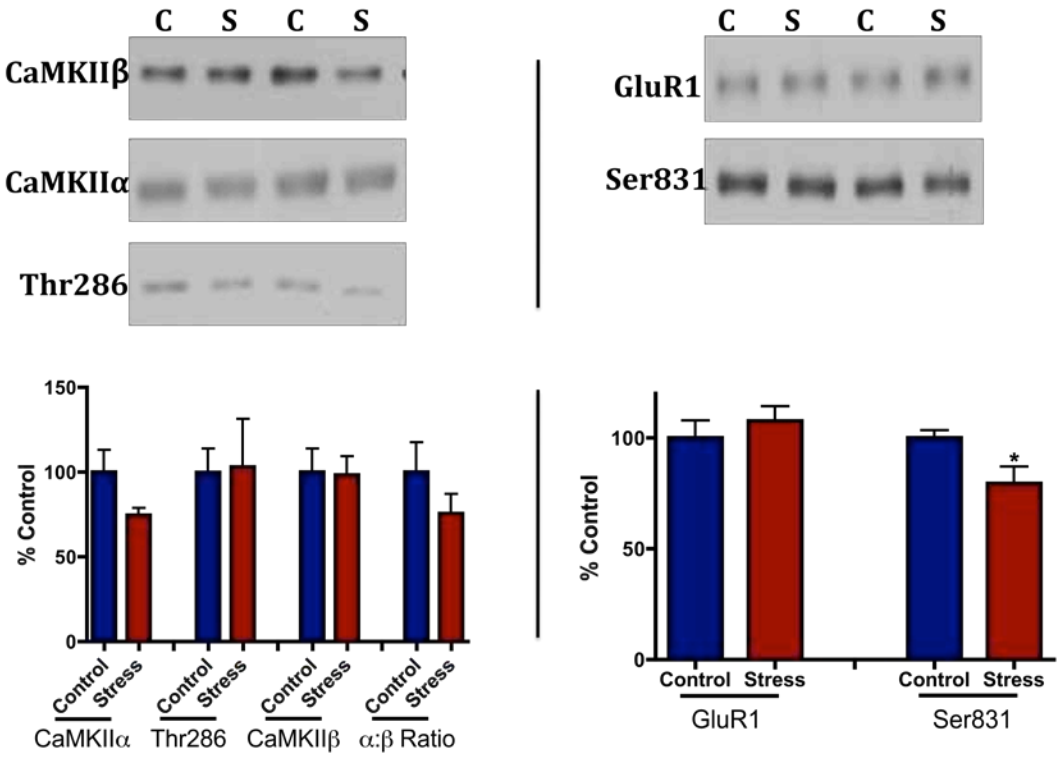

Figure 11. Western blot analysis of total homogenates from adult control and ES mice. Left panel: There was a trend for a 25% decrease in CaMKIIα levels in ES mice (p=0.10) with no change in CaMKIIβ levels when normalized to total protein loaded, leading to a slight non-significant trend for a reduced CaMKIIα:CaMKIIβ ratio. No change in the amount of Thr286 phosphorylation was detected when normalized to total CaMKIIα. Right panel: There was no decrease in the amount of total GluR1 in ES compared to control mice, but Ser831 phosphorylation was decreased 20% when normalized to total GluR1 (p=0.0374).
(Control=5; Stress=5)

Figure 12

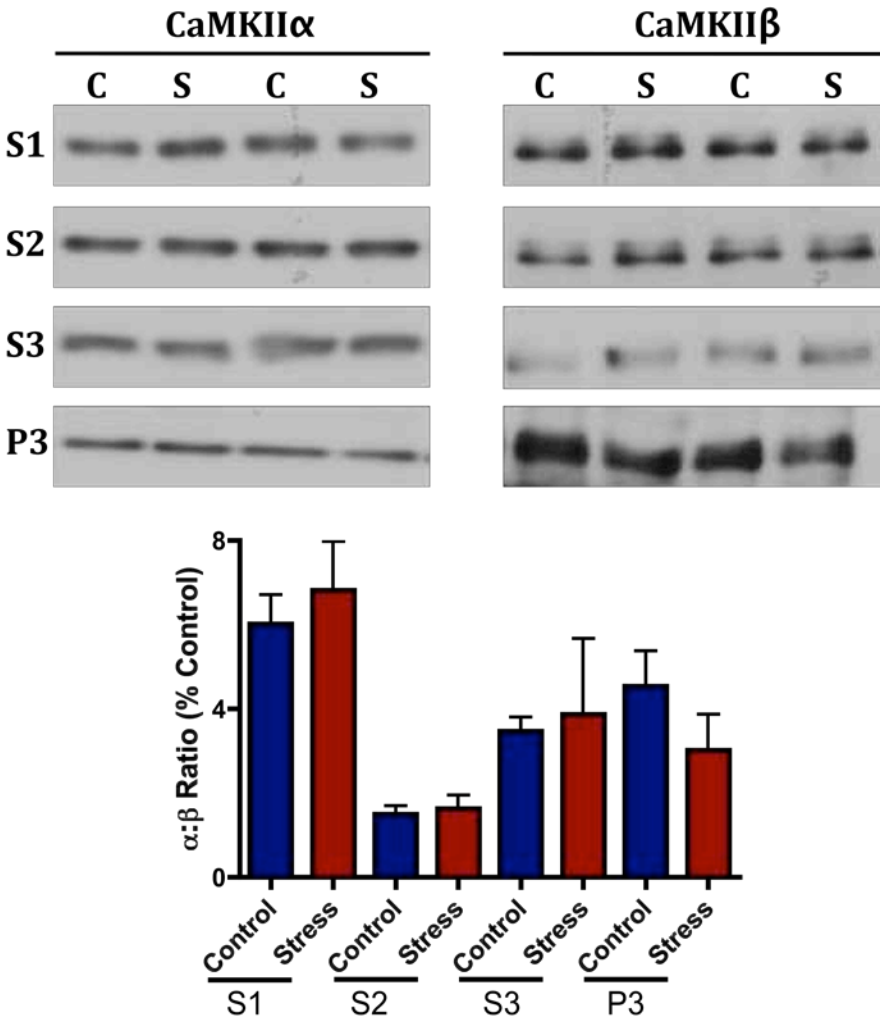

Figure 12. CaMKII western blots of subcellular fractions of hippocampal homogenates from adult control and ES mice. A trend for a decrease in CaMKIIα levels in S3 and P3 from ES mice, with no change in CaMKIIβ, leads to a non-significant 33% decrease in the CaMKIIα:CaMKIIβ ratio in the P3 fraction. (Control=5; Stress=5)

is a shift in subcellular populations of NMDARs that are being differentially regulated in the ES mice.

In adult mice, unlike adolescent mice, the GluR1 subunit of the AMPAR was readily detected in the P3 fraction, along with the S2 and S3 fractions. Furthermore, there is a strong trend for a decrease in the amount of GluR1 in the S3 and P3 fraction of adult ES mice compared to control mice, with no change in GluR1 levels in the S2 fraction (Figure 13). This redistribution of GluR1 was accompanied by a trend for a decrease in Ser831 phosphorylation in the S2 fraction (Figure 13).

Whole-cell patch clamp recordings revealed the amplitude of the sEPSCs was reduced 42% in adult ES cells versus control cells (Figure 14), as seen in adolescent mice. However, the frequency of sEPSCs was not changed between groups (Figure 14).

Discussion

Chronic early-postnatal stress is known to cause behavioral deficits lasting the life of the animal (MacQueen et al., 2003; Romeo et al., 2003; Rice et al., 2008). It is unknown how early-life stress alters neuronal processes, during these developmental periods, which creates a diseased state for the life of the animal. Through our work using an AS mouse model, we hypothesized that early-life stress would lead to misregulation of CaMKII during development that leads to long-lasting changes on a cellular level that cause behavioral deficits throughout the life of the animal.

Our biochemical data suggest there is a developmental effect on expression and localization of PSD proteins in the hippocampus of adolescent ES mice. At P25 ES mice have a reduction in PSD-95 levels in PSD-enriched fractions. This difference could be

Figure 13

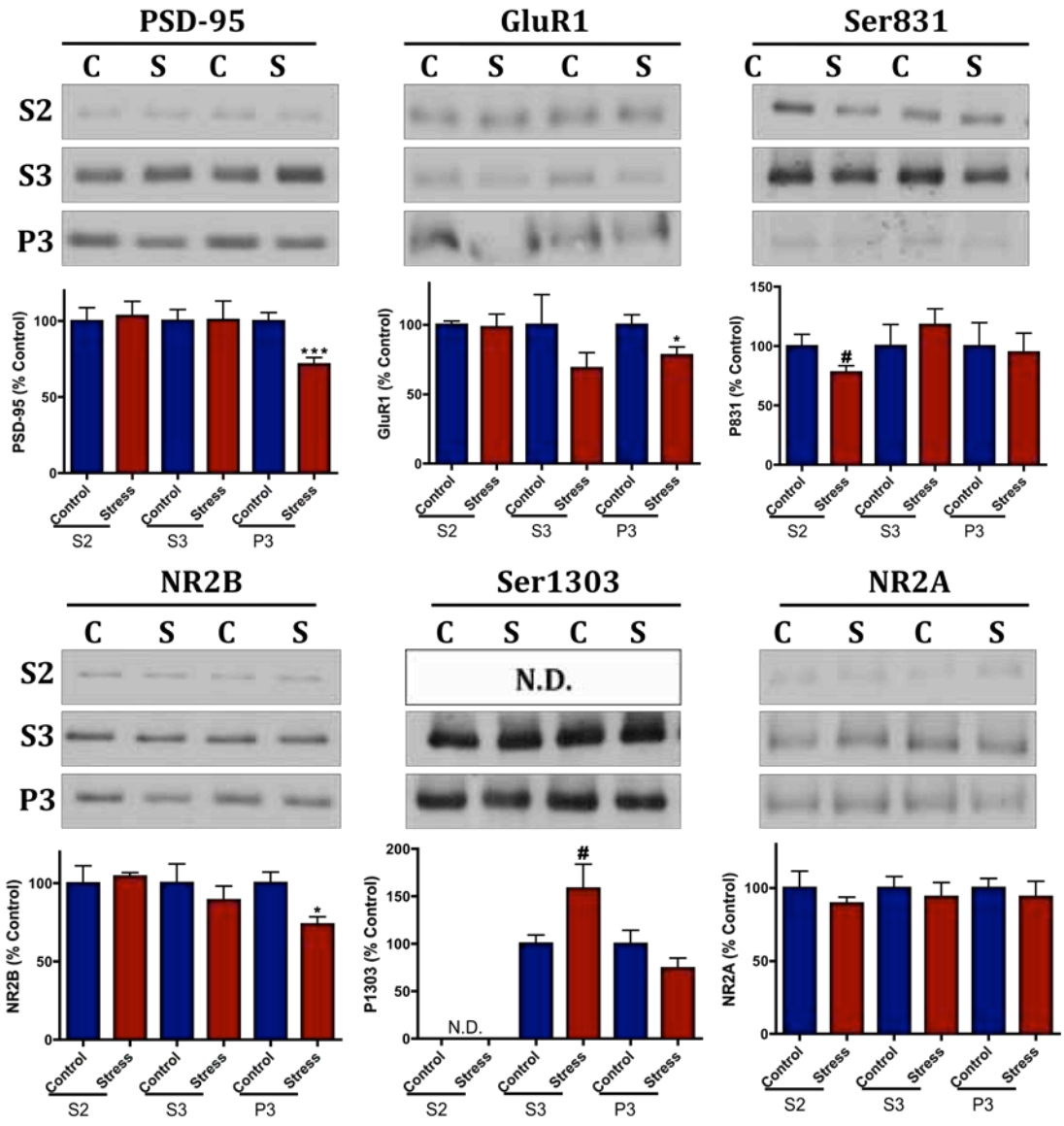

Figure 13. Subcellular fractionation of PSD-associated proteins in control and ES mice. Several proteins were shown to be decreased in the P3 fraction from ES mice, including PSD-95 (p=0.0038), GluR1 (p=0.0453), and NR2B (p=0.0148). When normalized to total NR2B in the S3 fraction there was a trend for an increase in the amount of Ser1303 phosphorylation of the NR2B subunit in ES mice (p=0.06). The level of Ser831 phosphorylation in the S2 fraction of ES mice showed a trend for a decrease when normalized to total GluR1 (p=0.08). (Control=5; Stress=5)

Figure 14

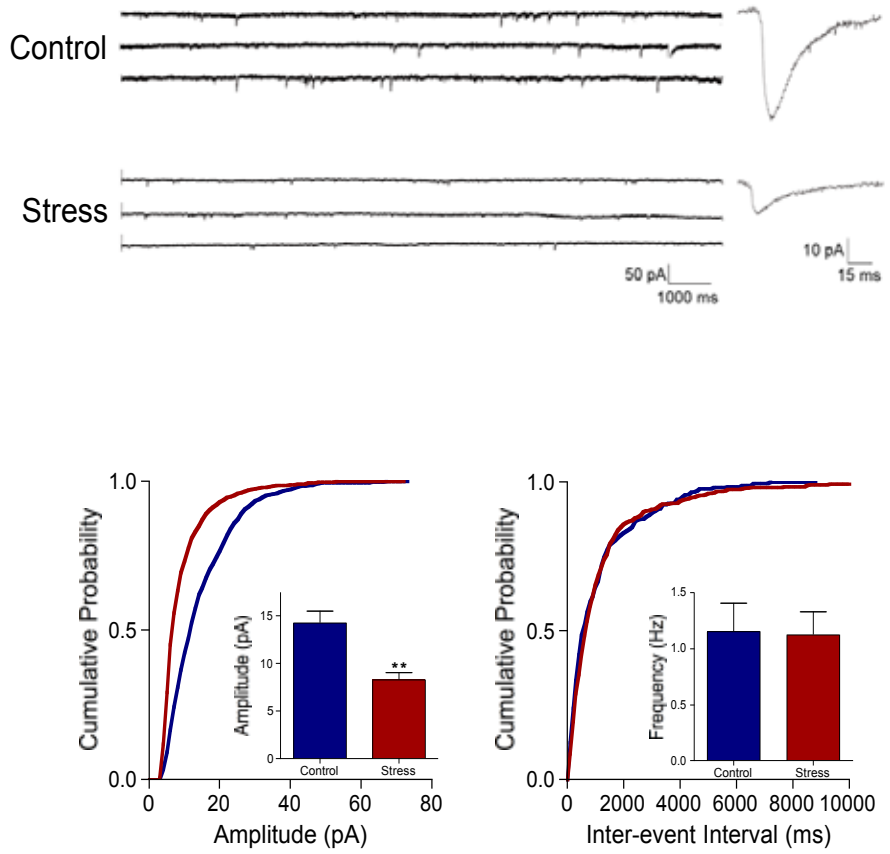

Figure 14. sEPSCs in whole-cell patch recordings from adult control and ES mice reveal a decrease in amplitude (p=0.0048) with no change in the frequency of the sEPSCs from ES mice.

due to a decrease in the number of PSDs in the ES mice or a restructuring of the PSD following early-life stress. There are data that demonstrate chronic stress leads to a dramatic decrease in dendritic arborization and spine number (Xu et al., 2009), consistent with a loss of PSD-95 from PSD-associated fractions. Furthermore, analysis of adult mice revealed a consistent reduction of PSD-95 in PSD-associated fractions from ES mice. Additionally, at these adult time points there are significant trends for a reduction in the NMDAR subunit, NR2B, as well as the AMPAR subunit, GluR1. Taken together, these data are consistent with a long-lasting change in PSD number or structure, induced by early-life stress in a specific developmental time window (P2-P9).

The redistribution of CaMKIIα, which leads to a decrease in the amount of CaMKIIα associated with the PSD-enriched fractions, could be due to a decrease in number or morphology of PSDs. Alternatively, misregulation of the kinase may be causing the alterations in the PSDs themselves. Support for this hypothesis can be seen when evaluating the subcellular localization of GluR1 and Ser831-phosphorylated GluR1 at P25. No changes in the total levels of GluR1 were detected between control and ES animals; however, there were significant ~50% decreases in the amount of Ser831 phosphorylation in the P3 fractions in the ES mice. This suggests that CaMKII function may be misregulated in PSD-associated fractions, leading to altered phosphorylation of Ser831 in GluR1 AMPAR subunits, and changes in AMPAR function, supported by decreased sEPSC amplitudes. Interestingly, this difference in Ser831 phosporylation is not detected in the S3 and P3 adult time points, but adult ES mice were shown to have a significant trend for reduced Ser831 phosphorylation in the S2 fraction, along with a trend for a reduction in phosphorylated Ser1303 of NR2B. The altered phosphorylation

of Ser831 across the different fractions, and Ser1303 in the S2 fraction, from control versus ES mice may suggest that AMPARs, and potentially NMDARs, are being differentially modulated at different membrane sites (i.e. synaptic versus exptrasynaptic). Current efforts are underway to create fractionation protocols coupled to biotinylation assays to identify biochemical changes in synaptic versus exptrasynaptic membranes. Together this may indicate that CaMKII misregulation, leading to alterations in GluR1 phosphorylation, is a component of a cellular mechanism leading to changes in the PSDs of ES mice.

CaMKII immunoprecipitation studies from the PSD-enriched fractions of ES mice revealed an altered association with PSD-95. Although less CaMKIIα was immunoprecipitated from the ES mice, there was a >60% increase in the amount of PSD-95 co-precipitated. We know that the ratio of CaMKIIα:Thr286 phosphorylation has not changed, so it does not appear that this increased interaction with PSD-95 is mediated through Thr286 phosphorylation. Could this be due to a shift in the CaMKIIα:CaMKIIβ ratio? Although not statistically significant, there does appear to be a 28% reduction in CaMKIIβ in the ES S3 fraction IP normalized to CaMKIIα.

The decrease in hippocampal LTP generation at P25 in ES hippocampal slices could be due to a decreased number synapses recruited, thus leading to a decrease in LTP. Additionally, the decrease in both frequency and amplitude of the sEPSCs points to a decrease in the total number of synapses on a particular neuron. Although the decrease in sEPSC amplitude is maintained into adulthood, the decrease in frequency returns to WT levels by P90. This suggests that there is a potential decrease in the number of PSDs due to a developmental delay, seen at P25, which is corrected for by adult time points.

The decrease in sEPSC amplitude that is maintained into adulthood implies that the proper regulation at the PSD remains altered at this later time point. These data appear to be in agreement with the hypothesis that there is a decrease in the number of spines or an alteration in spine morphology that is causing a decrease in postsynaptic responses.

The trend for reduced protein levels of CaMKIIα, NR2B, and GluR1 in PSD-associated fractions supports the hypothesis that there are either decreased PSD number or altered PSD morphology in the hippocampus of ES mice. This could potentially lead to the decrease in EPSC frequency seen in adolescent ES mice. Less activation of postsynaptic neurons would lead to a decrease in CaMKII activation, evidenced by the decrease in CaMKII localizing to the PSD-associated fractions in the ES mice. This in turn may be altering CaMKII dependent phosphorylation of Ser1303 of the NR2B subunit and Ser831 of the GluR1 subunit. A decrease in Ser831 could be seen electrophysiologically as a decrease in EPSC amplitude, which we do show in both adolescent and adult time points. Thus, we hypothesize the dysfunction in the ES mice is due to a combination of decreased PSD number with altered signaling of CaMKII, as well as additional signaling cascades that have yet to be tested.

Despite promising data obtained in these initial early-life stress experiments, changes in the animal care facility compromised our ability to reliably generate ES and control mice. A high percentage of pups in the ES environment died, and weights of the controls were not different from the ES survivors. This situation underscores the importance of having consistent proper maintenance of mouse colonies. Ongoing experiments have been moved into a more stable environment where the health of the mice will be appropriately maintained. The biochemical, electrophysiological, as well as

behavioral experiments will be continued to elucidate the role of CaMKII in the learning and memory deficit associated with earl-life stress.

These experiments demonstrate that environmental stressors, occurring during early postnatal development, can lead to persistent and evolving synaptic and molecular changes that last into adulthood. Although we were able to identify CaMKII misregulation and altered localization in the early-life stress mice we do not know if this is due to a direct effect on the kinase or a compensatory mechanism. To better understand the role of CaMKII regulation during development we decided to take advantage of the CaMKIIα-Thr286Ala knock-in transgenic mouse model.

CHAPTER V

CaMKII-Thr286Ala KNOCK-IN MICE

Introduction

Biochemical data generated using the early-life stress model (Chapter 4) suggest that CaMKII misregulation early in postnatal development can alter normal cellular processes for the life of the animal. Thus we sought an understanding of how normal development is affected by disrupting CaMKIIα auto-phosphorylation.

The phosphorylation of CaMKII is vital for proper subcellular localization and directing protein/protein interactions that are thought to be necessary for normal learning and memory (Chapter 1: Introduction) (Colbran and Brown, 2004). However, much of our understanding of these processes comes from work *in vitro* and/or in cultured neurons. To understand how altering CaMKIIα-Thr286 autophosphorylation affects CaMKII expression, localization, and protein/protein interactions *in vivo*, and in turn affecting learning and memory, we took advantage of the CaMKIIα-Thr286Ala knock-in mice (Giese et al., 1998). CaMKII regulation and the phenotypes seen in the knock-in mice were completely described in the introduction of chapter 1. Briefly, the CaMKIIα-Thr286Ala knock-in (KI) mice are able to undergo normal Ca^{2+}/calmodulin-dependent activation leading to a translocation of CaMKII to the PSD. However, due to the inability of the kinase to undergo autophosphorylation at Thr286, CaMKIIα is unable to become autonomously active as Ca^{2+} dissipates, reducing the binding of CaMKII to

several of its interacting partners, and decreasing the affinity of the kinase for PSDs. Until now this hypothesis has not been directly tested *in vivo*.

Research using CaMKIIα-Thr286Ala KI mice to understand how misregulation of CaMKIIα leads to memory deficits has focused solely on the adult. CaMKIIα expression begins at ~ P5 in the rodent, so these mice live there entire postnatal lives without proper CaMKIIα function. Thus, the adult phenotypes may represent acute neuronal deficits due to the lack of Thr286 autophosphorylation, or may reflect an altered functional state due to developmental compensation.

Results

CaMKII expression pattern in WT versus KI mice

We first wanted to describe the expression pattern of CaMKII in the hippocampus from P25 KI mice compared to WT controls (Figure 1). Western blot analysis of total hippocampal homogenates confirmed the genotypes of individual mice by readily detecting Thr286 phosphorylation in WT mice with an absence of Thr286 phosphorylation in the homogenates from the KI animals (Figure 1). A 40% reduction in total CaMKIIα, along with a 33% increase in total CaMKIIβ leads to a 58% reduction in the α:β ratio (Figure 1). Thus, the absence of Thr286 phosphorylation in the KI mice alters the expression pattern of total CaMKII in adolescence. We hypothesize that the lack of Thr286 phosphorylation and the change in α:β ratio will lead to altered subcellular localization of CaMKII as well as changes in normal protein/protein interactions.

Figure 1

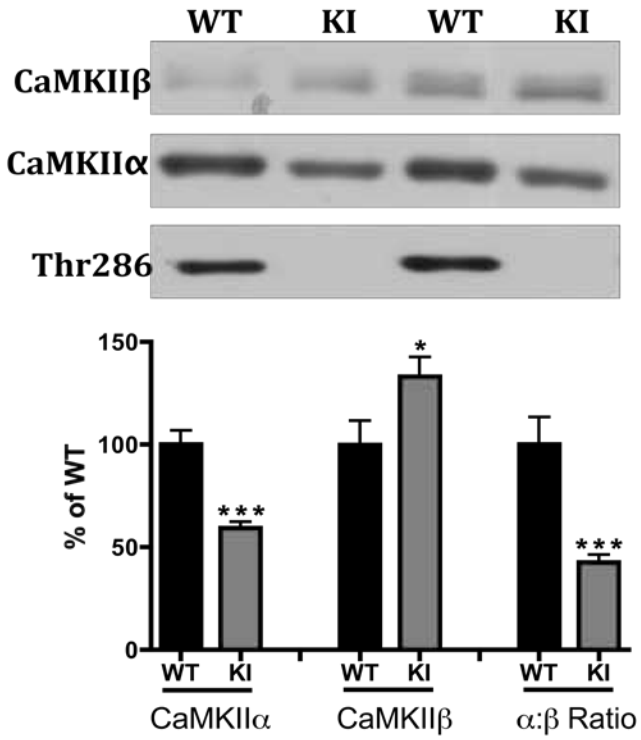

Figure 1. Western blot analysis of total hippocampal homogenates from P25 WT and KI mice. CaMKIIα levels were decreased 40% ($p<0.0001$) and CaMKIIβ levels were increased 33% ($p=0.0424$) in KI compared to WT mice. The change in CaMKII expression leads to an overall 58% decrease in the CaMKIIα:CaMKIIβ ratio ($p=0.0004$) in the KI mice. Probing for phosphorylated Thr286 reveals the total absence of Thr286 phosphorylation in the KI mice, confirming the genotyping. (WT=7; KI=9)

Subcellular fractionation was performed to identify if CaMKII localization was altered in P25 KI mice (Figure 2). The CaMKIIα levels were significantly reduced in the S1 fraction from the KI mice, whereas CaMKIIα levels in S2 were unchanged, although there was a slight trend for a decrease in the KI mice (Figure 2). The CaMKIIα levels in S3 and P3 fractions from the KI mice were dramatically decreased, 87% in S3 and 95% in P3 (Figure 2). CaMKIIβ in the S1 and S2 fractions of the KI mice were increased 130% and 60%, respectfully, whereas CaMKIIβ was decreased 70% in both S3 and P3 fractions (Figure 2). The changes in expression and localization of both CaMKII isoforms leads to a significant decrease in the α:β ratio in all fractions (Figure 2).

CaMKII immunoprecipitation in WT and KI mice

The altered CaMKII expression, localization, and isoform ratio led us to hypothesize that there were changes in CaMKII protein/protein interactions, specifically at the PSD. We used immunoprecipitation assays to probe for changes in interaction of CaMKII with several known interacting partners in the different subcellular fractions. Due to our interests in determining what is occurring at the PSD in the WT versus KI animals, I wanted to be able to perform the immunoprecipitation assays on the entire PSD-associated fraction (S3 and P3). To this end the pooled S3 and P3 fractions were used as inputs.

Levels of CaMKIIα immunoprecipitated from S3 fractions of KI mice were decreased 80% compared to WT when normalized to volume (Figure 3). CaMKIIβ levels were decreased 46% in PSD-associated fractions of KI mice compared to WT mice when normalized to volume. The decrease in the amounts of the CaMKII isoforms in the

Figure 2

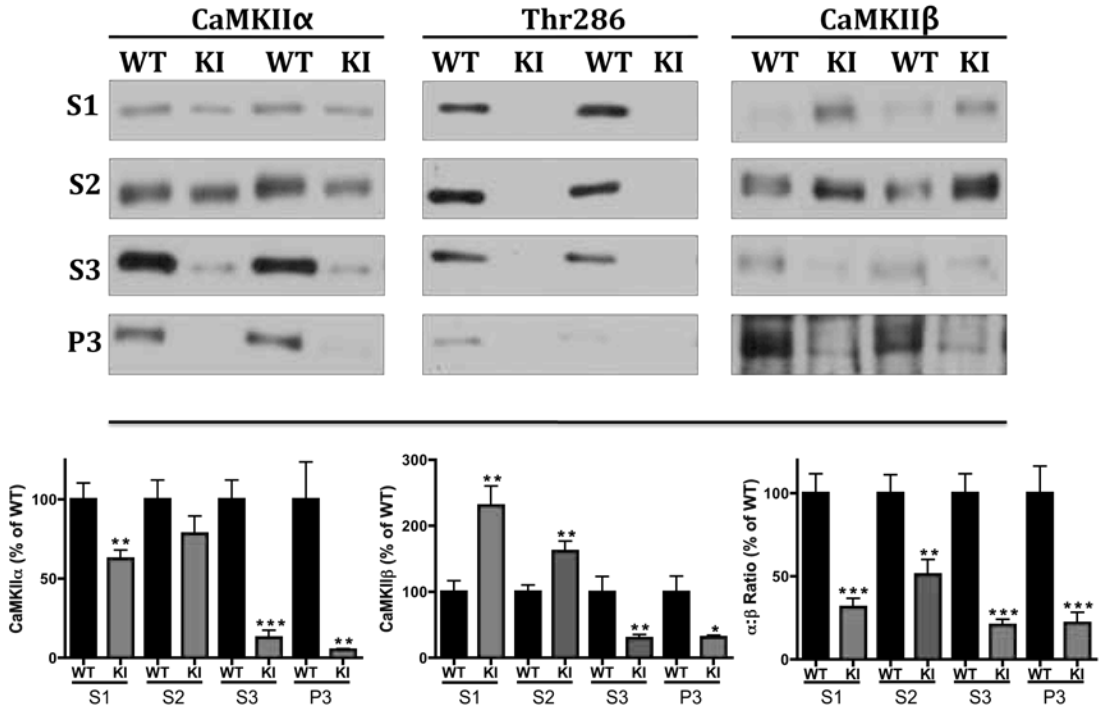

Figure 2. Western blot analysis of hippocampal subcellular fractions from P25 WT and KI mice. CaMKIIα levels were significantly decreased in S1 (40%; p=0.003), S3 (87%; p<0.0001), and P3 (95%; p=0.0016) KI fractions. CaMKIIβ levels were increased in S1 (130%; p=0.0016) and S2 (60%; p=0.0038) KI fractions and decreased in S3 (70%; p=0.007) and P3 (70%; p=0.015) KI fractions. Due to the shift in expression, CaMKIIα:CaMKIIβ ratio is decreased in all fractions S1 (69%; p<0.0001), S2 (49%; p=0.0025), S3 (80%; p<0.0001), and P3 (79%; p=0.0008) in the KI animals. No Thr286 phosporylation was detected in any fraction from the KI mice. (WT: S1=10, S2=10, S3=10, P3=7; KI: S1=12, S2=12, S3=12, P3=7)

Figure 3

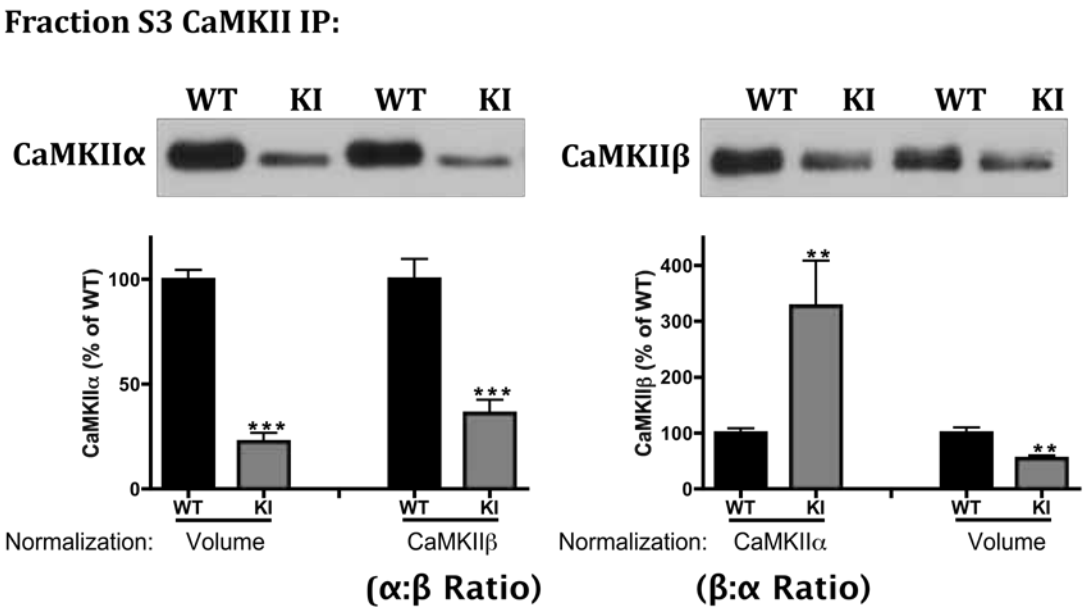

Figure 3. CaMKII immunoprecipitation from the PSD-associated fraction (S3) of hippocampal subcellular fractionation from P25 WT and KI mice. The amount of CaMKIIα in the KI IP was decrease 78% ($p<0.0001$) when normalized to volume. When normalized to the amount of CaMKIIβ, the CaMKIIα:CaMKIIβ ratio in the KI IP was decreased 64% ($p=0.0004$). CaMKIIβ, normalized to volume, was decreased 46% ($p=0.0033$). When normalized to the amount of CaMKIIα in the IP (CaMKIIβ:CaMKIIα) ratio, CaMKIIβ was increased significantly (225%; $p=0.0041$). Taken together, the KI mice have reduced holoenzyme in the PSD-associated fraction, but the holoenzyme that is present has an increase in the amount of CaMKIIβ per CaMKIIα subunits. (WT=10; KI=7)

PSD-associated fraction of the KI mice leads to a subsequent 64% decrease in the α:β ratio (Figure 3). These decreases in CaMKII isoforms seen in the immune complexes mirror those seen in the whole S3 and P3 fractions (Figure 2 and 3). CaMKIIβ-Thr287 phosphorylation could be compensating for the loss of CaMKIIα-Thr286 phosphorylation, creating an autonomously active kinase. To understand the contribution of Thr287 phosphorylation in the KI mice we quantified the amount of CaMKIIβ-Thr287 phosphorylation in the PSD-associated fraction (Figure 4). There was no change in the amount of phosphorylated Thr287 in the PSD-associated fraction from the KI mice when normalized to total CaMKIIβ (Figure 4). By normalizing to the Ponceau-S total protein stain, we revealed that the total amount of CaMKIIβ phosphorylated at Thr287 was decreased by 74% (Figure 4). Taken together this suggests that CaMKIIβ levels are down in the PSD-associated fraction of KI mice, but there is no change in the ratio of Thr287/CaMKIIβ. Additionally, this is shown when the amount of CaMKIIβ and the amount of Thr287 in the IP is normalized to the amount of CaMKIIα. In both cases there is a 2-fold increase in the KI versus the WT (Figure 3 and 4).

CaMKII-complexes in WT and KI mice

To begin to understand how CaMKII protein/protein interactions are altered in the KI mice we looked at changes in the co-immunoprecipitation with CaMKII of several known interacting proteins. The levels of NR1, NR2B, and NR2A in the PSD-associated fraction were unchanged between genotypes when normalized to Ponceau-S total protein stain (Figure 5). Co-immunoprecipitation of NR1, NR2B, and NR2A with CaMKII was significantly reduced in KI compared to WT when normalized to volume (Figure 5).

Figure 4

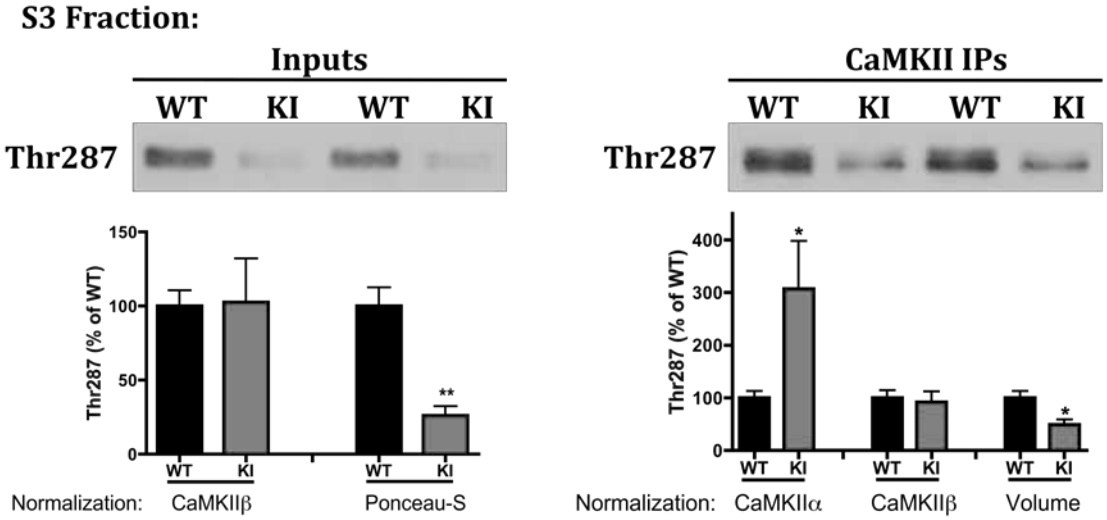

Figure 4. CaMKIIβ-Thr287 phosphorylation in PSD-associated fraction from P25 WT and KI mice. Left panel (S3 inputs): The amount of CaMKIIβ-Thr287 phosphorylation was unchanged in the S3 fraction when normalized to CaMKIIβ, revealing that the Thr287 phosphorylation was decreased to the same extent as the CaMKIIβ in the KI mice. This is visualized when normalizing Thr287 phosphorylation to total protein loading, where the Thr287 is decreased 74% in the KI compared to WT (p=0.0003). Right panel (S3 CaMKII IP): The amount of CaMKIIβ-Thr287 phosphorylation in the CaMKII IP from KI mice was decreased 52% (p=0.0118) when normalized to volume. No difference in the amount of Thr287 phosphorylation between WT and KI mice was observed when normalized to CaMKIIβ in the IPs, meaning the fraction of CaMKIIβ-Thr287 phosphorylation is unchanged. By normalizing to the amount of CaMKIIα in the IP, there is a 3-fold increase in the amount of CaMKIIβ-Thr287 phosphorylation per CaMKIIα in the KI mice (p=0.0161). (WT=9; KI=6)

This is not surprising due to the significant reduction in CaMKII in the IPs, from the KI mice (Figure 3). However, normalization to the amount of CaMKIIα in the IPs revealed, a significant ~2-fold increase in the amount of NR1 and NR2B in KI compared to WT mice (Figure 5). However, there was no difference in the amount of NR1 or NR2B present in the co-immunoprecipitaion in WT versus KI animals when normalized to levels of CaMKIIβ (Figure 5). This again suggests that CaMKIIβ may be directing these interactions at the PSD or potentially compensating for the mutant CaMKIIα in the KI mice.

The total amount of NR2A in the co-immunoprecipitation was decreased when normalized to volume; however, unlike NR1 and NR2B, when normalized to CaMKIIα there was no difference in the amount of NR2A relative to CaMKIIα (Figure 5). Furthermore, when normalized to the amount of CaMKIIβ in the IPs, there is a trend for a decrease in the amount of co-immunoprecipitated NR2A (Figure 5).

CaMKII is able to regulate NR2B containing NMDARs via phosphorylation of Ser1303 residue in the C-terminus (Sessoms-Sikes et al., 2005). We wanted to determine if the phosphorylation at Ser1303 is misregulated in PSD-associated fractions from KI mice, which could potentially affect learning and memory behaviors in these mice. Western blot analysis of the PSD-associated fraction of P25 mice revealed no change in the amount of Ser1303 normalized to total NR2B (Figure 6). Additionally, there was no change in the fraction of NR2B phosphorylated at Ser1303 in the co-immunoprecipitation, seen when normalizing the phospho-Ser1303 signal to total NR2B in the co-immunoprecipitation (Figure 6).

Figure 5

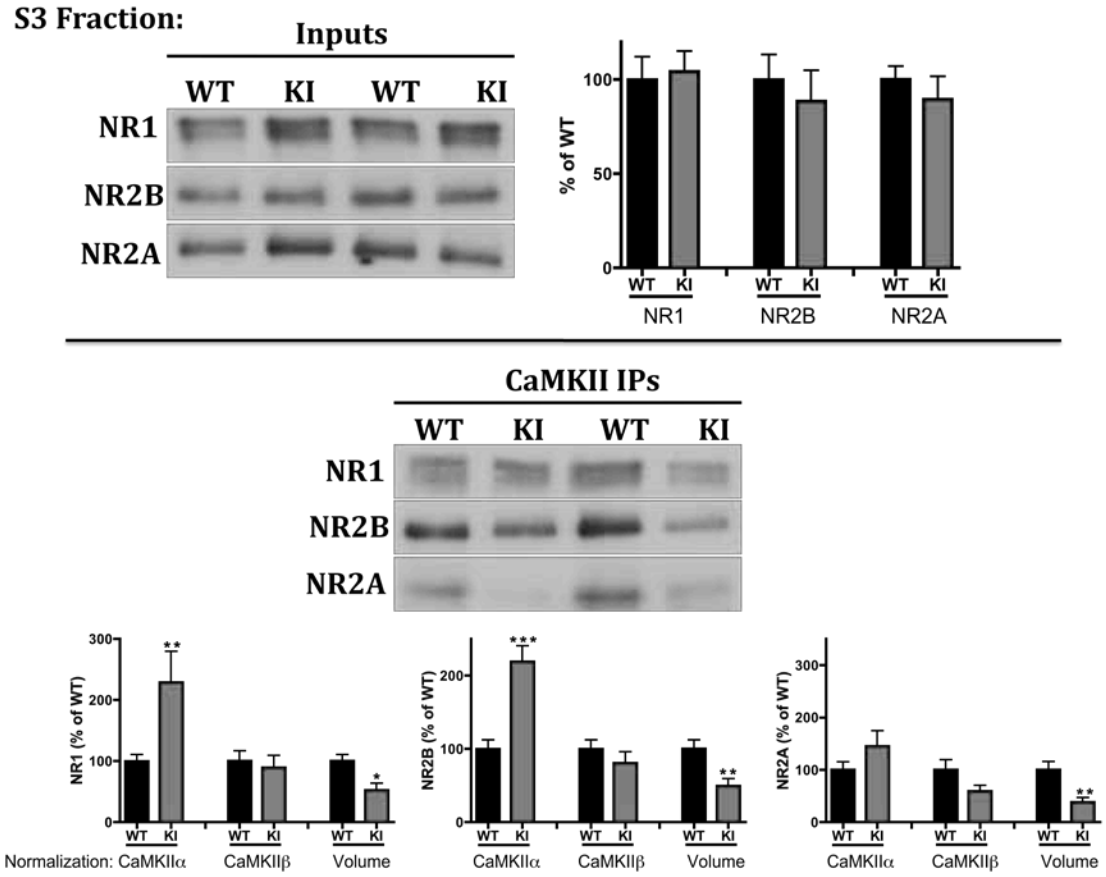

Figure 5. NMDAR complexes in hippocampal S3 fractions in P25 WT and KI mice. Top panel (S3 inputs): Total levels of NR1, NR2B, and NR2A are unchanged in KI compared to WT mice. Bottom panel (S3 CaMKII IPs): Co-immunoprecipitaion of NMDAR in S3 fractions from WT and KI mice. When normalized to the amount of CaMKIIα in the IP, there is a greater than 2-fold increase in the association of NR1 (128%; p=0.0072) and NR2B (118%; p=0.0001) in the KI mice. Normalizing to the amount of CaMKIIβ reveals that the relative amount of NR1 and NR2B is unchanged, meaning NR1 and NR2B decreased to the same extent as CaMKIIβ in the IPs. The amount of NR1 and NR2B are decreased in the IPs, seen when normalizing to volume, 48% (p=0.010) and 51% (p=0.0092), respectively. The amount of NR2A in the IPs was decreased 63% (p=0.0087) in the KI mice when normalized to volume. When normalized to CaMKIIα there was no difference in the fraction of NR2A coming down in the IP, but interestingly, when normalized to CaMKIIβ there was a trend for a 40% decrease in the fraction of NR2A (p=0.1) associating with CaMKIIβ. (WT=10; KI=7)

Figure 6

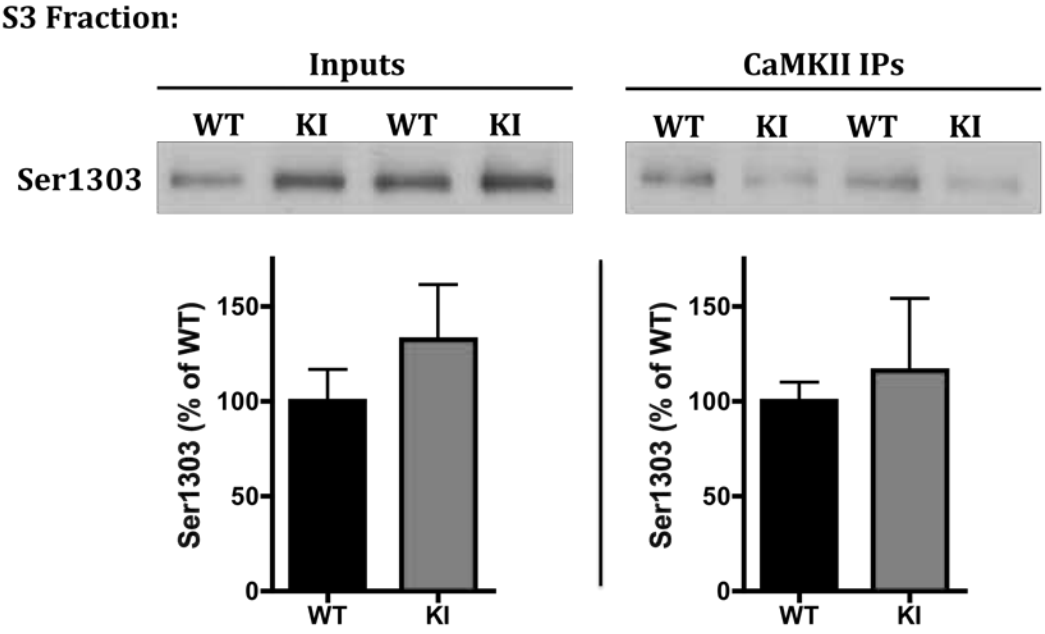

Figure 6. Expression and CaMKII co-immunoprecipitation of NR2B-Ser1303 phosphorylated subunits in WT and KI mice. When normalized to the amount of total NR2B in the S3 fraction there was no change in the amount of Ser1303 phosphorylation in the inputs (left panel) or in the CaMKII IPs (right panel). (WT=10; KI=7)

To determine if the increased interaction of CaMKIIα with NR1 and NR2B extends to additional PSD-associated proteins that complex with CaMKII, we also probed the co-immunoprecipitations for PSD-95. The amount of PSD-95 in the PSD-associated fraction was unchanged between WT and KI mice (Figure 7). There was a strong trend for a ~15% decrease in the amount of PSD-95 in the KI mice ($p=0.085$). Co-immunoprecipitation of PSD-95 with CaMKII was readily detected via western blot (Figure 7). The total amount of PSD-95 in the IPs was decreased by 45% in the KI mice when normalized to volume. The ratio of PSD-95 to CaMKIIα revealed a greater than 2-fold increase of PSD-95 associated with CaMKIIα in the KI compared to WT IPs, but no change when normalized to CaMKIIβ (Figure 7).

Behavioral deficits in adolescent KI mice

Hippocampal-dependent learning and memory deficits have been reported in adult (2-3 month old) KI mice in the Morris water maze (Giese et al., 1998). To date there has been no report on behavioral phenotypes that may be present in adolescent KI mice. Due to the biochemical changes we uncovered in the PSD-associated fractions of the KI mice we wanted to determine if a behavioral phenotype could be exposed in the adolescent animals (P24-P25). We adjusted the conditions of three behavioral tasks for assaying adolescent mice (see Chapter 2: Methods-Figure 5). Two hippocampal-dependent memory tasks, Y-Maze (working memory) and a variation of the Novel Object Recognition (short-term/long-term memory), were used to assay for hippocampal dysfunction in the KI mice. Additionally, the Elevated-Plus Maze (EPM) was used to assay for anxiety phenotypes, which also often includes a hippocampal component. We

Figure 7

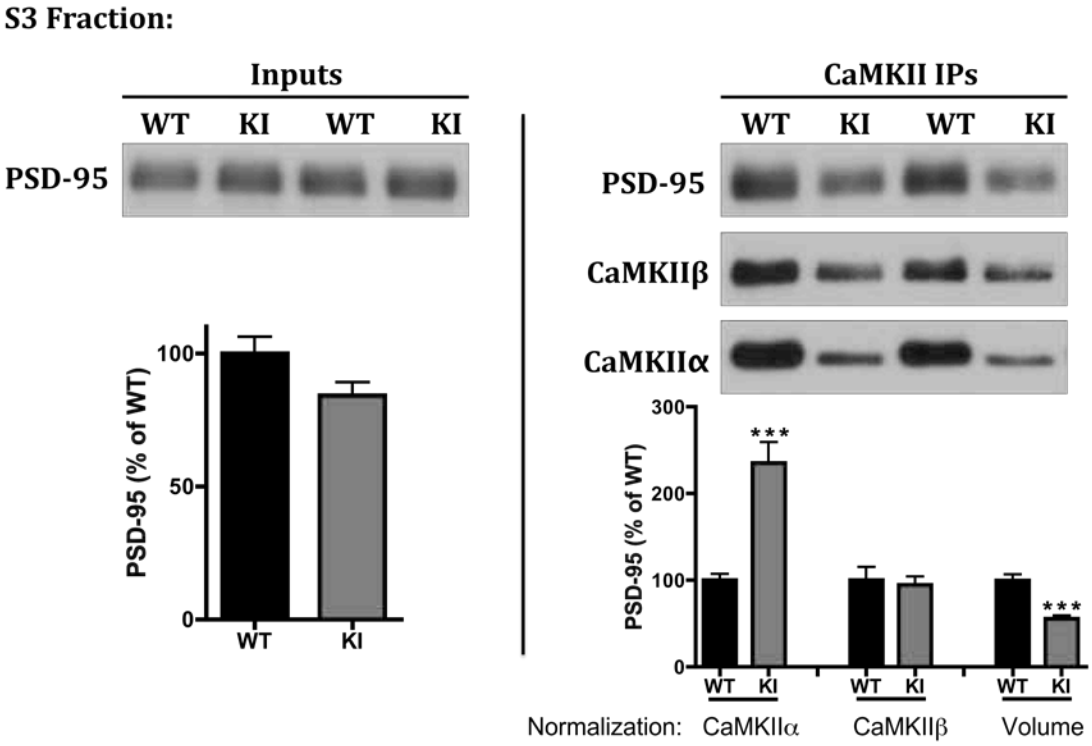

Figure 7. PSD-95 expression and CaMKII co-immunoprecipitation in hippocampal S3 fractions from P25 WT and KI mice. There was a trend for a slight decrease in the amount of PSD-95 (15%; p=0.0858) in the S3 fraction of KI compared to WT mice. PSD-95 co-immunoprecipitation mirrored CaMKIIβ in the IP, normalized to CaMKIIα there was a 135% ($p<0.0001$) increase of PSD-95 association, normalized to CaMKIIβ there was no change in the association of PSD-95, and normalizing to the volume showed that there was a 45% (p=0.0002) decrease in the amount of PSD-95 in the IP of KI mice. (WT=10; KI=7)

are interested in exploring an EPM phenotype in adolescent KI mice due to unpublished data in our laboratory that show adult KI mice have an increased center time in the open-field paradigm, eluding to a potential anxiolytic phenotype in these animals. Adult KI mice also display an increased overall activity in the open-field task (Rentz and Colbran unpublished).

These behavioral tasks were run on all mice, on three consecutive days. The experimental paradigm was as follows: 1. Mice were weaned at P21 (familiar object for novel object recognition placed in weanling home cage at this time-see Chapter 2: Methods for details). 2. Y-maze was performed on P24. 3. The variation of novel object recognition was performed on P25. 4. On P26 the mice were run on the EPM, and 5. Mice were sacrificed for biochemical analysis.

The Y-maze revealed no differences in spontaneous alternations between the WT, KI, or Heterozygous (HET) animals (Figure 8). Interestingly, the KI mice had a ~ 3-fold increase in the number of total arm entries compared to both WT and HET mice (Figure 8). This supports unpublished data that adult KI mice have increased activity in the open-field.

The novel object recognition paradigm that we performed was a short-term memory task, with associated long-term memory components. Adolescent WT and HET mice showed significant preference for the novel object over that of the familiar object (WT: 30% > chance HET: 23% > chance) (Figure 8). However, adolescent KI mice showed no preference for novel or familiar objects, revealing a memory deficit (Figure 8).

To determine if adolescent KI mice show an anxiety phenotype, EPM was

Figure 8

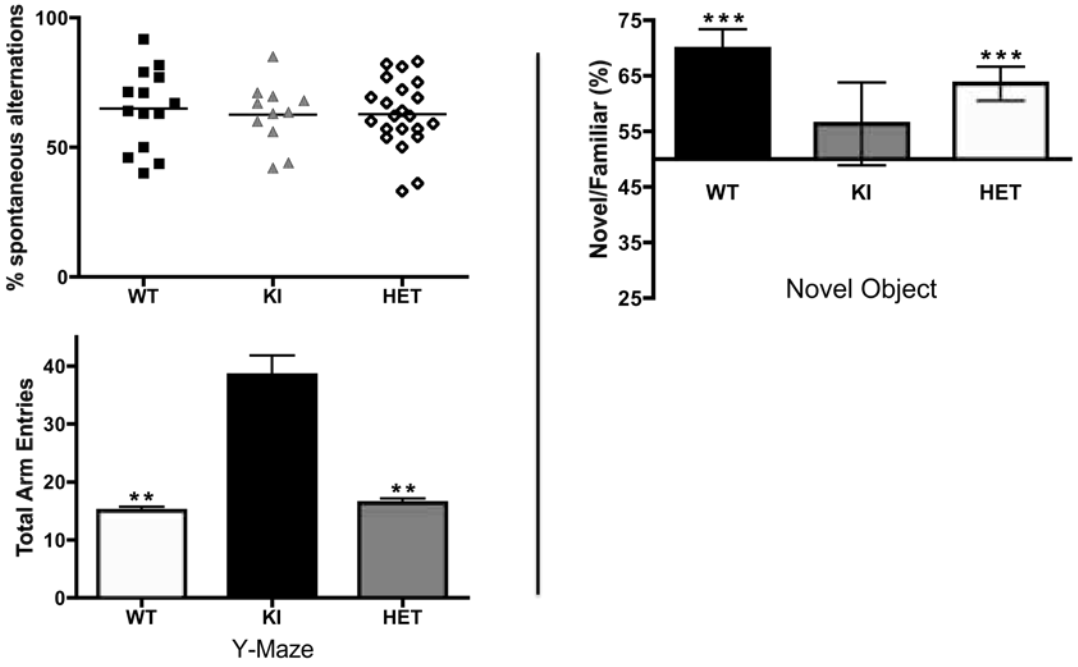

Figure 8. Hippcampal-dependent learning and memory tasks in adolescent WT and KI mice. Left panel: Spontaneous alternations in the y-maze are unchanged between WT, KI, and Thr286Ala heterozygous mice (N: WT=14; KI=11; HET=22). KI mice display an increase in total arm entries with an average of 38 entries in the y-maze compared to WT, 15 entries, and HET, 16 entries mice (ANOVA $p<0.0001$). Right panel: Both WT and HET mice spent significantly more time with the novel object compared to the familiar object over that of chance, whereas KI mice displayed no preference for the novel or familiar object (WT=70%; KI=56%; HET=64%) (N: WT=14; KI=8; HET=20).

Figure 9

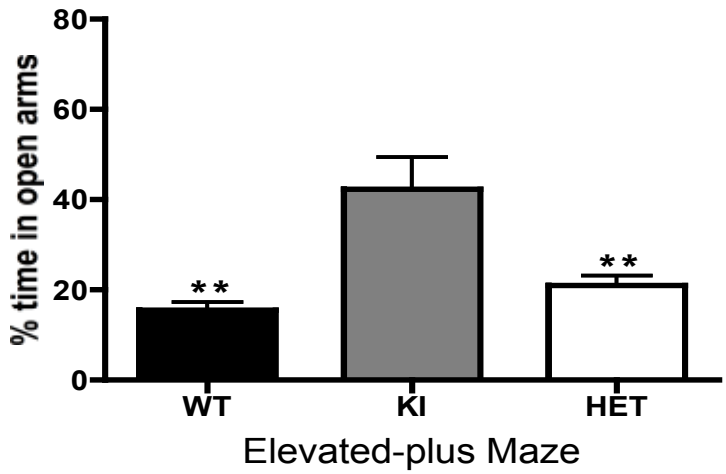

Figure 9. The elevated-plus maze reveals an anxiolytic phenotype in KI mice when compared to WT and HET mice. The percent time spent in the open-arm versus the closed-arm showed that the WT mice spent 15% of the time in the open-arms of the EPM, with the HET mice spending 21% of the time in the open-arms. The KI mice spent 42% of the time in the open-arms versus closed-arms. (ANOVA p=0.0011; bonferroni post-tests: WT<KI p=0.001, HET<KI p=0.001) (N: WT=13; KI=8; HET=21)

performed (Figure 9). WT and HET mice spent 15% and 20% of their time on the open-arms compared to closed-arms, respectively, whereas KI mice spent 42% of their time on the open-arms compared to closed-arms. The significant 2-fold increase in open-arm time from that of WT or HET mice reveals a dramatic anxiolytic phenotype in the KI mice (Figure 9).

Discussion

Hippocampal deficits in adult CaMKIIα-Thr286Ala KI mice have been well documented both electrophysiologically and behaviorally (Giese et al., 1998). Our understanding of how CaMKII functions within neurons, and specifically at the PSD, allows for the generation of hypotheses allowing us to test the mechanism underlying the memory deficits seen in these animals (see chapter 1: Introduction). Knowing that CaMKIIα expression begins postnatally in the rodent (~P5) as well as the role it plays in neuronal development (Wu and Cline, 1998), we wanted to understand if postnatal development was altered in the KI animals, due to the lack of Thr286 phosphorylation. Furthermore, does this altered development cause changes in intracellular signaling mechanisms that in turn lead to long-term behavioral deficits.

Thr286 phosphorylation of CaMKIIα confers autonomous activity to the kinase and increases the affinity of the kinase for the PSD (Lisman et al., 2002; Colbran, 2004; Griffith, 2004). Using our biochemical fractionation protocol, we were able to examine the direct contribution of Thr286 phosphorylation on subcellular localization of CaMKII and how the lack of Thr286 during development altered the kinase localization. CaMKIIα was readily detected in all subcellular fractions from hippocampal

homogenates of WT mice; however, CaMKIIα was enriched in the PSD-associated fractions. This was not too surprising since that CaMKII accounts for 1-2% of the total protein in the hippocampus, and 2-10% of the protein in the PSD (Hanson and Schulman, 1992b; Colbran, 2004). Thr286 phosphorylation stabilizes CaMKII localization to the PSD (Strack and Colbran, 1998). Thus, we expected to see a reduced amount of CaMKII at the PSD in WT versus KI mice. When compared to WT, the loss of CaMKIIα-Thr286 phosphorylation in KI animals drastically decreased the amount of CaMKII in the PSD-associated fractions, with CaMKIIα decreased 90-95% and CaMKIIβ decreased 70-75% from that of WT. This was the first time the decrease in PSD-associated CaMKII in KI mice has been quantified.

Along with this decrease in total CaMKII in the PSD-associated fractions, we detected a concurrent switch in CaMKII holoenzyme subunit composition decreasing the CaMKIIα:CaMKIIβ ratio, such that in the KI mice there are more CaMKIIβ subunits per CaMKIIα subunits at the PSD. Taking into account that CaMKIIβ contains an F-actin binding domain and can directly bind F-actin (Shen et al., 1998; Fink et al., 2003), along with a higher affinity for Ca^{2+}/CaM binding (Brocke et al., 1999), this altered CaMKIIα:CaMKIIβ ratio can potentially have significant effects on subcellular localization as well as normal protein/protein interactions that are necessary for proper CaMKII regulation of PSD-associated protein.

The change in levels of CaMKII in the PSD-associated fractions of the KI mice are most likely not solely due to a redistribution of the kinase, but also alterations in the total expression of CaMKII. Total hippocampal homogenates possessed a 40% decrease in CaMKIIα expression and a 33% increase in CaMKIIβ expression in KI compared to

WT mice. CaMKIIα levels were significantly decreased in both the cytosolic and PSD-associated fractions, which may point to a global CaMKIIα transcription/translation deficit throughout the hippocampus in KI mice (Bito et al., 1997; Ouyang et al., 1999; Thiagarajan et al., 2002; Atkins et al., 2004). Conversely, CaMKIIβ levels where significantly increased in cytosolic and membrane-associated non-PSD fractions and decreased in the PSD-associated fractions in KI mice, suggesting that Thr286 phosphorylation of CaMKIIα is regulating CaMKIIβ expression. Until now there has been no report on the effect of CaMKIIα-Thr286 phosphorylation on CaMKIIβ expression in the KI mice.

In attempts to more completely understand how the PSD-associated fraction was altered, from a biochemical standpoint, we investigated the expression of a number of proteins know to be crucial in proper PSD function. The total levels of PSD-95 as well as the NMDAR subunits, NR1, NR2B, and NR2A, were unchanged in the PSD-associated fractions of WT versus KI mice. Due to the decrease in the total amount of CaMKII in the PSD-associated fractions of the KI mice, along with no change in several PSD-associated proteins in these same fractions, we anticipated to see a significant decrease in the amount of interaction between CaMKII and these proteins that are known to complex with CaMKII (Strack and Colbran, 1998; Strack et al., 2000a; Robison et al., 2005b). Although the total amounts of PSD-95, NR1, NR2B, and NR2A are decreased in the CaMKII co-immunoprecipitations when normalized to volume, the amount of PSD-95, NR1, and NR2B normalized to the amount of CaMKIIα in the immunoprecipitation was significantly increased, revealing a difference in affinity of these protein/protein interactions. Interestingly, there was no change in the amount of NR2A co-precipitating

when normalized to CaMKIIα. When normalized to the amount of CaMKIIβ in the IPs there was no difference in the amount of PSD-95, NR1, or NR2B co-precipitating; however, there was a trend for a 40% decrease in the amount of NR2A co-precipitating in KI versus WT animals. This may be revealing a difference in the interactions of NR2B versus NR2A containing NMDARs with CaMKII isoforms, where CaMKIIβ is playing a dominant role in stabilizing interactions with NR2B containing NMDARs and having less of an effect on NR2A containing NMDARs and more so for NR2B containing NMDARs. Knowing that CaMKII, NR2B, and NR2A are developmentally regulated and critical for neuronal development and synaptogenesis (Wu and Cline, 1998; Stephenson et al., 2008), this differential CaMKII isoform affinity for specific NMDAR subunits could be part of the mechanism that drives neuronal development.

The difference in the apparent affinities of CaMKIIα and CaMKIIβ for the NMDAR subunits could be due to altered phosphorylation of CaMKII (Strack and Colbran, 1998). Specifically, is there an increase in CaMKIIβ-Thr287 phosphorylation in the KI mice that may be compensating for the lack of CaMKIIα-Thr286 phosphorylation? We were able to show that there is no difference in the ratio of CaMKIIβ phosphorylated at Thr287 in the PSD-enriched fractions comparing WT and KI mice, suggesting that the difference in CaMKII protein/protein interactions is not due to a compensation of CaMKIIβ-Thr287 phosphorylation.

We predicted that these biochemical changes would have functional consequences at the synaptic level that would affect behavior in the adolescent KI mice. The biochemical changes in CaMKII along with the altered protein/protein interactions in the PSD-enriched fractions translated to hippocampal-dependent dysfunction evidenced by

deficits in a novel object recognition paradigm. Taken together this confirms the crucial role of CaMKII in proper hippocampal function in adolescent mice. Additionally, the increase in total activity seen in the Y-maze, as well as the anxiolytic phenotype displayed in the EPM by the KI mice suggest important roles for proper CaMKII function in additional brain regions (amygdala, cortical, and striatal circuits) at these adolescent time points. It will be important to thoroughly establish these behavioral models in adolescent mice to be able to understand how early-life perturbations (genetic and otherwise) can alter the normal development of these complex behaviors.

In summary these studies revealed that the loss of CaMKIIα-Thr286 phosphorylation leads to memory deficits as early as postnatal day 25 in mice, demonstrated by a novel object recognition deficit. This behavioral deficiency was accompanied by alterations in CaMKII expression and localization that led to a shift in CaMKII holoenzyme composition, which we were able to show has profound effects on CaMKII protein/protein interactions. This demonstrates that altering CaMKII composition and changing CaMKII protein interactions can lead to significant effects on synaptic function and behavior.

CHAPTER VI

CONCLUSIONS

Introduction

The underlying theme of this dissertation project has been to understand the role of CaMKII during postnatal development. I have used three separate mouse models of environmental (early-life stress) and genetic (*UBE3A* M-/P+ and CaMKIIα-Thr286Ala knock-in mice) perturbations that are known to alter learning and memory in adult animals. We want to link the learning and memory deficits to the perturbations occurring in early postnatal development. To accomplish this we used mouse models where CaMKIIα phosphorylation has been shown (or documented in this dissertation) to be misregulated, to determine how aberrant phosporylation could change the expression, subcellular localization, as well as protein/protein interactions that are crucial for normal CaMKII function and proper learning and memory to occur. Our efforts focused on prepubescent, adolescent mice (P24-P28) so we could more completely understand how these perturbations, genetic or environmental, alter developmental regulation of expression, subcellular localization, and interactions of CaMKII and several proteins known to play crucial roles in adult learning and memory.

Angelman Syndrome

Angelman syndrome is a neurodevelopmental disorder that is normally caused by a chromosomal deletion of the *UBE3A* gene, which encodes for the E3-ubiquitin ligase,

E6-AP (Knoll et al., 1989; Kishino et al., 1997; Matsuura et al., 1997; Sutcliffe et al., 1997). The report linking abnormal synaptic transmission, in a mouse model of AS, to a misregulation (Weeber et al., 2003) of CaMKII prompted my interest in using this mouse model to establish the developmental progression of the AS phenotype and attempt to find a mechanistic link between E6-AP and CaMKII.

E6-AP expression in an Angelman Syndrome mouse model

Since development of the first AS mouse models, the dogma in the AS field has been that *UBE3A* is maternally imprinted solely in hippocampus, cerebellum, and olfactory bulbs. However, it is unclear how this selective maternal imprinting leads to such a vast array of disease phenotypes. We were successful in showing that the E6-AP protein in AS mice is decreased by ~90-95% compared to WT mice across all brain regions. Moreover, we identified a greater than 50% reduction in the E6-AP levels in the heart, liver, and kidney of AS compared to WT mice. This more global loss of E6-AP expression in AS might explain the broad phenotypes.

Attempts to determine the molecular mechanism of how the loss of maternal *UBE3A* can lead to the behavioral deficits seen in the AS mouse, research has focused on hippocampal and cerebellar dysfunction. These findings expand AS research to include a global understanding of how the loss of the maternal *UBE3A* gene can lead to the variety of phenotypes seen in AS. We are hopeful that a more complete knowledge of E6-AP expression will expand AS research that will lead to discovery of better therapeutic targets for the treatment of AS.

Although this research better defines E6-AP expression profiles in the AS mouse, the developmental expression pattern of E6-AP is not clearly understood. It is crucial to AS research that a complete developmental expression pattern of E6-AP across brain regions in WT compared to AS mice is done to determine when E6-AP is first expressed and what point in development E6-AP is most highly expressed. As an E3-ubiquitin ligase, E6-AP is involved in regulating protein degradation, however to date no target of E6-AP has been shown to be involved in the generation of AS phenotypes. Research focused on adult time points ignores the role of abnormal development that may be involved. If E6-AP is most highly expressed early in development, it may be playing a more dominant role early in life, which has not yet be evaluated. Alternatively, if there is a target of E6-AP that is involved in AS and it is developmentally regulated, we may be missing the time window to identify the protein of interest. A developmental role for E6-AP may be supported by the fact that the only difference in our biochemical analysis of CaMKII in the AS animals that we were able to identify was a decrease in Ca^{2+}/CaM-dependent CaMKII activity in the P10 time point.

Moving forward with evaluating *UBE3A* and E6-AP in WT versus AS mice, I propose to do a more complete developmental profile of both gene and protein expression. By establishing a timeline that encompasses embryonic, early development, adolescent, and adult time points, *in situ* hybridization studies evaluating *UBE3A* gene expression and concurrent immunohistochemistry/western blot analysis evaluating E6-AP protein expression could give clues to what point in development E6-AP is playing a dominate role. Along the same lines, subcellular localization studies could point to what

part of the cell E6-AP is acting. This information should guide a more systematic approach to identifying disease mechanisms.

CaMKII role in Angelman Syndrome

There are two reports in the literature implicating CaMKII as a player in the molecular mechanism underlying the disease phenotypes in a mouse model of AS (Weeber et al., 2003; van Woerden et al., 2007). My attempts to recapitulate the findings that support a role for CaMKII in AS were unsuccessful. However, the behavioral deficits along with the decrease in E6-AP expression confirmed that our mice still displayed characteristic AS phenotypes (see Chapter 3: Angelman Syndrome). Also, the genetic cross of AS mice with heterozygous CaMKIIα-Thr-Thr305/305Val-Ala mice did prevent several of the AS phenotypes, seen in the double mutant mice (van Woerden et al., 2007), further supporting the role of CaMKII in AS.

CaMKII is known to play a dominant role at the PSD in normal learning and memory, so is it realistic to expect that a mutation in CaMKII that prevents inhibitory phosphorylation and enhances total CaMKII at the PSD along with LTP (see Table I in Chapter 1: Introduction) would have the potential to prevent learning deficits from occurring. However, I hypothesize that if you cross a CaMKII mutant mouse that increases the effectiveness of CaMKII at the PSD, with any mouse model that displays a form of hippocampal learning and memory dysfunction that there will be some alteration of behavioral and/or electrophysiological phenotypes in the double mutants. If hippocampal deficits could be prevented by altering CaMKII activity or localization in numerous mouse models, this would suggest that CaMKII may not be directly involved

in the mechanisms leading to the deficits displayed in the AS mouse, but that changing normal CaMKII function can compensate for the deficiencies in the AS mouse.

The AS mouse phenotype was prevented by genetic cross of heterozygous CaMKIIα Thr-Thr305/306Val-Ala, which should reduce the inhibitory phosphorylation and increase the amount of total CaMKII at the PSD. If reducing CaMKII inhibition while increasing local concentrations at the PSD prevents the behavioral deficits in AS, then it would stand to reason that increasing inhibition by blocking phosphorylation genetically (Thr286Ala), which decreases total CaMKII at the PSD, would either have no effect or may enhance the behavioral deficits. To test this hypothesis we crossed heterozygous CaMKIIα-Thr286A mice with AS mice, which yielded four genotypes: WT, AS, T286A Heterozygous, and Double mutant (AS/T286A Heterozygous) mice. In rotarod assays for motor coordination, the WT and Heterozygous CaMKIIα-Thr286Ala latency to fall was not different on any of the days tested (Figure 1). The AS mice did not display any motor learning as there latency to fall did not significantly change throughout testing, if anything there was a reduction in the AS mice latency to fall on trial day 10 (Figure 1). Interestingly, the double mutants showed a partial prevention of the rotarod deficit seen in the AS mice, and showed a significant retention of motor memory when tested on day 10 compared to the AS mice (Figure 1). Although preliminary, this suggests that CaMKII is acting though compensatory pathways rather than being directly effected by the loss of E6-AP in the AS mice.

The major caveat to the AS studies, other than the effects of external stressors described in Chapter 3, is the confounding influences that murine strain differences can contribute to variation in behavioral and biochemical effects. I inherited a mouse colony

Figure 1

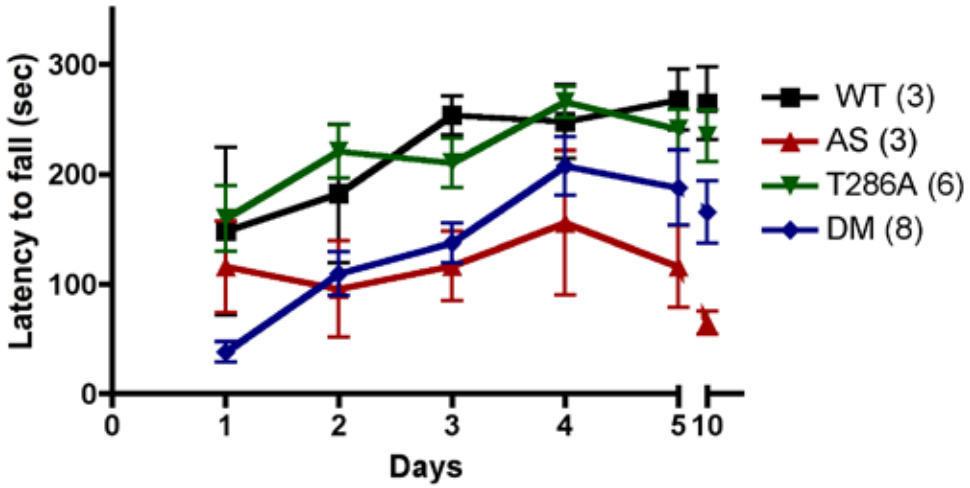

Figure 1. The genetic cross of AS with Thr286Ala HET mice yield four genotypes: WT, Thr286Ala (+/-), AS, and double mutant (DM) mice. Rotarod analysis recapitulates the known deficits in the AS mice. The Thr286Ala (+/-) mice performed as well as the WT mice, showing no deficits in the ability to learn the rotarod. The DM mice never reached the performance level of the WT mice, however they did perform at a higher level than the AS mice, revealing a partial prevention of the AS rotarod phenotype. Additionally, at day 10 the WT, Thr286Ala (+/-), and DM all were able to retain performance at the same level as at day 5, whereas the AS mice showed a loss of performance. (two-way ANOVA $p<0.0001$) (N: WT=3; Thr286Ala (+/-)=6; DM=8; AS=3)

with a wide range of C57/B6 and SV/129 stain contributing to the genetic makeup of the mice. I contemplated back crossing the mice nine generations to a pure C57/B6 strain, however time restraints made this unrealistic.

Early-life Stress

The additional environmental stressors that we predicted to be confounding the results obtained from the AS mouse model using the current breeding strategies lead us to adopt a model of early-life stress in attempts to identify roles for CaMKII across development. Using a model of maternal deficient care from P2-P9 (Rice et al., 2008), my goal was to determine whether CaMKII was misregulated early in development, potentially playing a role in long-term behavioral consequences.

Early-life stress induced PSD morphological changes

The reduction in levels of PSD-95 in the PSD-associated fraction of adolescent early-life stress mice compared to control animals is maintained into adulthood (P90) (Figure 2). This suggests that there could be an overall loss of PSDs in the hippocampus due to the early-life stress that is maintained throughout the life of the animal. There is evidence that shows chronic stress can decrease hippocampal dendrite and dendritic spine density (Xu et al., 2009), which one would predict there would be a loss of PSD-95 with decreasing numbers of dendritic spines. Another possibility that could account for the decrease in PSD-95 could be a change in PSD morphology while maintaining similar dendritic spine numbers. To gain insight into the mechanism underlying the learning deficits induced by early-life stress, I believe it will be important to determine changes in

Figure 2

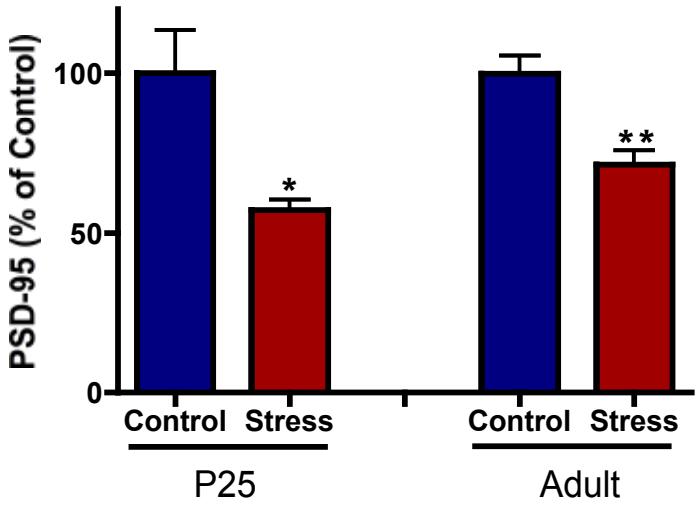

Figure 2. PSD-95 levels in PSD-associated fractions in control and early-life stress animals at P25 and P90. The loss of PSD-95 in the ES mice at P25 (43%) is maintained into adult time points (30%). (P25 p=0.0156 ; Adult p=0.0038).

dendrite and dendritic spine number and/or morphology. Golgi staining methods could be performed at different time points post early-life stress to determine if changes in dendrites and/or dendritic spines are occurring. Additionally, changes in specific subregions of the hippocampus could give insight into mechanism. If there is an overall loss of spines you may predict it is a global loss of signaling that is leading to dysfunction, whereas a change in spine morphology with no loss in total spines may point to a misregulation of specific signaling pathways.

Early-life stress induced plasticity changes

At both time points assayed (P25 and P90), there was a decrease in amplitude of evoked AMPAR mediated responses in neurons from early-life stress mice compared to controls. However, at P25 the early-life stress mice showed a decrease in frequency of the evoked AMPAR responses compared to controls, which was not seen at the P90 time point. The decrease in frequency at P25 could be due to alterations in presynaptic release mechanisms, however paired-pulse facilitation at this time point seems to be unchanged in early-life stress compared to control animals (data not shown), suggesting that the stress is not affecting presynaptic release. I hypothesize that the deceased frequency in the early-life stress mice at P25 is due to either an increase in silent synapses, or fewer synaptic sites in general and that this is corrected or compensated for in adulthood. To test this I propose to look, electrophysiologically and biochemically using biotinylation studies, at the number of silent synapses (those containing NMDAR, but no AMPAR) in adolescent time points to determine if there is a delay in the unsilencing of synapses (addition of AMPAR) in the early-life stress mice compared to that of control mice.

Developmental delay can also lead to an increase in the amount of LTD generated in mice later into life, and there is evidence that neonatal stress can induce this developmental delay (Ku et al., 2008). I would predict that the early-life stress mice have an increased hippocampal LTD at P25 compared to Control animals. We could induce LTD in hippocampal slices from adolescent control and early-life stress animals to assay the amount of depression of fEPSPs. The hypothesis is that P25 control animal fEPSPs would depotentiate, whereas early-life stress animal fEPSPs would depotentiate roughly 30%. Additionally, I would expect that the early-life stress animals would show significant depotentiation at P40, ages when control animals do not show fEPSP depotentiation. This hippocampal LTD is NMDAR dependent (Ku et al., 2008) and could reveal developmental changes or delays that are represented in the early-life stress animals.

Behavioral characterization

The early-life stress paradigm used in these studies was developed in the laboratory of Dr. Baram (Rice et al., 2008). These initial studies reported deficits in the Morris water maze and novel object recognition tasks. The authors of this study also reported no change in overall activity in the stress versus non-stressed animals, as well as no change in the center time in the open-field. Although these studies pointed towards a hippocampal-dependent learning and memory deficiency, the wide range in age of the mice used in these behavior studies (4-8 months) may add variability to these behavioral tasks that could potentially mask other deficits in these animals. Therefore a more complete behavioral characterization of the early-life stress animals is needed to more

fully understand the long-term adverse effects the early postnatal stress is having long-term.

In future experiments, I propose to do a more rigorous behavioral characterization over a timeline (adolescent, young adult, and mature adult) to determine how early-life stress induced behavioral deficits develop over time. This would also give insight into how normal behavioral development occurs, which would give us the potential to tie known biochemical and electrophysiological changes at these time windows to a behavioral output.

These experiments would need the development and/or conversion of a variety of behavioral tasks to be able to test adolescent mice. With the assistance of Dr. Gregg Stanwood's laboratory, we have developed behavioral paradigms (Y-maze, novel object, and elevated-plus maze) to assay behavioral deficits in adolescent mice with some success (see Chapter 2: Methods and Chapter 5: CaMKII-Thr286Ala). We are beginning attempts to identify behavioral deficits in adolescent early-stress mice using the y-maze, novel object, and EPM (Figure 3). With only a single cohort of animals (control N=3; stress N=3) it is too early to make any definitive conclusions. Assaying the percent of spontaneous alternations in the y-maze show no significant trend of difference between control and early-life stress animals (Figure 3). In the novel object recognition task time spent with the novel over the familiar object was not significantly different between groups (Figure 3). There may be a slight trend for an increase in novel object recognition in the early-life stress mice; however, we predict that this is due to inter-litter variability due to the fact that the control mice in these studies only spent 60% of their time with the novel object. We expect, from our other adolescent behavior studies that with an increase

in N, the control mice will spend ~70% of their time with the novel object. Finally, the initial EPM studies reveal no difference between control and early-life stress groups (Figure 3).

We may or may not be able to identify behavior deficits in the adolescent early-stress mice for several potential reasons. For one, at this age compensatory molecular mechanisms may be preventing deficits in the behaviors we are assaying. Alternatively, the complex brain circuitry that is needed to perform these tasks may not be completely established, which could mask subtle deficits in behavior. Additionally, brain plasticity at this age is able to overcome the early-life stress revealing the resiliency of young animals. Lastly, the behavioral paradigms that we have set up may not be sensitive enough to reveal subtle changes in behavior and better paradigms need to be created to test these behaviors in adolescent mice. For these reasons I believe it is important to establish that we are able to identify behavioral deficits in adult early-life stress mice prior to attempting to understand how these complex behaviors develop in the adolescent animals.

Therapeutic rescue of early-life stress deficits

There are many long-term benefits of identifying the molecular mechanisms underlying the behavioral deficits caused by early-life stress. With an understanding of how biochemical misregulation leads to the development of behavioral deficits we can identify therapeutic targets that can be pharmacologically manipulated to prevent or reverse the adverse effects of early-life stress. From a human health standpoint this is immensely important. Environmental factors, such as different forms of stress, can

Figure 3

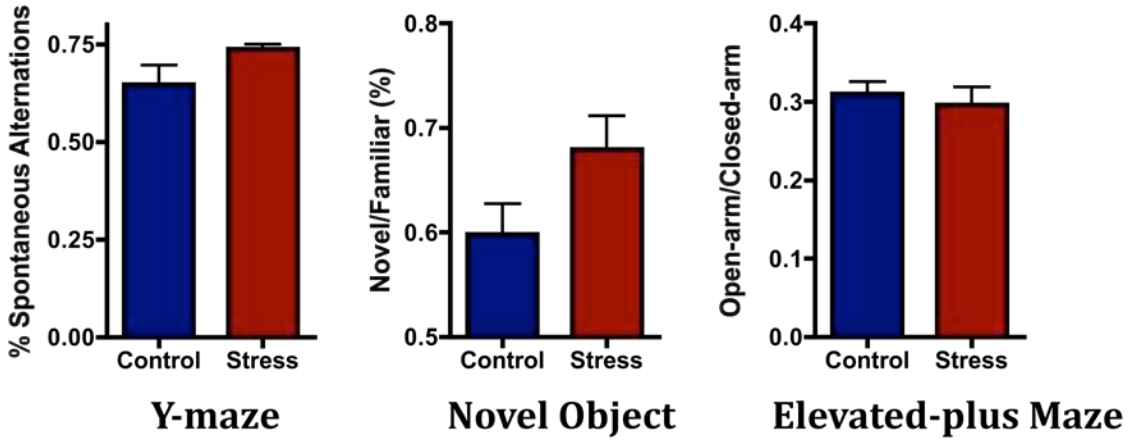

Figure 3. Behavioral tasks in adolescent control and early-life stress mice. Initial behavioral characterization of ES mice has not revealed any significant deficits in performance on the y-maze, novel object, or elevated-plus maze behavioral paradigms in the adolescent time point. (Control=3; Stress=3)

adversely affect brain development, which can lead to profound effects on cognition, depression, anxiety, as well as other behavior abnormalities later in life. The ability to identify these external stressors as well as their biochemical and behavioral effects could suggest novel therapeutic strategies to eliminate the long-term consequences of the adverse early-life stressors.

CaMKII and General Neuroscience Questions

Synaptic versus extra-synaptic surface receptors

A major caveat to the subcellular fractionation studies used in this dissertation is that we are isolating the total population of protein in any one particular fraction. Our method does not allow for differentiation of surface versus intracellular protein. Using our protocol, significant changes in synaptic membrane receptors may be masked by the total pool of receptor in the PSD-enriched fraction. Currently, we are attempting to use biotinylation techniques in hippocampal slices along with our fractionation protocol to be able to probe for changes in total versus surface protein expression in any given biochemical fraction.

The major goal of these studies is to develop a biotinylation/fractionation technique that will allow us to differentiate, not just between surface and total protein, but to identify synaptic versus extra-synaptic membrane fractions. This will allow for the identification of membrane proteins and subunits that may be differentially expressed in extra-synaptic versus synaptic membranes. Additionally, it will allow us to determine how different proteins are expressed, trafficked, and regulated in these various

membranes under differing conditions (i.e. early-life stress or genetic modification). To date we have had success combining the biotinylation with our fractionation protocol to be able to probe for surface versus total protein. We are currently trying to determine how to identify and isolate the synaptic from the extra-synaptic membranes. This may prove to be an extremely powerful technique, when coupled with electrophysiological techniques, to look at contributions of extra-synaptic and synaptic membrane associated receptor in learning and memory process.

Importance of the CaMKIIα:CaMKIIβ ratio in learning and memory

CaMKII exists as a docecameric holoenzyme consisting of a combination of α, β, δ, and γ subunits (see Chapter 1: Introduction). CaMKII research, relating to the hippocampus, has mainly focused on the role of CaMKIIα in describing learning and memory processes. However, it is important to understand the role the additional subunits play in regulation, activity, and localization of the holoenzyme to truly understand the function of CaMKII.

Our data suggests that the lack of CaMKIIα-Thr286 phosphorylation, as seen in the adolescent CaMKIIα-Thr286Ala knock-in mice, alters the CaMKIIα:CaMKIIβ ratio of the CaMKII holoenzyme at the PSD. This suggests that for every CaMKIIα subunit there is an increased number of CaMKIIβ subunits in the KI mice compared to WT mice. Immunoprecipitation experiments from WT and KI PSD-associated fractions show a significant increase in the co-immunoprecipitation of several NMDAR subunits and PSD-95 when normalized to the amount of CaMKIIα immunoprecipitated. However, when normalized to the amount of CaMKIIβ present in the immunoprecipitation there is no

change in the interaction of these proteins. This may suggest that CaMKIIβ is the major contributor to the scaffolding properties of the CaMKII holoenzyme. There is evidence that CaMKIIβ is playing a dominant role as a scaffold protein. CaMKIIβ has a F-actin binding domain, which allows targeting of CaMKIIβ containing holoenzymes to the actin cytoskeleton (Shen et al., 1998; Fink et al., 2003). The binding of Ca^{2+}/calmodulin modulates the actin interaction with CaMKIIβ. Additionally, CaMKIIβ has a higher affinity to Ca^{2+}/calmodulin than CaMKIIα. Taken together with the decrease in the CaMKIIα:CaMKIIβ ratio in the KI animals, CaMKIIβ may be compensating for a loss of CaMKII holoenzyme at the PSD, directing the interaction of the decreased CaMKII to the PSD and thereby positioning the remaining kinase in close vicinity to its interacting proteins. However, once there, when Ca^{2+} dissipates and CaMKIIα-Thr286 is unable to be phosphorylated, misregulation of CaMKII signaling occurs, leading to the electrophysiological and behavioral deficits seen in the KI animals.

Preliminary data suggests that increasing the amount of CaMKIIβ subunits may indeed increase the interactions with selected PSD-associated proteins (Figure 4). In these experiments CaMKII immunoprecipitations, using three different antibodies, were performed on whole-forebrain homogenates from WT and CaMKIIα knock-out mice (courtesy of Ype Elgersma). The three antibodies used were: 1. A goat-anti-CaMKII polyclonal antibody purified from a CaMKIIα filtration column, which is able to recognize both CaMKIIα and CaMKIIβ with a higher affinity for the α subunit. 2. A mouse-anti-CaMKIIα monoclonal antibody, which is unable to detect CaMKIIβ, and 3. A mouse-anti-CaMKIIβ monoclonal antibody, which is unable to detect CaMKIIα in western blot analysis. By performing immunoprecipitations using these three antibodies

we can determine the amount of CaMKIIα and CaMKIIβ that are present in the immunoprecipitation and how the changes in subunit contribution to the holoenzyme affects the interaction with CaMKII binding proteins, such as NR2B, and NR2A (Figure 4). There are significant differences in the amount of CaMKIIα versus CaMKIIβ present in the different immunoprecipitations from WT animals (α:β ratio from WT: GT-IP = 4.7; MS-α-IP = 2.5; MS-β-IP = 1.1). Although a CaMKIIα:CaMKIIβ ratio cannot be obtained from the CaMKIIα KO animals, there was a substantial difference in the amount of CaMKIIβ immunoprecipitated in the KO animals using the different antibodies, with the MS-CaMKIIβ specific antibody immunoprecipitating ~ 5.5-fold more CaMKIIβ compared to the GT-CaMKII immunoprecipitation (CaMKIIβ in KI: GT-IP = 2.1; MS-α-IP = N.D.; MS-β-IP = 11.7).

When normalized to the amount of CaMKIIβ in the IP there was a no difference in the amount of NR2A co-immunoprecipitated in GT-CaMKII IP versus the MS-CaMKIIβ IP from WT animals. However, when normalized to the amount of CaMKIIβ in the immunoprecipitations, the amount of NR2B in the co-immunoprecipitation was over 2-fold higher in the MS-CaMKIIβ IP versus the GT-CaMKII IP. Additionally, MS-CaMKIIβ immunoprecipitations from the CaMKIIα KO mice had an increase in the amount of NR2B associating with CaMKII compared to GT-CaMKII IP from WT animals; however, the amount of NR2A co-immunoprecipitating seems to be unchanged. Together this suggests that CaMKII holoenzymes consisting of more CaMKIIβ per CaMKIIα subunits may preferentially interact with NMDAR subunits and perhaps scaffold the CaMKII holoenzyme to specific areas of the cell for appropriate signaling to take place. Closer examination comparing the CaMKII co-immunoprecipitations from

Figure 4

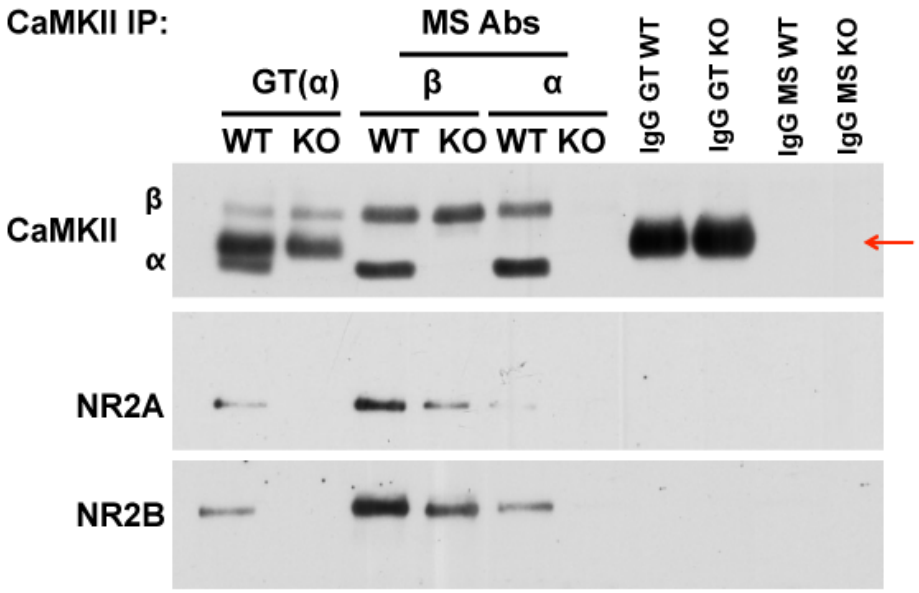

Figure 4. CaMKII immunoprecipitations using different antibodies to isolate CaMKII holoenzymes consisting of differential CaMKIIα:CaMKIIβ ratios in WT and CaMKIIα KO mice. Immunoprecipitations that contain higher fractions of CaMKIIβ are able to co-immunoprecipitate a larger amount of NR2B. The amount of NR2A co-immunoprecipitated seems to increase with the total amount of CaMKII holoenzyme that is IPed without showing preference to holoenzymes containing CaMKIIβ. (Red arrow identifies IgG recognized by the goat-CaMKII antibody)

WT and KI animals may be revealing this same potential differential interaction when CaMKII holoenzyme composition is altered (see Chapter 5, Figures 3, 5, and 6). In the CaMKII immunoprecipitation there is a decrease in both CaMKIIα and CaMKIIβ in the KI animals compared to WT controls. The extent to which these subunits are decreased is different, such that the CaMKIIα:CaMKIIβ ratio is decreased 60%. This leads to an overall decrease in PSD-95, NR1, NR2B, and NR2A in the KI mice when the co-immunoprecipitations are normalized to volume. This makes sense due to the decrease in total CaMKII in the immunoprecipitations from the KI animals. When these same proteins are normalized to the amount of CaMKIIα in the immunoprecipitation there is a significant increase the amount of PSD-95, NR1, and NR2B co-immunoprecipitating in the KI versus WT mice; however, NR2A is not significantly increased. Alternatively, when these proteins are normalized to the amount of CaMKIIβ in the immunoprecipitation there is no difference in the amount of PSD-95, NR1, and NR2B co-immunoprecipitating in WT and KI animals. This means that PSD-95, NR1, and NR2B are decreased to the same extent as CaMKIIβ in the KI animals. More interestingly, there is a significant trend for a decrease in the amount of NR2A when normalized to CaMKIIβ (~ 50%) in KI compared to WT mice.

I hypothesize that CaMKIIβ plays a predominate scaffolding role in targeting CaMKII to specific proteins, which allows for the construction of larger signaling complexes at the PSD that are crucial for learning and memory processes to occur. The role of CaMKIIβ in targeting CaMKII to specific proteins could be worked out using *in vitro*, heterologous cell system to overexpress the CaMKII subunits at different concentrations along with known interacting proteins (i.e. NR1, NR2B, and NR2A), to

see how different CaMKII holoenzymes consisting of different CaMKIIα:CaMKIIβ ratios can alter interactions and potentially localization within the cell. To this end, recent data in the lab using heterologous expression systems has shown that CaMKIIβ interacts with NR2B with a much higher affinity than does CaMKIIα (Dr. Yuxia Jiao and Nidhi Jalan-Sakrikar).

In the attempts to understand the differential roles of CaMKIIα and CaMKIIβ in the neuron as it pertains to function of the holoenzyme, there is a major caveat. We have not begun looking at the effects the other CaMKII subunits (i.e. δ and γ) may be having on protein/protein interactions, localization, or activity of the kinase. Although these CaMKII isoforms are minor in their contribution to the total amount of CaMKII in the hippocampus, their concentrations may be significant in pools of kinase that are selectively targeted to specific sites within the cell. Additionally, these other CaMKII isoforms may be playing important roles in other brain regions or in specific cell types where they are expressed to a great extent (Erondu and Kennedy, 1985; Bayer et al., 1999; Thiagarajan et al., 2002; van Woerden et al., 2009).

Conclusions

The role of CaMKII as a scaffolding protein is not a novel idea (Erondu and Kennedy, 1985; Colbran, 2004; Sheng and Hoogenraad, 2007; Bingol et al., 2010). CaMKIIα phosphorylated at Thr286 is able to translocate to the PSD bringing together signaling components from multiple signaling systems to orchestrate complex molecular events, in response to temporal and local changes in calcium concentration. However, the majority of research, to determine the role of CaMKII in learning and memory, has

focused on how changes in CaMKIIα expression, activation, localization, and phosphorylation affect these processes. This has given us a great understanding of how CaMKII functions in the cell; however, due to the complex structure and intersubunit regulation of CaMKII, not much is understood about how different isoform conformations contribute to CaMKII localization and function *in vivo*. Additionally, a complete understanding of the modulation of function of CaMKII by alternative phosphorylation sites (i.e. Thr253) has not been determined.

This dissertation project begins to tie together biochemical, electrophysiological, and behavioral techniques that will allow for the understanding of how learned behaviors are developed over time. Moving forward, must establish how neuronal circuits can be developed and become functional, and how the development of these circuits are crucial for specific learned behaviors. Understanding the role of CaMKII in these processes and how these behaviors develop overtime, we may be able to identify specific target for therapeutic manipulation to prevent or reverse disease.

LITERATURE CITED

Ahmed T, Frey JU, Korz V (2006) Long-term effects of brief acute stress on cellular signaling and hippocampal LTP. J Neurosci 26:3951-3958.

Albrecht U, Sutcliffe JS, Cattanach BM, Beechey CV, Armstrong D, Eichele G, Beaudet AL (1997) Imprinted expression of the murine Angelman syndrome gene, Ube3a, in hippocampal and Purkinje neurons. Nat Genet 17:75-78.

Angleman H (1965) "Puppet" Children A Report on Three Cases Developmental Medicine & Child Neurology 7:681-688.

Anson LC, Chen PE, Wyllie DJ, Colquhoun D, Schoepfer R (1998) Identification of amino acid residues of the NR2A subunit that control glutamate potency in recombinant NR1/NR2A NMDA receptors. J Neurosci 18:581-589.

Atkins CM, Nozaki N, Shigeri Y, Soderling TR (2004) Cytoplasmic polyadenylation element binding protein-dependent protein synthesis is regulated by calcium/calmodulin-dependent protein kinase II. J Neurosci 24:5193-5201.

Bach ME, Hawkins RD, Osman M, Kandel ER, Mayford M (1995) Impairment of spatial but not contextual memory in CaMKII mutant mice with a selective loss of hippocampal LTP in the range of the theta frequency. Cell 81:905-915.

Banke TG, Traynelis SF (2003) Activation of NR1/NR2B NMDA receptors. Nat Neurosci 6:144-152.

Barria A, Malinow R (2002) Subunit-specific NMDA receptor trafficking to synapses. Neuron 35:345-353.

Barria A, Muller D, Derkach V, Griffith LC, Soderling TR (1997) Regulatory phosphorylation of AMPA-type glutamate receptors by CaM-KII during long-term potentiation. Science 276:2042-2045.

Barry MF, Ziff EB (2002) Receptor trafficking and the plasticity of excitatory synapses. Curr Opin Neurobiol 12:279-286.

Bayer KU, Lohler J, Schulman H, Harbers K (1999) Developmental expression of the CaM kinase II isoforms: ubiquitous gamma- and delta-CaM kinase II are the early isoforms and most abundant in the developing nervous system. Brain Res Mol Brain Res 70:147-154.

Beckung E, Steffenburg S, Kyllerman M (2004) Motor impairments, neurological signs, and developmental level in individuals with Angelman syndrome. Dev Med Child Neurol 46:239-243.

Behe P, Stern P, Wyllie DJ, Nassar M, Schoepfer R, Colquhoun D (1995) Determination of NMDA NR1 subunit copy number in recombinant NMDA receptors. Proc Biol Sci 262:205-213.

Bingol B, Wang CF, Arnott D, Cheng D, Peng J, Sheng M (2010) Autophosphorylated CaMKIIalpha acts as a scaffold to recruit proteasomes to dendritic spines. Cell 140:567-578.

Bito H, Deisseroth K, Tsien RW (1997) Ca2+-dependent regulation in neuronal gene expression. Curr Opin Neurobiol 7:419-429.

Bliss TV, Lomo T (1973) Long-lasting potentiation of synaptic transmission in the dentate area of the anaesthetized rabbit following stimulation of the perforant path. J Physiol 232:331-356.

Bliss TV, Collingridge GL (1993) A synaptic model of memory: long-term potentiation in the hippocampus. Nature 361:31-39.

Boehm J, Kang MG, Johnson RC, Esteban J, Huganir RL, Malinow R (2006) Synaptic incorporation of AMPA receptors during LTP is controlled by a PKC phosphorylation site on GluR1. Neuron 51:213-225.

Bourne JN, Harris KM (2008) Balancing structure and function at hippocampal dendritic spines. Annu Rev Neurosci 31:47-67.

Bradshaw JM, Hudmon A, Schulman H (2002) Chemical quenched flow kinetic studies indicate an intraholoenzyme autophosphorylation mechanism for Ca2+/calmodulin-dependent protein kinase II. J Biol Chem 277:20991-20998.

Bredt DS, Nicoll RA (2003) AMPA receptor trafficking at excitatory synapses. Neuron 40:361-379.

Brocke L, Chiang LW, Wagner PD, Schulman H (1999) Functional implications of the subunit composition of neuronal CaM kinase II. J Biol Chem 274:22713-22722.

Brown AM, Deutch AY, Colbran RJ (2005) Dopamine depletion alters phosphorylation of striatal proteins in a model of Parkinsonism. Eur J Neurosci 22:247-256.

Catani M, Jones DK, ffytche DH (2005) Perisylvian language networks of the human brain. Ann Neurol 57:8-16.

Cattanach BM, Barr JA, Beechey CV, Martin J, Noebels J, Jones J (1997) A candidate model for Angelman syndrome in the mouse. Mamm Genome 8:472-478.

Chang FL, Greenough WT (1984) Transient and enduring morphological correlates of synaptic activity and efficacy change in the rat hippocampal slice. Brain Res 309:35-46.

Chen C, Rainnie DG, Greene RW, Tonegawa S (1994) Abnormal fear response and aggressive behavior in mutant mice deficient for alpha-calcium-calmodulin kinase II. Science 266:291-294.

Chen C, Kim JJ, Thompson RF, Tonegawa S (1996) Hippocampal lesions impair contextual fear conditioning in two strains of mice. Behav Neurosci 110:1177-1180.

Chen HX, Otmakhov N, Strack S, Colbran RJ, Lisman JE (2001) Is persistent activity of calcium/calmodulin-dependent kinase required for the maintenance of LTP? J Neurophysiol 85:1368-1376.

Chowdhury S, Shepherd JD, Okuno H, Lyford G, Petralia RS, Plath N, Kuhl D, Huganir RL, Worley PF (2006) Arc/Arg3.1 interacts with the endocytic machinery to regulate AMPA receptor trafficking. Neuron 52:445-459.

Chung HJ, Xia J, Scannevin RH, Zhang X, Huganir RL (2000) Phosphorylation of the AMPA receptor subunit GluR2 differentially regulates its interaction with PDZ domain-containing proteins. J Neurosci 20:7258-7267.

Cohen P (1989) The structure and regulation of protein phosphatases. Annu Rev Biochem 58:453-508.

Cohen P (1991) Classification of protein-serine/threonine phosphatases: identification and quantitation in cell extracts. Methods Enzymol 201:389-398.

Colas D, Wagstaff J, Fort P, Salvert D, Sarda N (2005) Sleep disturbances in Ube3a maternal-deficient mice modeling Angelman syndrome. Neurobiol Dis 20:471-478.

Colbran RJ (2004) Targeting of calcium/calmodulin-dependent protein kinase II. Biochem J 378:1-16.

Colbran RJ, Soderling TR (1990) Calcium/calmodulin-independent autophosphorylation sites of calcium/calmodulin-dependent protein kinase II. Studies on the effect of phosphorylation of threonine 305/306 and serine 314 on calmodulin binding using synthetic peptides. J Biol Chem 265:11213-11219.

Colbran RJ, Brown AM (2004) Calcium/calmodulin-dependent protein kinase II and synaptic plasticity. Curr Opin Neurobiol 14:318-327.

Crombag HS, Sutton JM, Takamiya K, Holland PC, Gallagher M, Huganir RL (2008) A role for alpha-amino-3-hydroxy-5-methylisoxazole-4-propionic acid GluR1 phosphorylation in the modulatory effects of appetitive reward cues on goal-directed behavior. Eur J Neurosci 27:3284-3291.

De Koninck P, Schulman H (1998) Sensitivity of CaM kinase II to the frequency of Ca2+ oscillations. Science 279:227-230.

Deacon RM, Bannerman DM, Kirby BP, Croucher A, Rawlins JN (2002) Effects of cytotoxic hippocampal lesions in mice on a cognitive test battery. Behav Brain Res 133:57-68.

Dillon GM, Qu X, Marcus JN, Dodart JC (2008) Excitotoxic lesions restricted to the dorsal CA1 field of the hippocampus impair spatial memory and extinction learning in C57BL/6 mice. Neurobiol Learn Mem 90:426-433.

Dindot SV, Antalffy BA, Bhattacharjee MB, Beaudet AL (2008) The Angelman syndrome ubiquitin ligase localizes to the synapse and nucleus, and maternal deficiency results in abnormal dendritic spine morphology. Hum Mol Genet 17:111-118.

Dosemeci A, Tao-Cheng JH, Vinade L, Winters CA, Pozzo-Miller L, Reese TS (2001) Glutamate-induced transient modification of the postsynaptic density. Proc Natl Acad Sci U S A 98:10428-10432.

Elgersma Y, Sweatt JD, Giese KP (2004) Mouse genetic approaches to investigating calcium/calmodulin-dependent protein kinase II function in plasticity and cognition. J Neurosci 24:8410-8415.

Elgersma Y, Fedorov NB, Ikonen S, Choi ES, Elgersma M, Carvalho OM, Giese KP, Silva AJ (2002) Inhibitory autophosphorylation of CaMKII controls PSD association, plasticity, and learning. Neuron 36:493-505.

Erondu NE, Kennedy MB (1985) Regional distribution of type II Ca2+/calmodulin-dependent protein kinase in rat brain. J Neurosci 5:3270-3277.

Esteban JA, Shi SH, Wilson C, Nuriya M, Huganir RL, Malinow R (2003) PKA phosphorylation of AMPA receptor subunits controls synaptic trafficking underlying plasticity. Nat Neurosci 6:136-143.

Fink CC, Meyer T (2002) Molecular mechanisms of CaMKII activation in neuronal plasticity. Curr Opin Neurobiol 12:293-299.

Fink CC, Bayer KU, Myers JW, Ferrell JE, Jr., Schulman H, Meyer T (2003) Selective regulation of neurite extension and synapse formation by the beta but not the alpha isoform of CaMKII. Neuron 39:283-297.

Forrest D, Yuzaki M, Soares HD, Ng L, Luk DC, Sheng M, Stewart CL, Morgan JI, Connor JA, Curran T (1994) Targeted disruption of NMDA receptor 1 gene abolishes NMDA response and results in neonatal death. Neuron 13:325-338.

Fumagalli F, Pasini M, Frasca A, Drago F, Racagni G, Riva MA (2009) Prenatal stress alters glutamatergic system responsiveness in adult rat prefrontal cortex. J Neurochem 109:1733-1744.

Gerges NZ, Aleisa AM, Schwarz LA, Alkadhi KA (2004) Reduced basal CaMKII levels in hippocampal CA1 region: possible cause of stress-induced impairment of LTP in chronically stressed rats. Hippocampus 14:402-410.

Giese KP, Fedorov NB, Filipkowski RK, Silva AJ (1998) Autophosphorylation at Thr286 of the alpha calcium-calmodulin kinase II in LTP and learning. Science 279:870-873.

Greer PL, Hanayama R, Bloodgood BL, Mardinly AR, Lipton DM, Flavell SW, Kim TK, Griffith EC, Waldon Z, Maehr R, Ploegh HL, Chowdhury S, Worley PF, Steen J, Greenberg ME (2010) The Angelman Syndrome protein Ube3A regulates synapse development by ubiquitinating arc. Cell 140:704-716.

Griffith LC (2004) Regulation of calcium/calmodulin-dependent protein kinase II activation by intramolecular and intermolecular interactions. J Neurosci 24:8394-8398.

Gustin RM, Bichell TJ, Bubser M, Daily J, Filonova I, Mreshavili D, Deutch AY, Colbran RJ, Weeber EJ, Haas KF (2010) Tissue-specific variation of Ube3a protein expression in rodents and in a mouse model of Angelman syndrome. Neurobiol Dis.

Hanson PI, Schulman H (1992a) Inhibitory autophosphorylation of multifunctional Ca2+/calmodulin-dependent protein kinase analyzed by site-directed mutagenesis. J Biol Chem 267:17216-17224.

Hanson PI, Schulman H (1992b) Neuronal Ca2+/calmodulin-dependent protein kinases. Annu Rev Biochem 61:559-601.

Hayashi Y, Shi SH, Esteban JA, Piccini A, Poncer JC, Malinow R (2000) Driving AMPA receptors into synapses by LTP and CaMKII: requirement for GluR1 and PDZ domain interaction. Science 287:2262-2267.

Herzing LB, Cook EH, Jr., Ledbetter DH (2002) Allele-specific expression analysis by RNA-FISH demonstrates preferential maternal expression of UBE3A and imprint maintenance within 15q11- q13 duplications. Hum Mol Genet 11:1707-1718.

Hinds HL, Goussakov I, Nakazawa K, Tonegawa S, Bolshakov VY (2003) Essential function of alpha-calcium/calmodulin-dependent protein kinase II in neurotransmitter release at a glutamatergic central synapse. Proc Natl Acad Sci U S A 100:4275-4280.

Hollmann M, Heinemann S (1994) Cloned glutamate receptors. Annu Rev Neurosci 17:31-108.

Hollmann M, O'Shea-Greenfield A, Rogers SW, Heinemann S (1989) Cloning by functional expression of a member of the glutamate receptor family. Nature 342:643-648.

Huang CC, Lin HR, Liang YC, Hsu KS (2007) Effects of neonatal corticosteroid treatment on hippocampal synaptic function. Pediatr Res 62:267-270.

Huibregtse JM, Scheffner M, Howley PM (1991) A cellular protein mediates association of p53 with the E6 oncoprotein of human papillomavirus types 16 or 18. Embo J 10:4129-4135.

Isaac JT, Nicoll RA, Malenka RC (1995) Evidence for silent synapses: implications for the expression of LTP. Neuron 15:427-434.

Jiang YH, Armstrong D, Albrecht U, Atkins CM, Noebels JL, Eichele G, Sweatt JD, Beaudet AL (1998) Mutation of the Angelman ubiquitin ligase in mice causes increased cytoplasmic p53 and deficits of contextual learning and long-term potentiation. Neuron 21:799-811.

Kameyama K, Lee HK, Bear MF, Huganir RL (1998) Involvement of a postsynaptic protein kinase A substrate in the expression of homosynaptic long-term depression. Neuron 21:1163-1175.

Kandel ER (2001) The molecular biology of memory storage: a dialogue between genes and synapses. Science 294:1030-1038.

Kessels HW, Malinow R (2009) Synaptic AMPA receptor plasticity and behavior. Neuron 61:340-350.

Kishino T, Lalande M, Wagstaff J (1997) UBE3A/E6-AP mutations cause Angelman syndrome. Nat Genet 15:70-73.

Knoll JH, Nicholls RD, Magenis RE, Graham JM, Jr., Lalande M, Latt SA (1989) Angelman and Prader-Willi syndromes share a common chromosome 15 deletion but differ in parental origin of the deletion. Am J Med Genet 32:285-290.

Kolodziej SJ, Hudmon A, Waxham MN, Stoops JK (2000) Three-dimensional reconstructions of calcium/calmodulin-dependent (CaM) kinase IIalpha and truncated CaM kinase IIalpha reveal a unique organization for its structural core and functional domains. J Biol Chem 275:14354-14359.

Ku HY, Huang YF, Chao PH, Huang CC, Hsu KS (2008) Neonatal isolation delays the developmental decline of long-term depression in the CA1 region of rat hippocampus. Neuropsychopharmacology 33:2847-2859.

Kuhne C, Banks L (1998) E3-ubiquitin ligase/E6-AP links multicopy maintenance protein 7 to the ubiquitination pathway by a novel motif, the L2G box. J Biol Chem 273:34302-34309.

Kumar S, Talis AL, Howley PM (1999) Identification of HHR23A as a substrate for E6-associated protein-mediated ubiquitination. J Biol Chem 274:18785-18792.

Laan LA, v Haeringen A, Brouwer OF (1999) Angelman syndrome: a review of clinical and genetic aspects. Clin Neurol Neurosurg 101:161-170.

Lai Y, Nairn AC, Greengard P (1986) Autophosphorylation reversibly regulates the Ca2+/calmodulin-dependence of Ca2+/calmodulin-dependent protein kinase II. Proc Natl Acad Sci U S A 83:4253-4257.

Lee HK, Barbarosie M, Kameyama K, Bear MF, Huganir RL (2000) Regulation of distinct AMPA receptor phosphorylation sites during bidirectional synaptic plasticity. Nature 405:955-959.

Lee HK, Takamiya K, Han JS, Man H, Kim CH, Rumbaugh G, Yu S, Ding L, He C, Petralia RS, Wenthold RJ, Gallagher M, Huganir RL (2003) Phosphorylation of the AMPA receptor GluR1 subunit is required for synaptic plasticity and retention of spatial memory. Cell 112:631-643.

Li W, Okano A, Tian QB, Nakayama K, Furihata T, Nawa H, Suzuki T (2001) Characterization of a novel synGAP isoform, synGAP-beta. J Biol Chem 276:21417-21424.

Liao D, Hessler NA, Malinow R (1995) Activation of postsynaptically silent synapses during pairing-induced LTP in CA1 region of hippocampal slice. Nature 375:400-404.

Lin HJ, Huang CC, Hsu KS (2006) Effects of neonatal dexamethasone treatment on hippocampal synaptic function. Ann Neurol 59:939-951.

Lisman J, Schulman H, Cline H (2002) The molecular basis of CaMKII function in synaptic and behavioural memory. Nat Rev Neurosci 3:175-190.

Lledo PM, Hjelmstad GO, Mukherji S, Soderling TR, Malenka RC, Nicoll RA (1995) Calcium/calmodulin-dependent kinase II and long-term potentiation enhance synaptic transmission by the same mechanism. Proc Natl Acad Sci U S A 92:11175-11179.

Lossie AC, Whitney MM, Amidon D, Dong HJ, Chen P, Theriaque D, Hutson A, Nicholls RD, Zori RT, Williams CA, Driscoll DJ (2001) Distinct phenotypes distinguish the molecular classes of Angelman syndrome. J Med Genet 38:834-845.

Lou LL, Lloyd SJ, Schulman H (1986) Activation of the multifunctional Ca2+/calmodulin-dependent protein kinase by autophosphorylation: ATP modulates production of an autonomous enzyme. Proc Natl Acad Sci U S A 83:9497-9501.

MacQueen GM, Ramakrishnan K, Ratnasingan R, Chen B, Young LT (2003) Desipramine treatment reduces the long-term behavioural and neurochemical

sequelae of early-life maternal separation. Int J Neuropsychopharmacol 6:391-396.

Malinow R, Malenka RC (2002) AMPA receptor trafficking and synaptic plasticity. Annu Rev Neurosci 25:103-126.

Mammen AL, Kameyama K, Roche KW, Huganir RL (1997) Phosphorylation of the alpha-amino-3-hydroxy-5-methylisoxazole4-propionic acid receptor GluR1 subunit by calcium/calmodulin-dependent kinase II. J Biol Chem 272:32528-32533.

Marrs GS, Green SH, Dailey ME (2001) Rapid formation and remodeling of postsynaptic densities in developing dendrites. Nat Neurosci 4:1006-1013.

Matsuda S, Launey T, Mikawa S, Hirai H (2000) Disruption of AMPA receptor GluR2 clusters following long-term depression induction in cerebellar Purkinje neurons. EMBO J 19:2765-2774.

Matsuura T, Sutcliffe JS, Fang P, Galjaard RJ, Jiang YH, Benton CS, Rommens JM, Beaudet AL (1997) De novo truncating mutations in E6-AP ubiquitin-protein ligase gene (UBE3A) in Angelman syndrome. Nat Genet 15:74-77.

Matynia A, Kushner SA, Silva AJ (2002) Genetic approaches to molecular and cellular cognition: a focus on LTP and learning and memory. Annu Rev Genet 36:687-720.

Mayford M, Wang J, Kandel ER, O'Dell TJ (1995) CaMKII regulates the frequency-response function of hippocampal synapses for the production of both LTD and LTP. Cell 81:891-904.

Mayford M, Baranes D, Podsypanina K, Kandel ER (1996) The 3'-untranslated region of CaMKII alpha is a cis-acting signal for the localization and translation of mRNA in dendrites. Proc Natl Acad Sci U S A 93:13250-13255.

McHugh SB, Niewoehner B, Rawlins JN, Bannerman DM (2008) Dorsal hippocampal N-methyl-D-aspartate receptors underlie spatial working memory performance during non-matching to place testing on the T-maze. Behav Brain Res 186:41-47.

McNeill RB, Colbran RJ (1995) Interaction of autophosphorylated Ca2+/calmodulin-dependent protein kinase II with neuronal cytoskeletal proteins. Characterization of binding to a 190-kDa postsynaptic density protein. J Biol Chem 270:10043-10049.

Meyer T, Hanson PI, Stryer L, Schulman H (1992) Calmodulin trapping by calcium-calmodulin-dependent protein kinase. Science 256:1199-1202.

Miano S, Bruni O, Elia M, Musumeci SA, Verrillo E, Ferri R (2005) Sleep breathing and periodic leg movement pattern in Angelman Syndrome: a polysomnographic study. Clin Neurophysiol 116:2685-2692.

Migues PV, Lehmann IT, Fluechter L, Cammarota M, Gurd JW, Sim AT, Dickson PW, Rostas JA (2006) Phosphorylation of CaMKII at Thr253 occurs in vivo and enhances binding to isolated postsynaptic densities. J Neurochem 98:289-299.

Miller S, Yasuda M, Coats JK, Jones Y, Martone ME, Mayford M (2002) Disruption of dendritic translation of CaMKIIalpha impairs stabilization of synaptic plasticity and memory consolidation. Neuron 36:507-519.

Miller SG, Kennedy MB (1986) Regulation of brain type II Ca2+/calmodulin-dependent protein kinase by autophosphorylation: a Ca2+-triggered molecular switch. Cell 44:861-870.

Milner B, Squire LR, Kandel ER (1998) Cognitive neuroscience and the study of memory. Neuron 20:445-468.

Mishkin M (1978) Memory in monkeys severely impaired by combined but not by separate removal of amygdala and hippocampus. Nature 273:297-298.

Miura K, Kishino T, Li E, Webber H, Dikkes P, Holmes GL, Wagstaff J (2002) Neurobehavioral and electroencephalographic abnormalities in Ube3a maternal-deficient mice. Neurobiol Dis 9:149-159.

Mohrmann R, Kohr G, Hatt H, Sprengel R, Gottmann K (2002) Deletion of the C-terminal domain of the NR2B subunit alters channel properties and synaptic targeting of N-methyl-D-aspartate receptors in nascent neocortical synapses. J Neurosci Res 68:265-275.

Monyer H, Sprengel R, Schoepfer R, Herb A, Higuchi M, Lomeli H, Burnashev N, Sakmann B, Seeburg PH (1992) Heteromeric NMDA receptors: molecular and functional distinction of subtypes. Science 256:1217-1221.

Moretti P, Levenson JM, Battaglia F, Atkinson R, Teague R, Antalffy B, Armstrong D, Arancio O, Sweatt JD, Zoghbi HY (2006) Learning and memory and synaptic plasticity are impaired in a mouse model of Rett syndrome. J Neurosci 26:319-327.

Moriyoshi K, Masu M, Ishii T, Shigemoto R, Mizuno N, Nakanishi S (1991) Molecular cloning and characterization of the rat NMDA receptor. Nature 354:31-37.

Morris EP, Torok K (2001) Oligomeric structure of alpha-calmodulin-dependent protein kinase II. J Mol Biol 308:1-8.

Morris RG, Anderson E, Lynch GS, Baudry M (1986) Selective impairment of learning and blockade of long-term potentiation by an N-methyl-D-aspartate receptor antagonist, AP5. Nature 319:774-776.

Moser MB, Trommald M, Andersen P (1994) An increase in dendritic spine density on hippocampal CA1 pyramidal cells following spatial learning in adult rats suggests the formation of new synapses. Proc Natl Acad Sci U S A 91:12673-12675.

Mukherji S, Brickey DA, Soderling TR (1994) Mutational analysis of secondary structure in the autoinhibitory and autophosphorylation domains of calmodulin kinase II. J Biol Chem 269:20733-20738.

Nikandrova YA, Jiao Y, Baucum AJ, Tavalin SJ, Colbran RJ (2010) Ca2+/calmodulin-dependent protein kinase II binds to and phosphorylates a specific SAP97 splice variant to disrupt association with AKAP79/150 and modulate alpha-amino-3-hydroxy-5-methyl-4-isoxazolepropionic acid-type glutamate receptor (AMPAR) activity. J Biol Chem 285:923-934.

Nuber U, Schwarz SE, Scheffner M (1998) The ubiquitin-protein ligase E6-associated protein (E6-AP) serves as its own substrate. Eur J Biochem 254:643-649.

Ohta Y, Nishida E, Sakai H (1986) Type II Ca2+/calmodulin-dependent protein kinase binds to actin filaments in a calmodulin-sensitive manner. FEBS Lett 208:423-426.

Ouyang Y, Rosenstein A, Kreiman G, Schuman EM, Kennedy MB (1999) Tetanic stimulation leads to increased accumulation of Ca(2+)/calmodulin-dependent protein kinase II via dendritic protein synthesis in hippocampal neurons. J Neurosci 19:7823-7833.

Planells-Cases R, Sun W, Ferrer-Montiel AV, Montal M (1993) Molecular cloning, functional expression, and pharmacological characterization of an N-methyl-D-aspartate receptor subunit from human brain. Proc Natl Acad Sci U S A 90:5057-5061.

Polydoro M, Acker CM, Duff K, Castillo PE, Davies P (2009) Age-dependent impairment of cognitive and synaptic function in the htau mouse model of tau pathology. J Neurosci 29:10741-10749.

Poncer JC, Esteban JA, Malinow R (2002) Multiple mechanisms for the potentiation of AMPA receptor-mediated transmission by alpha-Ca2+/calmodulin-dependent protein kinase II. J Neurosci 22:4406-4411.

Ramamoorthy S, Nawaz Z (2008) E6-associated protein (E6-AP) is a dual function coactivator of steroid hormone receptors. Nucl Recept Signal 6:e006.

Reiter LT, Seagroves TN, Bowers M, Bier E (2006) Expression of the Rho-GEF Pbl/ECT2 is regulated by the UBE3A E3 ubiquitin ligase. Hum Mol Genet 15:2825-2835.

Rial Verde EM, Lee-Osbourne J, Worley PF, Malinow R, Cline HT (2006) Increased expression of the immediate-early gene arc/arg3.1 reduces AMPA receptor-mediated synaptic transmission. Neuron 52:461-474.

Rice CJ, Sandman CA, Lenjavi MR, Baram TZ (2008) A novel mouse model for acute and long-lasting consequences of early life stress. Endocrinology 149:4892-4900.

Robison AJ, Bartlett RK, Bass MA, Colbran RJ (2005a) Differential modulation of Ca2+/calmodulin-dependent protein kinase II activity by regulated interactions with N-methyl-D-aspartate receptor NR2B subunits and alpha-actinin. J Biol Chem 280:39316-39323.

Robison AJ, Bass MA, Jiao Y, MacMillan LB, Carmody LC, Bartlett RK, Colbran RJ (2005b) Multivalent interactions of calcium/calmodulin-dependent protein kinase II with the postsynaptic density proteins NR2B, densin-180, and alpha-actinin-2. J Biol Chem 280:35329-35336.

Roche KW, O'Brien RJ, Mammen AL, Bernhardt J, Huganir RL (1996) Characterization of multiple phosphorylation sites on the AMPA receptor GluR1 subunit. Neuron 16:1179-1188.

Roche KW, Standley S, McCallum J, Dune Ly C, Ehlers MD, Wenthold RJ (2001) Molecular determinants of NMDA receptor internalization. Nat Neurosci 4:794-802.

Romeo RD, Mueller A, Sisti HM, Ogawa S, McEwen BS, Brake WG (2003) Anxiety and fear behaviors in adult male and female C57BL/6 mice are modulated by maternal separation. Horm Behav 43:561-567.

Rosenmund C, Stern-Bach Y, Stevens CF (1998) The tetrameric structure of a glutamate receptor channel. Science 280:1596-1599.

Rougeulle C, Glatt H, Lalande M (1997) The Angelman syndrome candidate gene, UBE3A/E6-AP, is imprinted in brain. Nat Genet 17:14-15.

Sanhueza M, McIntyre CC, Lisman JE (2007) Reversal of synaptic memory by Ca2+/calmodulin-dependent protein kinase II inhibitor. J Neurosci 27:5190-5199.

Schworer CM, Colbran RJ, Soderling TR (1986) Reversible generation of a Ca2+-independent form of Ca2+(calmodulin)-dependent protein kinase II by an autophosphorylation mechanism. J Biol Chem 261:8581-8584.

Sessoms-Sikes S, Honse Y, Lovinger DM, Colbran RJ (2005) CaMKIIalpha enhances the desensitization of NR2B-containing NMDA receptors by an autophosphorylation-dependent mechanism. Mol Cell Neurosci 29:139-147.

Shen K, Teruel MN, Subramanian K, Meyer T (1998) CaMKIIbeta functions as an F-actin targeting module that localizes CaMKIIalpha/beta heterooligomers to dendritic spines. Neuron 21:593-606.

Sheng M, Hoogenraad CC (2007) The postsynaptic architecture of excitatory synapses: a more quantitative view. Annu Rev Biochem 76:823-847.

Sheng M, Cummings J, Roldan LA, Jan YN, Jan LY (1994) Changing subunit composition of heteromeric NMDA receptors during development of rat cortex. Nature 368:144-147.

Shepherd JD, Rumbaugh G, Wu J, Chowdhury S, Plath N, Kuhl D, Huganir RL, Worley PF (2006) Arc/Arg3.1 mediates homeostatic synaptic scaling of AMPA receptors. Neuron 52:475-484.

Shi S, Hayashi Y, Esteban JA, Malinow R (2001) Subunit-specific rules governing AMPA receptor trafficking to synapses in hippocampal pyramidal neurons. Cell 105:331-343.

Shi SH, Hayashi Y, Petralia RS, Zaman SH, Wenthold RJ, Svoboda K, Malinow R (1999) Rapid spine delivery and redistribution of AMPA receptors after synaptic NMDA receptor activation. Science 284:1811-1816.

Silva AJ, Stevens CF, Tonegawa S, Wang Y (1992a) Deficient hippocampal long-term potentiation in alpha-calcium-calmodulin kinase II mutant mice. Science 257:201-206.

Silva AJ, Paylor R, Wehner JM, Tonegawa S (1992b) Impaired spatial learning in alpha-calcium-calmodulin kinase II mutant mice. Science 257:206-211.

Soderling TR (2000) CaM-kinases: modulators of synaptic plasticity. Curr Opin Neurobiol 10:375-380.

Son GH, Geum D, Chung S, Kim EJ, Jo JH, Kim CM, Lee KH, Kim H, Choi S, Kim HT, Lee CJ, Kim K (2006) Maternal stress produces learning deficits associated with impairment of NMDA receptor-mediated synaptic plasticity. J Neurosci 26:3309-3318.

Song I, Huganir RL (2002) Regulation of AMPA receptors during synaptic plasticity. Trends Neurosci 25:578-588.

Squire LR, Zola-Morgan S (1991) The medial temporal lobe memory system. Science 253:1380-1386.

Stephenson FA, Cousins SL, Kenny AV (2008) Assembly and forward trafficking of NMDA receptors (Review). Mol Membr Biol 25:311-320.

Strack S, Colbran RJ (1998) Autophosphorylation-dependent targeting of calcium/ calmodulin-dependent protein kinase II by the NR2B subunit of the N-methyl- D-aspartate receptor. J Biol Chem 273:20689-20692.

Strack S, McNeill RB, Colbran RJ (2000a) Mechanism and regulation of calcium/calmodulin-dependent protein kinase II targeting to the NR2B subunit of the N-methyl-D-aspartate receptor. J Biol Chem 275:23798-23806.

Strack S, Choi S, Lovinger DM, Colbran RJ (1997a) Translocation of autophosphorylated calcium/calmodulin-dependent protein kinase II to the postsynaptic density. J Biol Chem 272:13467-13470.

Strack S, Barban MA, Wadzinski BE, Colbran RJ (1997b) Differential inactivation of postsynaptic density-associated and soluble Ca2+/calmodulin-dependent protein kinase II by protein phosphatases 1 and 2A. J Neurochem 68:2119-2128.

Strack S, Robison AJ, Bass MA, Colbran RJ (2000b) Association of calcium/calmodulin-dependent kinase II with developmentally regulated splice variants of the postsynaptic density protein densin-180. J Biol Chem 275:25061-25064.

Suenaga T, Morinobu S, Kawano K, Sawada T, Yamawaki S (2004) Influence of immobilization stress on the levels of CaMKII and phospho-CaMKII in the rat hippocampus. Int J Neuropsychopharmacol 7:299-309.

Sutcliffe JS, Jiang YH, Galijaard RJ, Matsuura T, Fang P, Kubota T, Christian SL, Bressler J, Cattanach B, Ledbetter DH, Beaudet AL (1997) The E6-Ap ubiquitin-protein ligase (UBE3A) gene is localized within a narrowed Angelman syndrome critical region. Genome Res 7:368-377.

Thiagarajan TC, Piedras-Renteria ES, Tsien RW (2002) alpha- and betaCaMKII. Inverse regulation by neuronal activity and opposing effects on synaptic strength. Neuron 36:1103-1114.

Tsui J, Malenka RC (2006) Substrate localization creates specificity in calcium/calmodulin-dependent protein kinase II signaling at synapses. J Biol Chem 281:13794-13804.

van Woerden GM, Harris KD, Hojjati MR, Gustin RM, Qiu S, de Avila Freire R, Jiang YH, Elgersma Y, Weeber EJ (2007) Rescue of neurological deficits in a mouse model for Angelman syndrome by reduction of alphaCaMKII inhibitory phosphorylation. Nat Neurosci 10:280-282.

van Woerden GM, Hoebeek FE, Gao Z, Nagaraja RY, Hoogenraad CC, Kushner SA, Hansel C, De Zeeuw CI, Elgersma Y (2009) betaCaMKII controls the direction of plasticity at parallel fiber-Purkinje cell synapses. Nat Neurosci 12:823-825.

Wang H, Feng R, Phillip Wang L, Li F, Cao X, Tsien JZ (2008) CaMKII activation state underlies synaptic labile phase of LTP and short-term memory formation. Curr Biol 18:1546-1554.

Wang H, Shimizu E, Tang YP, Cho M, Kyin M, Zuo W, Robinson DA, Alaimo PJ, Zhang C, Morimoto H, Zhuo M, Feng R, Shokat KM, Tsien JZ (2003) Inducible protein knockout reveals temporal requirement of CaMKII reactivation for memory consolidation in the brain. Proc Natl Acad Sci U S A 100:4287-4292.

Weeber EJ, Jiang YH, Elgersma Y, Varga AW, Carrasquillo Y, Brown SE, Christian JM, Mirnikjoo B, Silva A, Beaudet AL, Sweatt JD (2003) Derangements of hippocampal calcium/calmodulin-dependent protein kinase II in a mouse model for Angelman mental retardation syndrome. J Neurosci 23:2634-2644.

Wenthold RJ, Petralia RS, Blahos J, II, Niedzielski AS (1996) Evidence for multiple AMPA receptor complexes in hippocampal CA1/CA2 neurons. J Neurosci 16:1982-1989.

Williams CA, Beaudet AL, Clayton-Smith J, Knoll JH, Kyllerman M, Laan LA, Magenis RE, Moncla A, Schinzel AA, Summers JA, Wagstaff J (2006) Angelman syndrome 2005: updated consensus for diagnostic criteria. Am J Med Genet A 140:413-418.

Wu GY, Cline HT (1998) Stabilization of dendritic arbor structure in vivo by CaMKII. Science 279:222-226.

Xu Y, Lin D, Li S, Li G, Shyamala SG, Barish PA, Vernon MM, Pan J, Ogle WO (2009) Curcumin reverses impaired cognition and neuronal plasticity induced by chronic stress. Neuropharmacology 57:463-471.

Yashiro K, Riday TT, Condon KH, Roberts AC, Bernardo DR, Prakash R, Weinberg RJ, Ehlers MD, Philpot BD (2009) Ube3a is required for experience-dependent maturation of the neocortex. Nat Neurosci 12:777-783.